

Fluid Manipulation Using a Thermoexpandable Polymer Based on Polydimethylsiloxane and Expancel

THÈSE N° 4889 (2010)

PRÉSENTÉE LE 10 DÉCEMBRE 2010

À LA FACULTÉ SCIENCES ET TECHNIQUES DE L'INGÉNIEUR

LABORATOIRE DE MICROSYSTÈMES 4

PROGRAMME DOCTORAL EN MICROSYSTÈMES ET MICROÉLECTRONIQUE

ÉCOLE POLYTECHNIQUE FÉDÉRALE DE LAUSANNE

POUR L'OBTENTION DU GRADE DE DOCTEUR ÈS SCIENCES

PAR

Lynda METREF

acceptée sur proposition du jury:

Prof. M. Gijs, président du jury
Prof. Ph. Renaud, directeur de thèse
Dr F. Bianchi, rapporteur
Prof. H. Hofmann, rapporteur
Prof. G. Stemme, rapporteur



ÉCOLE POLYTECHNIQUE
FÉDÉRALE DE LAUSANNE

Suisse
2010

*To my mother, who left too soon
to see the result of her encouragements and support.*

Abstract

Nowadays, manipulation of liquids in miniaturised environments finds applications in many fields in biology and medicine such as diagnostics, toxicity analysis, drug delivery and so on. In those domains, the use of disposable devices has the great advantage of removing any surface contamination which could result in device malfunction. In this context, the present work revolves around the use of a thermoexpandable material, composed of expandable beads in an elastomeric matrix, used as actuator for liquids. This material is expandable only once, providing a good actuation for disposable devices. It also allows to keep the material inflated without additional energy input. This thesis has three main goals: understanding the expansion properties of this material through characterisation and modelling, proposing implementation of the heating source, and investigating possible applications.

Characterisation of the material reviews its capability to create movement. The two main parameters characterised are the volumetric expansion of the material and the pressure it can provide. To better understand those behaviours, a morphological study of Expancel® beads is also undertaken. Expansion of the composite is then theoretically modelled to provide a tool for future designs.

The following part of this thesis focuses on solutions to implement the material for liquid actuation. Before this investigation, the main solution used to heat the material was the resistive heating of copper tracks on a circuit board. Here, alternative solutions are provided such as the use of clean room facilities, screen-printing and polymeric conductors. The pros and cons of the proposed solutions are stated in a way to allow the reader to choose the best option for his application.

Finally, some applications of this actuation system are implemented and tested to highlight the limitations and advantages of this technology when put into application.

Keywords: thermoexpandable material, microfluidic, actuator, PDMS, Expancel

Version abrégée

De nos jours, la manipulation de liquides dans des environnements miniaturisés peut être appliquée dans de nombreux domaines en biologie et médecine; comme le diagnostic, l'analyse de toxicité, l'administration de médicaments, etc. Dans ces domaines, l'emploi d'un appareil jetable a le grand avantage de supprimer les contaminations de surfaces, qui pourraient provoquer un dysfonctionnement de l'appareil. Tenant compte de ce contexte, le présent travail se base sur l'utilisation d'un matériau thermo-expansible, composé de billes expansibles dans une matrice élastomère, pour déplacer des liquides. Ce matériau n'est expansible qu'une seule fois, fournissant ainsi un bon actionneur pour appareils jetables. Il reste également dans l'état expansé sans apport d'énergie supplémentaire. Cette thèse a trois buts principaux: comprendre les propriétés d'expansion de ce matériau à l'aide de caractérisations et de modélisations, proposer une implémentation du système de chauffage, et investiguer les applications possibles de cette technologie.

La caractérisation du matériau évalue sa capacité à créer du mouvement. Les deux paramètres principalement caractérisés sont l'expansion volumique du matériau et la pression qu'il peut fournir. Afin de mieux comprendre son comportement, une étude morphologique des billes d'Expancel[®] est entreprise. Le gonflement du composite sera ensuite modélisé, fournissant ainsi un outil de conception pour le futur.

La partie suivante de cette thèse se penchera sur la mise en oeuvre de ce matériau pour déplacer des liquides. Précédemment, la façon la plus courante de chauffer le composite était le chauffage par résistance électrique de pistes de cuivre sur un circuit imprimé. Dans ce travail, des solutions alternatives de chauffage sont proposées; comme l'utilisation de techniques de production en salle blanche, la sérigraphie ou des polymères conducteurs. Les avantages et inconvénients de chaque solution sont exposés. Le lecteur pourra donc choisir la meilleure en fonction de son application.

Finalement, quelques applications de ce système actionneur sont implémentées et testées pour mettre en évidence les limites et avantages de cette technologie en pratique.

Mots-clés: matériel thermo-expansible, microfluidique, actionneur, PDMS, Expancel

Acknowledgements

I would like to thank a lot of people for helping me bring this work to fruition. Some on more technical level and others for their constant support.

I would like to thank Prof. Philippe Renaud for welcoming me in his lab to carry out this work, as well as for his support and scientific advice, and Frédéric Neftel from Debiotech for offering me this PhD position. Thank you also to the members of the jury, Prof. Göran Stemme, Prof. Heinrich Hofmann and Dr. François Bianchi, for taking the time to judge my work and for providing an insightful discussion in the course of my exam; as well as to Prof. Martin Gijs for presiding over my thesis defence.

Many people helped me carry out the different scientific works presented here: thank you to (in random order) Ludger Weber, Christopher Plummer, Sarah Levy, the ACI members, the LTP members, the LPM workshop staff, the Biop staff, Anne Aimable, Sébastien Jiguët, Nathalie Serra, the LPM members, Nicolas Blanc, Michael Canonica, Charly Azra, Pau Mato-sabat, Patrick Thévoz, Raphaël Goetschman, Marc Laurent, François Bianchi, Véronique Vallet, Selma Mefti, Pierre Lemaire, Stephan Gamper, Arnaud Tourvieille, Niklaus Schneeberger, Eric Chappel, Philippe Berton, André Colas, Anne Agellilo-Cherrer, Christiane Gerschheimer.

Thank you to my office mates for their company and their open ear to my scientific and every day problems: Mina Todorova, Pontus Linderholm, Nicolas Durand, Harsha Kasi and Robert Meissner

A more general thank to my (past and present) lab mates at LMIS for their help: Anja, Sophie, Pierre, Guillaume, Ludovica, Fabian, Nina, Ana, Harald, Arnaud, Shady, Urban, Matteo, Mario, Thomas, Raph (Tweedy says thank you too), Nicolas, André and the others I may have forgotten. Thank you also to all my colleagues at Debiotech.

To help me proof reading and proof hearing this text and my presentation, a big thank you to Marie Dysli, Arnaud Bertsch, Mina Todorova, Stéphane Magnenat and Etienne Dysli.

Finally I want to thank my friends and my family. Thank you to my sister Nadia, my father Salem and my mother Anne-Lise. The last months of this work have been hard due to the passing of my mother and your support was inestimable. Last but not least, thank you Etienne for supporting (and suffering) me during those years.

Contents

1	Introduction	1
1.1	Introduction to composite materials	3
1.2	State of the art of microfluidic actuation	7
1.3	Motivations and goals	16
2	Characterisation of PDMS - Expancel® composite	17
2.1	Particles morphological study	19
2.2	Expansion profile as function of temperature	24
2.3	Young's modulus measurement	28
2.4	Zero expansion pressure analysis	32
2.5	Volumetric expansion ratio characterisation	36
2.6	Characterisation roundup	41
3	Modelling	43
3.1	Expansion of a single Expancel® bead	44
3.2	Model of expansion for a PDMS coated bead	46
3.3	Beads' internal pressure after expansion	54
3.4	Modelling roundup	58
4	Heating system for PDMS - Expancel® composite activation	59
4.1	Screen-printed heaters with temperature control	60

4.2	Other activation methods	70
4.3	Heating system roundup	72
5	Applications of PDMS - Expancel® composite	73
5.1	Micro-injector	74
5.2	Miniaturized blood coagulation testing tool	81
5.3	Applications roundup	88
6	Conclusion	89
6.1	Summary of results	90
6.2	Perspectives	92
	Bibliography	93
	List of Symbols	107
A	Detailed experimental protocol	111
A.1	PDMS-Expancel® composite preparation	112
A.2	Crosslinked PDMS removal procedure	114
A.3	Density measurement protocol	115
A.4	Conducting PDMS preparation protocol	116
A.5	Ti/Pt electrode fabrication and implementation with composite . .	118
B	Detailed calculus	119
B.1	Variation of volume in a micro injector cavity	120
	Curriculum Vitae	123

勝兵先勝而後求戰
敗兵先戰而後求勝

*Vanquishing warriors seek victory first and then go to war,
while defeated warriors fight first and then strive for victory.*

- Sun Tzu, The art of War

Contents

1.1	Introduction to composite materials	3
1.1.1	Polydimethylsiloxane (PDMS)	3
1.1.2	Expancel®	5
1.2	State of the art of microfluidic actuation	7
1.2.1	Liquid management in microchannels	7
1.2.2	Microfluidic actuation in channels based on polymers	8
1.2.3	PDMS - Expancel® composite	11
1.3	Motivations and goals	16

Diagnostics and biology are fields of research and development where liquid analyses are omnipresent. From disease or body malfunction detection to understanding principles of life, analytical tools are needed. In those analyses, fluid control is essential. Dosing, mixing and fluid manipulation are ubiquitous. For several years, microfluidic systems have been developed in order to find new and more competitive tools in the fields of chemistry, biology and diagnostics [1–3]. Advantages of such systems have been praised for more than a decade. Needs of fewer reagents and samples, non turbulent flows, high miniaturisation and portability potential are the most cited.

One of the challenges to overcome in this domain is the prevention of any kind of cross contamination between analyses. This is easily achieved by the use of disposable or partially disposable devices.

To bring such a system to the market, one must be able to produce it on a large scale and at a low cost. Polymers are materials of choice for disposable devices, including microfluidic devices [4]. They are cheap and can be mass produced.

One of the competitors and predecessors of polymers in Microelectromechanical System (MEMS) is silicon. It offers many possibilities in terms of integration, because electronic sensors and channels can be produced on the same substrate. Its main drawback is its cost both for raw material and manufacturing process.

In order to add more functionalities to polymer systems, smart materials have been developed. From moving to sensing, they are now getting more and more of the functionalities of silicon [5–7].

The present work will focus on the study of a thermoexpandable material usable as disposable microfluidic actuator in point-of-care devices. It is a composite polymer where a Polydimethylsiloxane (PDMS) matrix embeds Expancel[®] microspheres. Since PDMS is already widely used in microfluidics [8, 9], this composite can use well-known fabrication methods and fits well within other PDMS systems.

1.1 Introduction to composite materials

As previously stated, this work will aim at assessing the possibilities and limitations of an actuating system based on a composite made of Expancel® beads embedded in a PDMS matrix shown in Figure 1.1. In order to have all the required tools to understand its working principle, this section will give a technical introduction on its two components.

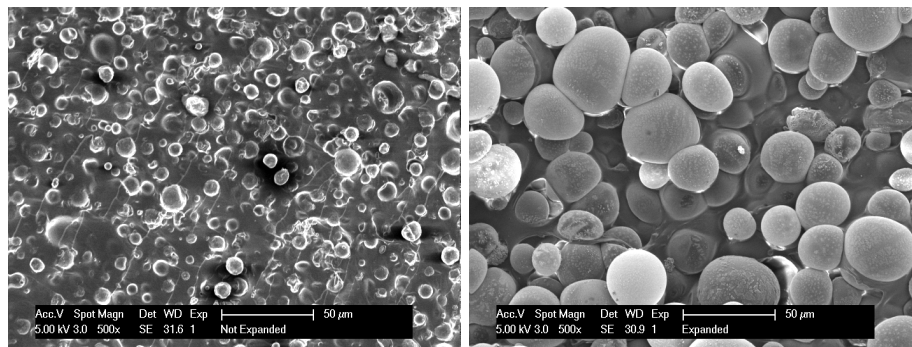


Figure 1.1 SEM images of Expancel® particles embedded in PDMS before (left) and after (right) expansion.

1.1.1 Polydimethylsiloxane (PDMS)

The first organic compounds based on silicon were presented in 1863 by Friedel and Crafts [10]. Kipping, around 1900, did further investigation and synthesis of siloxane compounds [11] and gave them the name “silicone”. Silicone as stable elastomer was developed after World War II by Dr. J. Franklin Hyde from Dow Corning [12, 13]. It was first employed as ignition sealing compound to prevent corona discharge [14] in aviation, making high altitude flights possible [15]. PDMS and other silicones of variable molecular weight were then used in many industries such as industrial lubrication, textile treatments, personal care and biomedicine [15]. This long carrier as industrial material gave time to scientists to characterise many of its properties [16].

PDMS elastomer is a network of crosslinked oligomers. Oligomers are a repetition of an Si-O backbone with two CH₃ groups covalently bond to each Si atom. This structure results in several intrinsic properties of the material. Crosslinking points between oligomers are quite far from each other. This gives important spaces in the molecular structure of the material. This results in a rather high permeability to small molecules such as oxygen or helium as well as high absorption

1.1. Introduction to composite materials

of low molecular weight liquids such as alcohol, isopropanol, *etc.* . A high compressibility can also be observed [17].

The surface tension of the PDMS oligomer before crosslinking is low enough to allow precise moulding with resolution reaching 10 nm [18]. Using replica moulding as fabrication process allows for the creation of a large variety of devices such as mixers, valves and pumps [19].

PDMS can be bonded to itself both permanently and reversibly. Reversible bonding occurs simply by putting into contact two PDMS surfaces which stick together by static forces. Such systems can withstand pressures from 0.34 [18] to 1 bar [20]. This can also be performed on PDMS/glass interfaces. Irreversible bonding is done by creating covalent O-Si-O bonds by a condensation reaction of two Si-based surfaces exposed to oxygen plasma [18]. Irreversible bonding can withstand pressures around 3 bars [18, 21]. Other methods such as varying curing ratio [19], curing agent [22] or uncured PDMS [23] gluing and partial PDMS curing [24] have been reported.

The ease of fabrication by replica moulding makes PDMS systems cheap and rapidly fabricated. Its permeability to gas allows the oxygenation of cell cultures in such systems [18, 25, 26]. It is mostly inert and resistant to many solvents and chemicals [27]. However, drawbacks like hydrophobicity and consequent hydrophobic molecule absorption can be noted. Water evaporation due to permeability to gas [28] also makes it improper to solution storage.

The CH₃ groups contained in PDMS make it hydrophobic. In microfluidic systems holding water, hydrophobic walls are not desirable. Several methodologies have been proposed to make the surface hydrophilic [29] such as ultraviolet polymer grafting [30], corona discharges [31], ultraviolet light exposure [32] or oxygen plasma exposure [33]. Studies have been made on hydrophobicity recovery time [31, 34–37]. In the case of oxygen plasma, the hydrophobic behaviour recovery can be slowed down by thermal treatment [38] or storage under water or polar organic solvent [27].

The high flexibility of this material, the development of a variety of flow control systems, its simplicity of implementation, high resolution and permeability to oxygen have made it a material of interest in the development of biological systems [18]. In microsystem technologies, it has been used to create microfluidic systems [8, 19, 39–41] and stamps for micro contact printing [42].

1.1.2 Expancel[®]

Expancel[®] is an expandable material manufactured by Azko Nobel in Sweden [43]. It is composed of microspheres which multiply their volume up to 40-fold when heated above a certain temperature.

The first patent regarding this material was submitted in 1967. The main inventor is Donald S. Morehouse and the assignee The Dow Chemical Company. The file was accepted and patented in 1971 [44].

As shown in Figure 1.2, the microspheres are hollowed thermoplastic beads filled with a small amount of liquid isobutane (10-15 % weight) [45, 46]. The vaporisation temperature at ambient pressure of this hydrocarbon is -11°C , meaning isobutane is maintained in its liquid phase by the thermoplastic shell of the bead. When the thermoplastic shell is heated above its glass transition temperature, it softens and isobutane goes from liquid to gaseous state, thus expanding the bead. Once the system cools down, the bead shell hardens again but the gas does not return to liquid form. The expansion is thus permanent.

This product exists in two different states (expanded or not expanded) and has various activation temperatures. The activation temperature variety is achieved by controlling the glass phase transition of the shell. A sample of existing variants is shown on Table 1.1. The shell's polymer is a composite of several thermoplastics with different phase change temperatures. The main components of the shell polymer are acrylonitrile, methacrylate and acrylate [45].

Name	Size [μm]	Expansion temperature [$^{\circ}\text{C}$]
820 DU 40	10-16	76-81
031 DUX 40	10-16	80-95
551 DU 40	10-16	95-100
551 DU 20	6-9	95-100
551 DU 80	18-24	95-100

Table 1.1 Overview of Expancel[®] expansion temperatures and particles' size from Expancel[®] datasheets [45]

The applications of Expancel[®] are very wide. Microbeads are used both in already expanded forms and expandable ones. The expanded form is used as filler for weigh reduction of products like paints, or thermoplastic. It has also been used to increase the strength and toughness of cement [47] and the resiliency of vinyl

1.1. Introduction to composite materials

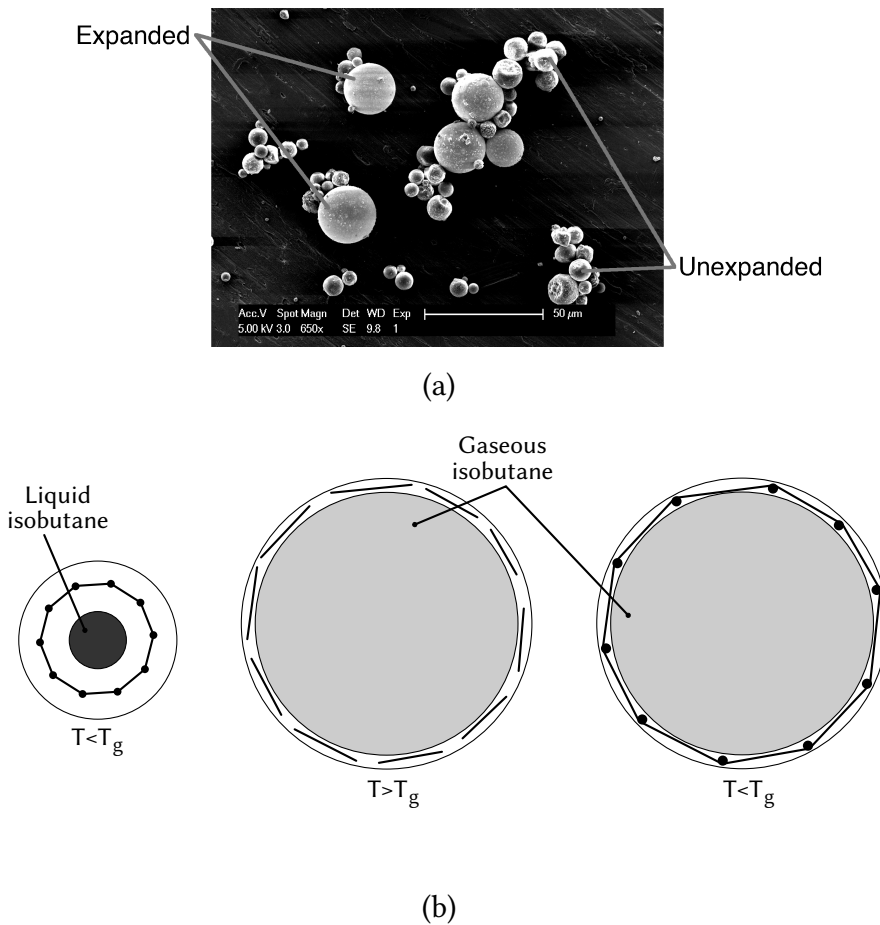


Figure 1.2 Scanning Electron Microscopy image of Expancel[®] beads in both unexpanded and expanded states (a). Expansion principle of Expancel[®] microspheres (b). Below expansion temperature, the thermoplastic shell of the sphere is rigid and is holding under liquid form isobutane, which evaporation temperature is around -11 °C. When the bead is heated, the shell softens and cannot hold the pressure applied by liquid isobutane any more. The isobutane is thus free to evaporate, the shell deforms and the overall volume of the sphere grows up to 40-fold. When the temperature decreases and the thermoplastic regains its rigidity, isobutane does not return to liquid state because no pressure is applied to it, resulting in a rigid larger sphere.

[48]. The unexpanded beads can be used to create raised patterns on cloth painting or swelling thermal insulator [43].

In this work, all studies were performed on 820 DU 40 Expancel[®], due to its low expansion temperature.

1.2 State of the art of microfluidic actuation

“Microfluidics” describes the manipulation of fluid in the sub millimetre range. Evident advantages are directly connected to their small size. Portability, lower reagents need and diminution of waste produced are among them. Beside their small size, the interest of such systems also lies in the fact that some phenomena do not scale linearly with size. The ratio of inertial and viscous forces, also call Reynold’s number, lower with size resulting in laminar flows. Mass and heat transfer are much more efficient on a small scale, resulting in faster reactions [1–3, 49–51].

1.2.1 Liquid management in microchannels

The first “Lab-on-chip” or micro total analysis system (μ TAS) was a gas chromatograph developed by S.C. Terry at Stanford University [52] during the seventies. This field did not get a high interest until the publication of the conceptual article laying the main ideas of on-chip analysis [53]. Since then, μ TAS systems have been widely studied [1, 54].

In order to analyse liquids, flow control elements such as valves [55], mixers [56] or actuation devices like pumps have been widely studied. This literature review will focus on fluid actuation [57, 58].

Analyses relying on capillarity to drive the liquid trough reagents are called “lateral flow assays”. They rely on passive liquid transport within porous material or capillaries. This method has been tremendously used since the sixties in various diagnostic and analysis systems. Most widely-known applications are diabetes testing, pregnancy testing, pH measurement, *etc.* [59]. By being deeply implanted in industry, it is still considered the best actuation system for portable disposable devices due to its simplicity, the fact that it does not require power supply and its low cost. The main drawback of such a system is the lack of protocol flexibility as well as the poor accuracy of volume used.

Centrifugation systems are not yet as much used as capillary systems, but are getting more and more interest from the industry [60]. They rely on circular movement to move liquid in channels [61, 62]. They are implanted on circular substrates like compact disks. By choosing the layout of channels, chambers, stop-valves and mixers can be implemented. The advantage of such a system is that centrifuges for

1.2. State of the art of microfluidic actuation

cell/plasma separation use the same principle and are ubiquitous in labs. Another alternative is the use of standard compact disk reader [63].

Electrical energy can be used to drive liquids as in electrohydrodynamic systems [64], electro-osmotic flows [65] and electro-wetting systems [66]. In those cases, the electrical energy is directly used to create a displacement of liquid. It is thus highly dependant on the electrical properties of the actuated liquid. Those methods are not recommended if the liquid is sensitive to electrical fields.

Electrical energy can also be used to induce another chemical or physical reaction. Electrochemical gas generation (in the liquid itself [67] or in an intermediate medium [68, 69]), fluid thermal dilatation [70] or evaporation[71] are some of the methods used. When the reaction takes place in the liquid itself, not any fluid can be used. Such process could modify liquids sensitive to electrical currents. To prevent modification of the results, it is not often used to perform analyses.

A pressurized gas can also be used as actuator. A pneumatic pressure is applied on a reservoir holding the liquid, transferring a force driving the liquid in the channels [72]. Pressure can also be applied on flexible membranes to act like mechanically driven pumps [19]. This system has been deeply studied and many applications have been proposed [73–76]. It allows the integration of elements on a very large scale [77] and this method is safe for the actuated liquid integrity, but a large system needs to be implemented outside the chip to create and distribute the pressure.

Mechanical pumps use moving parts such as valves and membranes to move liquids. Those systems are mainly based on macroscale principles, scaled down to the micrometer scale. Many mechanical micropumps have been developed like valve membrane pumps [78–80], peristaltic pumps [81], valveless rectification pumps [82] and rotary pumps [83].

Other actuation systems based on intrinsic deformations of polymers will be described in the next section.

1.2.2 Microfluidic actuation in channels based on polymers

Since this work will focus on thermoexpandable polymers, it is of interest to present similar systems with the common properties of being based on polymeric materials. In other words, systems where the needed momentum to actuate the liquid is

provided by a polymer. Two main classes of polymer actuator can be described: the form changing polymers and the expanding ones.

Form changing polymers

Shape Memory Polymers (SMP) have been proposed as fluidic actuators [84]. Those materials have the property to change their geometrical shape when activated. More precisely, they have a permanent shape and a temporary shape. When in temporary shape, an external stimulus (temperature, light, electricity...) makes them return to their permanent state.

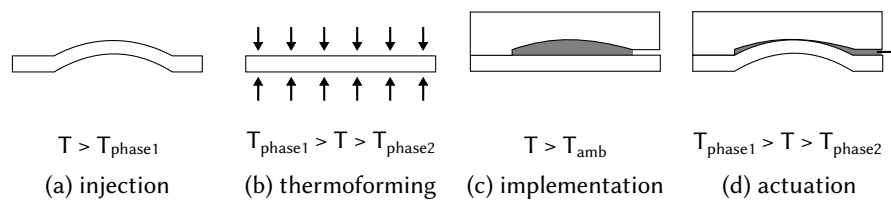


Figure 1.3 Implementation of SMP as microfluidic actuator. The polymer is first formed above the glass transition temperature of the first phase, T_{phase1} (a). This gives it its permanent form. Then the temporary form is given at a temperature between the glass transition temperature of the two phases (b). Once the system is implemented in the microfluidic system (c), the temperature can be raised again above the glass transition temperature of the second phase to recover the permanent form and actuate a liquid (d).

SMP are formed of at least two different phases [85]. We will develop the case of temperature stimulated SMP. The phase with the higher glass transition temperature (phase I), is responsible for holding the permanent shape. The composite is formed above this temperature. The second phase (phase II) can hold the temporary shape. As the glass transition temperature of phase I is higher than phase II's the permanent shape is memorised in phase I's network as phase II retains the temporary shape. When this material is heated above phase II's glass transition temperature, phase II melts and allows the permanent shape to recover. A typical implementation of SMP as fluidic actuator is shown in Figure 1.3

1.2. State of the art of microfluidic actuation

Polymer	Stimulus
Poly(Nisopropylacrylamide) (PNIPAAm)	Temperature, 32 °C
PEO–PPO–PEO copolymer	Temperature, 50 °C
Poly(acrylic acid) (PAAc)	pH 5-6 (Poylacid)
Poly(N,N'-dimethyl aminoethyl methacrylate) (PDMAEMA)	pH 7.5 (Polybase)
N,N-dimethyl aminoethyl methacrylate (DMAEMA)	Glucose concentration

Table 1.2 Examples of hydrogels and their stimulus [86].

Expanding polymers

These polymers change their volume under a certain stimulus. Their swelling results in mechanical displacement actuating a liquid.

Hydrogels are the main example of this category of actuators. An hydrogel is a crosslinked polymer with an hydrophilic network accepting water [86]. The expansion of hydrogels relies on physical changes of the matrix to allow water to enter or to go out of the material network, making it swell or shrink. These changes can be induced by different stimuli. Heat, electrical potential, pH and light can be cited as example. Table 1.2 cites some hydrogels and their activation principle [86].

In microfluidics, hydrogels have been used as liquid actuators [87–89] or flow controllers [90–92] like valves. The principle used most often to package hydrogels as microfluidic actuator is show in Figure 1.4. Hydrogels are structured in a cavity closed on top by a membrane out of flexible material such as PDMS. This chamber is connected to a water reservoir to allow the osmotic balance change to collect liquid and let the swelling occur. The fluidic channel or the reservoir is placed on top of the flexible membrane. In this way, when the hydrogel swells, the volume increase deforms the membrane and closes the upper space, emptying the cavity or blocking the liquid flow.

Phase change polymer actuators rely on liquefaction of a solid polymer. To the knowledge of the author, only poly ethylene glycol (PEG) has been reported as phase changing polymer actuator [93, 94]. The principle of the device is to embed

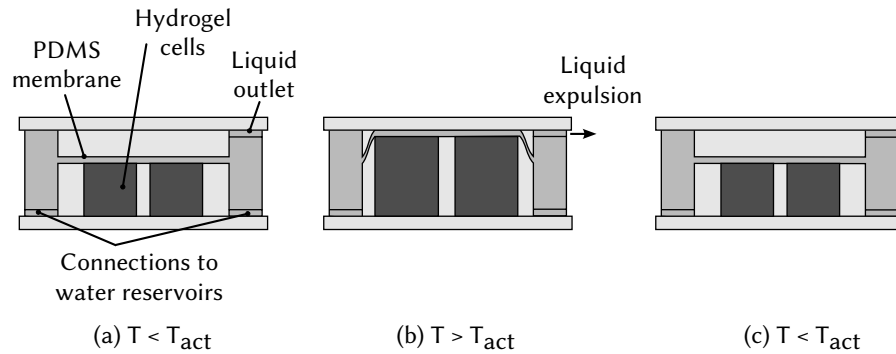


Figure 1.4 Structure and operation of a hydrogel based liquid dispenser: (a) This kind of system is usually composed of two cavities separated by a flexible membrane. In one of those cavities, the liquid to dispense is stored, as in the other one lay the hydrogels. (b) While a stimulus is applied to hydrogel cells, they expand by getting filled with water. This volume increase deforms the membrane resulting in the expulsion of the stored liquid. (c) The effect is reversible and if the stimulus stops, the hydrogel cells regain their original form.

solid PEG under a flexible membrane with heaters. A liquid channel is put on top of the flexible membrane and when the heaters are activated, the PEG will melt and increase its volume by 25 %, closing the fluidic channel in the same manner as for hydrogel shown in Figure 1.4. This system is reversible, but as long as the channel needs to be kept closed, energy is required to maintain the fusion temperature. It can be used to dispense a single dose of liquid or, by putting several systems in series, as a peristaltic pump.

1.2.3 PDMS - Expancel[®] composite

Actuation based on Expancel beads has been first implemented by using only Expancel[®] in a microchannel [46]. In following studies, Expancel[®] has been included in an elastomer matrix to make its use more simple. This also allows to localise Expancel[®] precisely and avoid its dissemination in the microfluidic circuit.

Liquid actuators and valves with PDMS - Expancel[®] composite

This kind of thermoexpandable composite made of PDMS holding Expancel[®] beads has been used to make complete microfluidic systems with fluidic actuators and valves [95, 96].

1.2. State of the art of microfluidic actuation

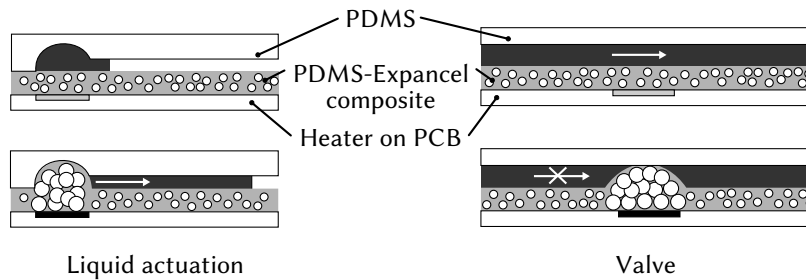


Figure 1.5 Structure and operation of PDMS technology: The system is composed of three layers, the PCB holding the heaters, the composite layer and a moulded PDMS part containing the microfluidic network. In the liquid dispensing case, a cavity is preloaded with the liquid to dispense. Under this cavity lie the heaters. When they are activated, the composite layer locally expands, filling the cavity and ejecting the liquid through the outlet. In the valve implementation, the setup is the same, but the heaters are under a channel where the liquid can freely flow. Once the heaters are powered, the expansion will obstruct the channel like an irreversible valve and will prevent the liquid from flowing.

Figure 1.5 describes liquid dispensing and flow control with valves. In the first implementation, a copper track on a Printed Circuit Board (PCB) was used as heater. Then, a non polymerised mix of Expancel[®] and PDMS is poured on the PCB and spin-coated, before being thermally cured. Finally, channels moulded in PDMS are bonded on top of the cured composite. By powering the copper tracks on the PCB, the composite is locally heated and thus expands, allowing to actuate liquid or to obstruct a channel.

Actuation of liquids and valves have been realised using such technology. Typical volume actuated by this method were in the nanoliter range [96] and the maximum pressure held by the valves was around 140 kPa.

Aspiration and dispensing system

A more complex system allowing to perform an aspiration and dispensing has been developed by Samel *et al.* [97]. Such device is presented in Figure 1.6.

The main concept of this system is to heat a ring of composite to create a “volcano” in its centre to suck in liquid and load the system. Secondly, the centre of the ring is also heated to eject the loaded liquid into its destination.

The system is composed of four layers. At the bottom lays the PCB with the heating tracks, then the composite layer, the closing layer and the rigidifying layer.

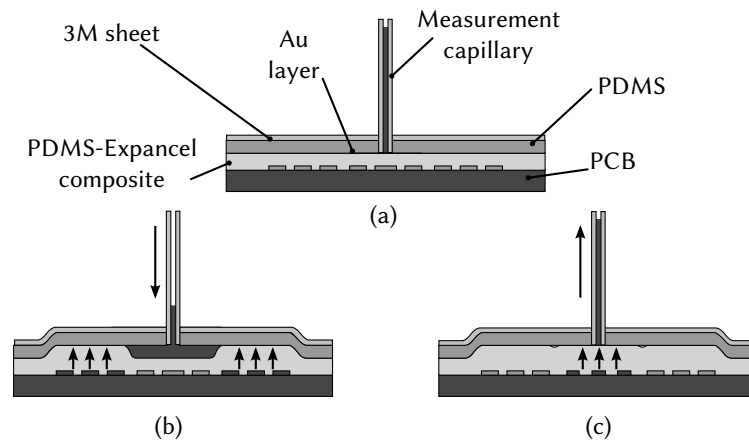


Figure 1.6 Structure and operation of fluidic aspiration and dispensing: (a) The system is composed of a PCB holding the heaters on top of which is spin coated a layer of PDMS - Expancel[®]. PDMS is spin coated and cured on a sheet of 1022-release-liner 3.0 mil (3M). Both parts are selectively coated with gold to prevent the bounding of the cavity. Finally, a capillary is fixed on the connection hole to allow the study of the liquid's movements. (b) The aspiration is performed by powering the external heater. The periphery of the system expands under the action of heat, a cavity is formed and the liquid is sucked in. (c) In a second step, the central heater is powered and the composite's expansion closes the cavity, ejecting the liquid.

The closing and composite layers are bonded together except inside the external heater ring. In this way, when the external ring is expanded, the closing ring rises on the border and in the middle, forming a cavity. If some liquid stands at the connection of the system, the depression created will suck it in. The expansion of the central part then ejects this liquid. Combined with valves, this system can act as a micro syringe by aspirating the liquid from a reservoir and re-injecting it in a microfluidic system.

Typical volumes dispensed by this system are in order of several hundreds nanoliters.

Augmentation of dispensed volumes with buckling membranes

To increase the volume dispensed by PDMS - Expancel[®] composite based systems, another variation of the technology was proposed [98]. In earlier versions of the system, the displacement of liquid was only based on the volume increase of the material. In this alternative approach, the volume increase implies a deformation

1.2. State of the art of microfluidic actuation

of the composite layer until its buckling, allowing to fill bigger cavities and thus to eject more liquid as Figure 1.7 shows. Typical ejected volumes are around $4.5 \mu\text{l}$.

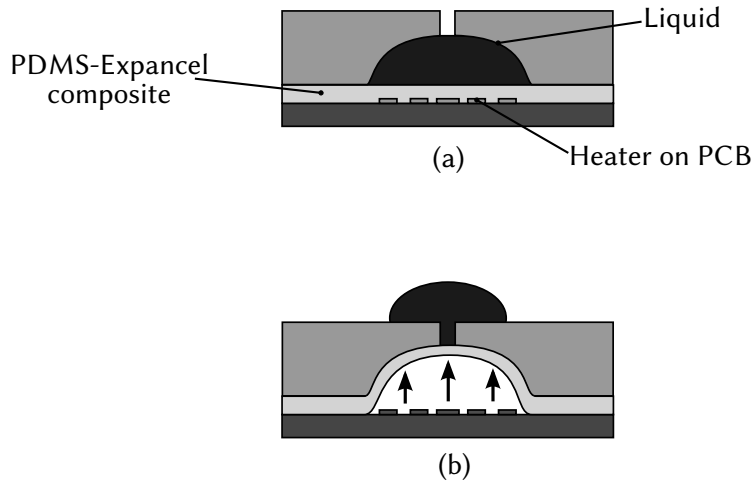


Figure 1.7 An alternative use of PDMS - Expancel[®] composite film is to profit from its ability to buckle and create a hollow bubble between the film and the PCB. In this case, the layer structure is the same as for the system presented in Figure 1.5 . The only difference is the size of the upper cavity which is bigger to accommodate more liquid. With more space, the film can also leave the PCB, forming a wrinkle and ejecting liquid.

Material characterisation

The bulk PDMS - Expancel[®] composite was characterised in terms of expansion ratio [95] and “in situ” thermal propagation in the system [96].

Expansion ratio results are shown in Figure 1.8. They show a strong correlation between expansion ratio and beads’ proportion in composite. Typical expansion ratios observed are between 1.6 and 2.8.

In order to determine possible liquid alteration due to temperature, a study of the temperature of the composite at its surface during the heating required to expand it was performed. Thermal analysis was performed on a $100 \mu\text{m}$ thick layer of PDMS - Expancel[®] with a temperature sensor [96]. Temperature for power supply of 220 mW heated the sample to $43 \text{ }^\circ\text{C}$ if activated during 2 s . If activation is reduced to 1 s the temperature reached is $35 \text{ }^\circ\text{C}$.

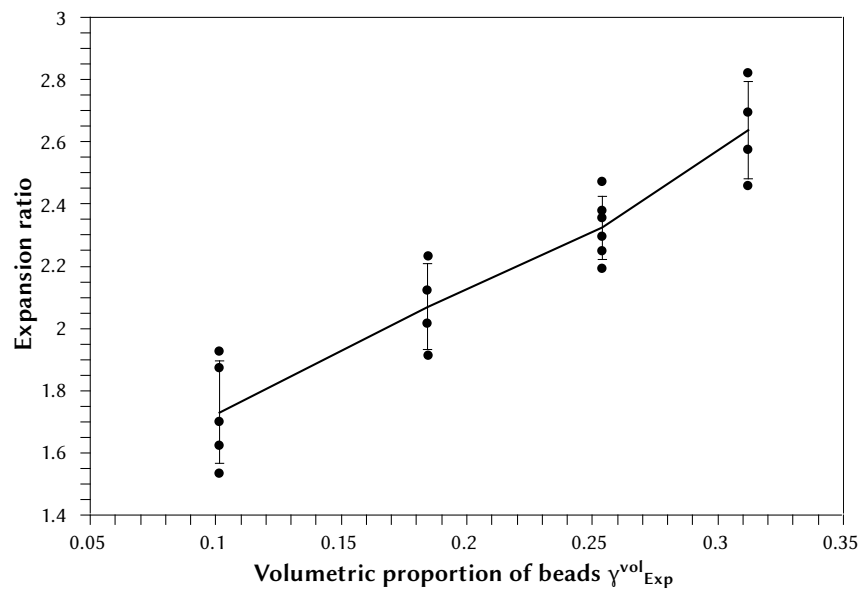


Figure 1.8 Data from Samel *et al.* [95] converted into expansion ratio as function of volumetric proportion. Typical expansion ratios are between 1.6 and 2.8 and are correlated to Expancel[®] proportion in the mix.

1.3 Motivations and goals

To our knowledge, no model of PDMS - Expancel[®] composite behaviour has been proposed. Characterisation in term of expansion ratio versus beads' proportion was performed [95], but no model was given to explain it. In this context, the motivation of this work is to provide an explanation of the behaviour of the PDMS - Expancel[®] composite. Providing a model for the expansion phenomenon is thus the first goal of this work.

Another aspect of this material which has not yet been studied, is its actuation power or the pressure it can provide to a fluid in order to actuate it. We tried to answer this by measuring the pressure provided by the material itself as well as the reduction of expansion ratio due to pressure.

Activation threshold of such material have been roughly described, but no substantial study has been performed. Thus a characterisation of expansion ratio as a function of temperature was undertaken to determine how the temperature can affect the expansion of the composite.

The properties of the components and how they will affect the expansion parameters are important since they will directly impact on the reproducibility of actuation. In this way, Expancel[®] was characterised in terms of particles' sizes to evaluate the presence of unwanted elements and possible variability.

All characterisations and models will be presented in Chapter 2 and 3.

Another point of interest is the investigation of alternative implementations of the composite in a miniaturised environment. Until now, the only heating system proposed was to use PCB copper tracks as heater. The only control was on the power dissipated in the resistors. Here, we want to demonstrate a way to control temperature directly instead of power, to allow a better control of the expansion. This will be treated in Chapter 4.

Finally, more complex systems are studied to determine the use of such material in diagnostic or medical devices. First, a device previously proposed was tested in automatised condition in order to assess its reproducibility in a stand-alone product. Then, a system testing coagulation was developed and tested. Chapter 5 will present this work.

All characterisation and application studies shall be able to determine the way in which such a material could be used. The industrial application of the material in the field of diagnostic and medical devices will be focused.

Characterisation of PDMS - Expancel[®] composite

Contents

2.1	Particles morphological study	19
2.1.1	Experimental conditions	19
2.1.2	Results and Discussion	19
2.1.3	Conclusion	22
2.2	Expansion profile as function of temperature	24
2.2.1	Experimental conditions	24
2.2.2	Results and Discussion	24
2.2.3	Conclusions	27
2.3	Young's modulus measurement	28
2.3.1	Experimental conditions	28
2.3.2	Results and Discussion	28
2.3.3	Summary	31
2.4	Zero expansion pressure analysis	32
2.4.1	Experimental conditions	32
2.4.2	Results and Discussion	33
2.4.3	Conclusions	35
2.5	Volumetric expansion ratio characterisation	36
2.5.1	Experimental conditions	36
2.5.2	Results and Discussion	37
2.5.3	Conclusions	40
2.6	Characterisation roundup	41

In this Chapter will be presented a characterisation of PDMS - Expancel[®] composite as a bulk material. The goal of such an investigation is to highlight the relevant properties of this material when it will be implemented in a microsystem.

Particles' analysis Expancel[®] was not developed with the purpose of microfluidic actuation. In this context, it is important to evaluate its purity and the potential impact on its expansion properties. Particles' sizes distribution will give data on presence of impurities and imaging morphological informations.

Expansion as function of temperature The impact of heating temperature on expansion ratio will be studied using Dynamical Mechanical Analysis (DMA). It will give information about optimal heating temperature and consequences of errors in temperature control.

Young's modulus Elasticity of both unexpanded and expanded states will be discussed. Impact of the volume of rigid beads within the matrix will also be investigated.

Zero expansion pressure analysis Actuating fluid through microfluidic channels requires pressure. This study will evaluate the upper limit of pressure provided by PDMS - Expancel[®] composite in the case of no volumetric expansion.

Expansion ratio The ability of the material to expand is its core property. It will rule the design of microsystems by defining the amount of fluid to be displaced. Its characterisation will be completed by analytical modelling in Chapter 3.

2.1 Particles morphological study

The Expancel® data sheet specifies a size of beads from 10 to 16 μm . To get a better view of this distribution a size analysis on the beads was performed. To have information about the morphology of the beads and thus on their expansion potential, Secondary Electron Microscopy (SEM) was used. Those data will also allow to evaluate the expansion reproducibility of the PDMS - Expancel® composite by detecting impurities in the raw material.

2.1.1 Experimental conditions

To analyse the size of the particles, a measurement was done using a Mastersizer 2000, Malvern Instruments, Malvern, UK. This system uses laser diffraction to analyse size distribution of particles in suspension. The powder was dispersed in water and then inserted in the apparatus reservoir. Expanded beads have a density close to the one of air. Thus, it is not possible to suspend them in water or in other liquid solvents to perform a comparable measurement. For this reason, the size distribution was studied only in the unexpanded state.

In order to evaluate the particle in expanded state, SEM was used to make a qualitative visual analysis. SEM images were taken using a XLF30-FEG (FEI, Hillsboro, USA) at the “Centre interdisciplinaire de microscopie électronique” at EPFL (CIME).

2.1.2 Results and Discussion

The results obtained from the particle size analysis are shown in Figure 2.1.

A first peak of the distribution is observed around 430 nm and a second one is present around 13 μm . Those values have been determined by fitting each peak to a gaussian function to find the peak location. On some measurements a smaller peak was seen between 30 and 100 μm .

The 30–100 μm peak is most probably due to aggregation of smaller particles (430 nm or 13 μm). Expancel® 820DU40 beads are quite hydrophobic and aggregates were observed in polar solution. Another source of large particles lies in the fabrication principle. Expancel® beads are manufactured using an emulsion process [44] making some elements imperfect. Some beads are merged together forming apparently bigger particles as shown in Figure 2.2.

2.1. Particles morphological study

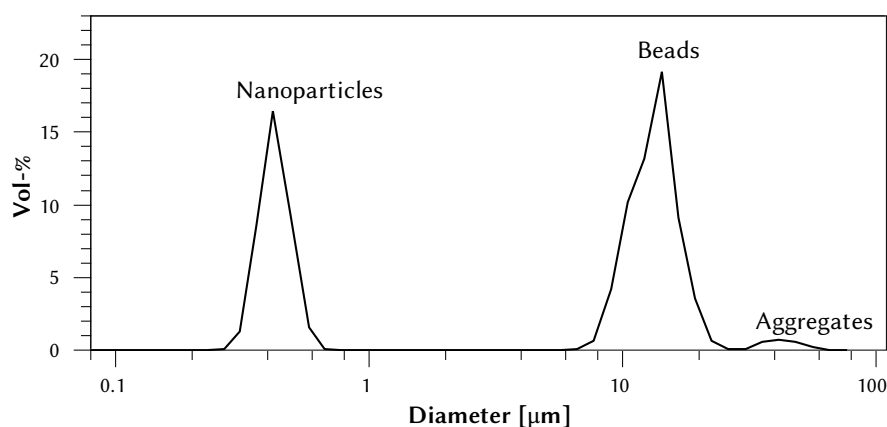


Figure 2.1 Typical particles' sizes distribution. A first mode is observed around 430 nm and a second one near 13 μm . In this figure, a third smaller mode is present between 30 and 100 μm .

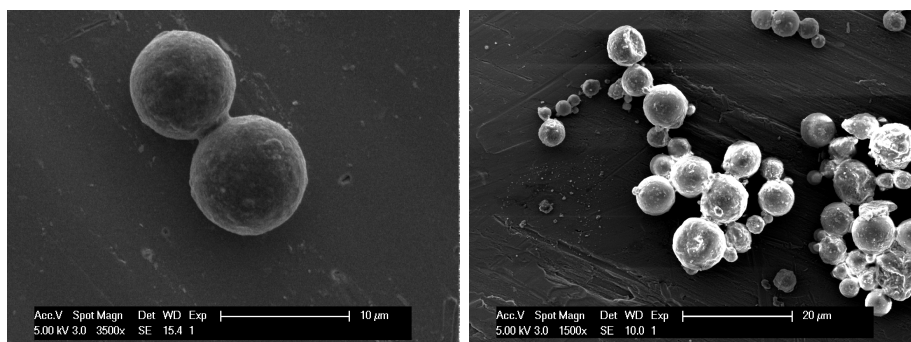


Figure 2.2 Expancel[®] particles. On the left, two particles have merged during the fabrication process to create a larger element. On the right lies an aggregate formed of single particles.

Deeper investigations have been made on 430 nm particles. By integrating the signal found in the graph of Figure 2.1, the proportion of smaller particles is shown to be around 40% in Figure 2.3.

SEM images of the beads reveal the actual presence of those smaller particles as shown in Figure 2.4. Representing an important volume of the product, it is important to investigate their contribution to expansion of the material. Indeed smaller particles have a tendency to sediment in powder of wide size distribution. It is quite difficult to maintain their proportion precisely, thus resulting in variable size distribution from one sample to another.

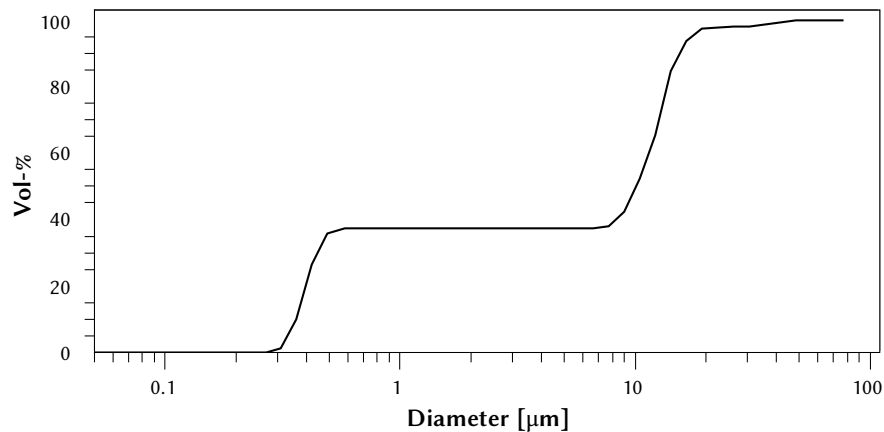


Figure 2.3 Integral of the beads' distribution. It shows that 40% of the overall volume are objects between 200 nm and 400 nm in diameter. Then 55 % of the volume are 10 µm to 20 µm diameter. The rest of the particles are between 30 and 100 µm.

Their morphology is variable, going from agglomerated spherical elements (Figure 2.4 (b)) to more angular shapes (Figure 2.4 (c)). They also have shown a high tendency to stick on larger beads (Figure 2.4 (d)).

They can be created by different phenomenon. They can be smaller droplets in the beads' fabrication emulsion or residue of fragmented larger particles. It is unsure if they have the capacity to expand like the standard-sized Expancel® beads. In the case of inactive small particles, this might greatly influence the expansion ratio of the PDMS - Expancel® composite. As their proportion is hard to control, they are a variable element in the proportion between shell composite and blowing agent. This material's properties greatly influence the expansion ratio of the composite, as will be discussed in Chapter 3. This is most probably the case of angular shaped particles. They might not be the product of polymerisation in an emulsion since droplets in an emulsion are rounded due to surface tension. The rounded particles may contain some blowing agent. On the other hand, their different size might make their constitution different than the one of bigger beads. Their expansion properties might thus be different.

Some refining techniques have been investigated, but did not give satisfactory results. The main solutions tested were filtration and sedimentation, but due to the nature of the beads' shell composite, smaller particles systematically aggregate to bigger ones unless sheer stress is applied. In future development, work needs to be done on surface tension of the beads in a solution to avoid such sticking, or on

2.1. Particles morphological study

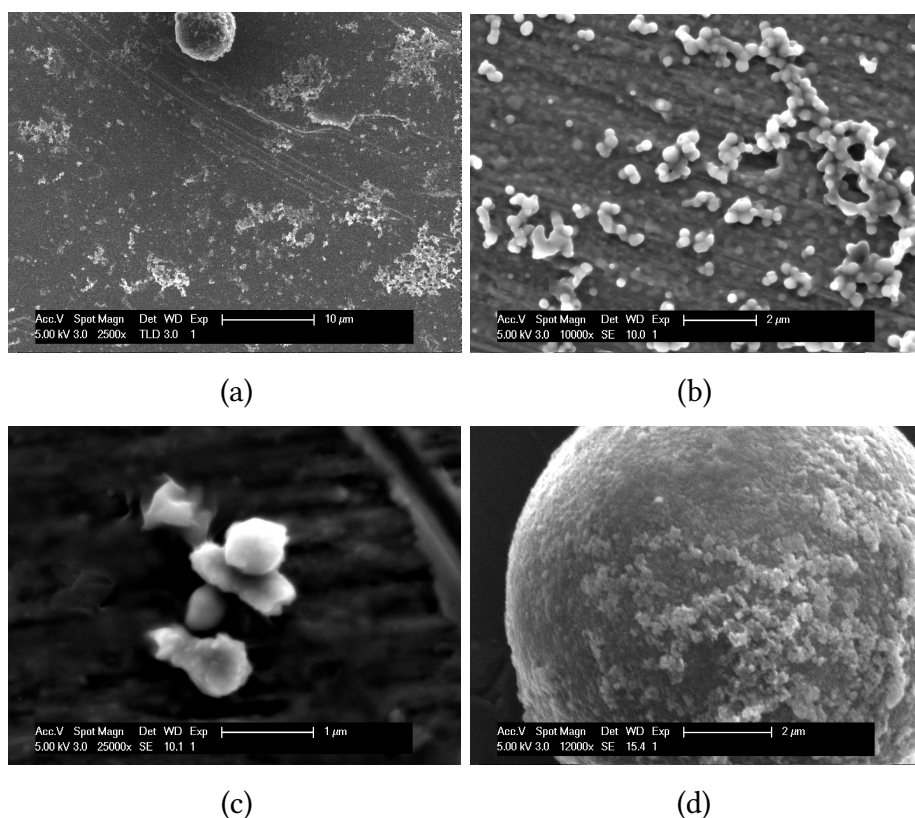


Figure 2.4 SEM images of Expancel® smaller particles. These particles are 50 to 100 times smaller than standard Expancel® particles (a). Various shapes have been observed. Some have round shapes (b) while other are more like flakes or nuggets (c). By observing standard Expancel® particles' surfaces, we notice that they seem to be covered with smaller ones forming a crust (d).

a system to continually applying shear stress on the solution and at the same time allowing sedimentation. Since those experiments were performed, Azko Nobel has developed a new version of this product, Expancel® 031 DUX 40, which is less subject to aggregation. This new product might make it possible to use the simple separation process proposed here.

2.1.3 Conclusion

In the datasheet of Expancel® provided by the manufacturer, [45] some properties are given with a huge variation, such as gas proportion (between 10 and 15 weight-%). This reflects the fact that Expancel® is not a very well controlled material in terms of bead size and purity. From our SEM study, the smaller elements of nanometric sizes may not expand like the other particles. Since their proportion is

Chapter 2. Characterisation of PDMS - Expancel[®] composite

hardly controllable, they might be the source of poor precision on gas proportion provided by the manufacturer. Separation methods tried in this work did not give sufficient results to homogenise the particles' sizes.

2.2. Expansion profile as function of temperature

2.2 Expansion profile as function of temperature

In order to determine the expansion temperature of the beads while encapsulated in PDMS, an experiment measuring the thickness of a composite sample as function of temperature was performed. The measurement was made using a DMA system allowing the measurement of the specimen thickness while enduring a temperature ramp. The temperature was raised from room temperature to expansion temperature at a very slow and controlled rate to allow an homogeneous temperature all over the sample. The normalised thickness of the sample represents the volumetric ratio of expanded beads since the sample undergoes an isotropic expansion.

2.2.1 Experimental conditions

This experiment was performed with a Dynamic Mechanical Analyser Q800, TA Instruments, New Castle, USA. The compression module in dynamical mode was used to determine the thickness of the sample. Samples were prepared as described in Appendix A.1 with standard curing process on a levelled surface. To be able to observe a larger deformation and thus reduce measurement noise, this measurement was done with a composite of 32.9 % volumetric Expancel[®] ratio. Samples were around 1 mm thick and 12 mm in diameter. The temperature ramp was set to begin at 50 °C and to end at 120 °C with a rate of 1 °C/min (2 N, 1 Hz). To reduce stick-and-slip, silicon oil was placed between the sample and the system plates.

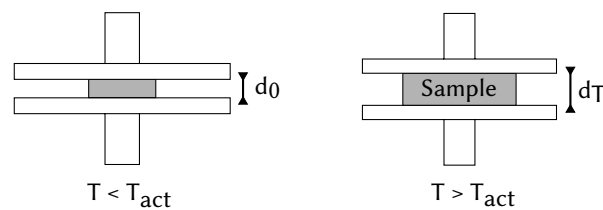


Figure 2.5 Measurement principle for determining the expansion of material as function of temperature. The thickness of the sample as function of temperature (d_T) is recorded while the temperature is raised from 50 °C to 120 °C. The initial thickness (d_0) is taken as reference to calculate the linear expansion ratio

2.2.2 Results and Discussion

The relation between thickness and temperature is represented in Figure 2.6.

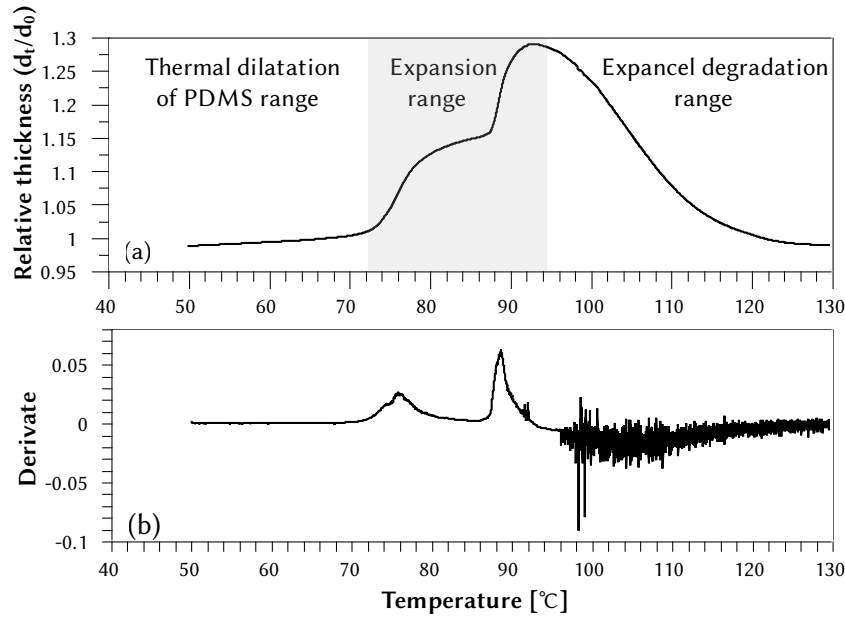


Figure 2.6 Evolution of thickness of the sample with temperature (a) and its derivative (b). The left of the graphs shows the thermal dilatation of PDMS due to the rise of temperature. From 70 °C onwards, a volumetric augmentation due to beads' expansion is observed. The expansion seems to occur in two phases separated by a plateau. Finally, above 92 °C beads degradation and/or explosion begins to occur.

Thermal dilatation

On the first part of the curve in Figure 2.6, a linear expansion of the sample can be observed. This is due to the thermal dilatation of the PDMS matrix. The thermal expansion coefficient of PDMS is given by Equation 2.1 [16], where T is the temperature:

$$\alpha(T) = 0.9 \cdot 10^{-3} + T \cdot 2.76 \cdot 10^{-7} + T^2 \cdot 10^{-10} \quad (2.1)$$

At 50 °C the theoretical thermal dilatation is $9.13 \cdot 10^{-4} \text{ K}^{-1}$. It was calculated on the 12 experiments performed by linear fitting between 50 and 65 °C. The mean was $8.8 \cdot 10^{-4} \text{ K}^{-1}$ with a standard deviation of 84 %. This huge variation makes it irrelevant to measure a thermal dilatation coefficient with this method. The non homogeneity of the composite and its roughness in the expanded state might explain such variations between measurements.

2.2. Expansion profile as function of temperature

Degradation of Expancel® beads

From 100 °C onwards, thickness decreases. The thermal degradation of the beads' shells results in the isobutane contained inside getting out. PDMS being permeable to gas, gas leakage cannot be prevented. The consequence of this loss of gas is the reduction of the overall volume since the PDMS is not under constraint any more and returns to its original shape. The high noise ratio observed in this part of the derivative is mainly due to stick-and-slip effect of the sample due to a loss in diameter and sticking to the surface of the apparatus.

Expansion of Expancel® beads

Figure 2.6 (a) represents the progression of thickness normalised to the original sample thickness. This analysis shows that the expansion does not take place at a very precise temperature, but occurs in a range between 70 and 90 °C. Since the polymer used for the shell of the beads does not have a precise glass transition temperature, the beads have different expansion temperatures. At 90 °C, more than 95 % of the final thickness is reached.

Expansion distribution

Another interesting feature is the presence of a plateau in the thickness progression. By studying the derivative of the thickness curve as shown in Figure 2.6 (b), it appears that two steps of expansion take place. It has been observed on almost all performed experiments and seems to always occur around 80°C, but the amount expanded before the plateau varies from one experiment to another. This two steps expansion might be correlated to the bimodal distribution of bead size observed in Section 2.1. If nanoparticles are expandable, their expansion temperature might be different than the one of microparticles explaining such a plateau. Another explanation would be the composition of the shell of the beads. The fabrication process might induce different “kinds” of beads resulting in this bimodal distribution. More investigations on the shell polymer properties are needed to explain this phenomenon precisely.

2.2.3 Conclusions

The main part of the expansion occurs between 70 °C and 90 °C. After 100-110 °C the beads degrade and the composite shrinks. In applications of such material, the temperature should be controlled to stay between 90 °C and 100 °C to obtain the highest expansion ratio. At a lower temperature, not all the beads will expand, and above, the composite will deteriorate. The expansion was also observed to be irregular. It stops around 80 °C. No reliable explanations could be given with the presented characterisation, but we suspect the inhomogeneities in beads' properties (size or composition) to be the source of this phenomenon.

2.3. Young's modulus measurement

2.3 Young's modulus measurement

2.3.1 Experimental conditions

DMA was used to determine Young's modulus of composites of different Expancel[®] proportions. A dynamical mechanical analyser Q800, TA Instruments, New Castle, USA was used. The essay was performed in traction and samples were prepared as described in Appendix A.1 with crosslinking on a flat surface to have planar samples. Sample dimensions were in the range of 1x5x10 mm³. Measurement was done at a constant temperature and at a frequency of 1Hz. Several "series" of samples (samples whose preparation and crosslinking where done simultaneously) were prepared.

2.3.2 Results and Discussion

Measurements of Young's modulus of the composite for different proportions are reported in Figure 2.7.

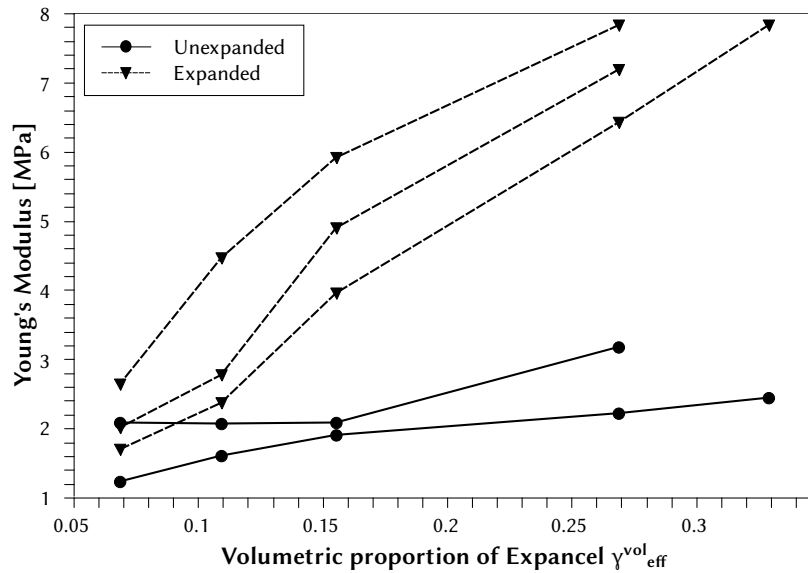


Figure 2.7 Young's modulus of the composite as a function of the proportion of Expancel[®] before and after expansion. Plain curves represent unexpanded samples and dashed curves expanded ones. As expected, Young's modulus rises with the proportion of rigid particles inside the material.

In those results, the Young's modulus of expanded composite is higher than the Young's modulus of unexpanded one. But since the expanded composite contains bigger beads, the effective volumetric ratio of hard particles inside the composite is much higher than in its unexpanded state. A quantitative analysis can be made by using the density of the expanded composite. The effective volume ratio of beads in the expanded composite, γ_{eff}^{vol} , is defined as:

$$\begin{aligned}\gamma_{eff}^{vol} &= \frac{V_{Exp}}{V_{tot}} \\ &= \frac{V_{tot} - V_{PDMS}}{V_{tot}} = 1 - \frac{V_{PDMS}}{V_{tot}}\end{aligned}\quad (2.2)$$

V_{tot} is the volume of the expanded sample, V_{Exp} the volume of beads inside the expanded sample, and V_{PDMS} the volume of PDMS in it. This last value is dependant on the initial proportion of Expancel[®] in the mix. V_{tot} depends on the mass of the sample, which does not change over expansion, and the density of the expanded sample.

$$\begin{aligned}V_{PDMS} &= \frac{m_{PDMS}}{\rho_{PDMS}} \\ V_{tot} &= \frac{m_{Exp} + m_{PDMS}}{\rho_{Exp}}\end{aligned}\quad (2.3)$$

Here, ρ_{Exp} is the measured density of expanded composite, m_{Exp} the mass of Expancel[®] beads in the mix, m_{PDMS} the mass of PDMS, and ρ_{PDMS} the density of PDMS.

Giving finally the beads' effective volumetric ratio:

$$\gamma_{eff}^{vol} = 1 - \frac{m_{PDMS}}{\rho_{PDMS}} \frac{\rho_{Exp}}{m_{Exp} + m_{PDMS}}\quad (2.4)$$

Density was previously measured as detailed in Section 2.5. Numerical values used here are shown on Table 2.1.

By applying the effective volume ratio of beads to the previously presented data, a new graph shown of Figure 2.8 is obtained.

This result shows that Young's modulus seems to be linearly dependant on the volumetric proportion of beads even if absolute variations seem to apply to different series of PDMS. Young's modulus of PDMS is very variable [99–101] depending on the preparation and the crosslinking, probably explaining the reason

2.3. Young's modulus measurement

PDMS:Expancel [®] ratio	Unexpanded density [kg/l]	Expanded density [kg/l]
10:1	1.14	1.26
6:1	1.13	1.12
4:1	1.15	0.89
2:1	1.17	0.47
1.5:1	1.26	0.37

Table 2.1 Densities of different ratio composites for expanded and unexpanded states.

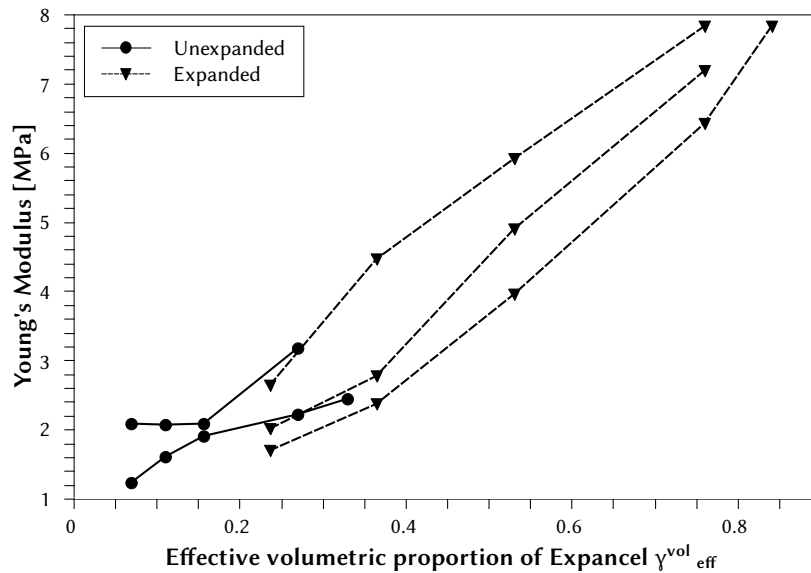


Figure 2.8 Young's modulus of the composite as a function of the effective proportion of Expancel[®] before and after expansion. Plain curves represent unexpanded samples and dashed curves expanded ones. Young's modulus seems to be linearly dependant on the volumetric proportion of beads even if absolute variations apparently apply to different series of PDMS.

of such variations as the slope of the curves varies less. Indeed, This slope is primarily affected by the variation of proportion of beads in the mix which is a more controllable parameter of the composite preparation.

2.3.3 Summary

PDMS - Expancel[®] Young's modulus linearly depends on volumetric proportion of hard particles in the mix. In this way, we can think that no interaction between beads and matrix altering mechanical properties of the two parts occurs. Mechanically, the composite can be seen as a linear combination of its two components. Moreover, the expanded state shows that the deformation of PDMS does not change its Young's modulus, confirming that its elastomer properties are conserved in the composite. Finally, large variations of absolute values of elasticity show the impact of preparation and curing of PDMS on its mechanical properties. It highlights the need of a precisely controlled preparation protocol to obtain a reliable Young's modulus.

2.4. Zero expansion pressure analysis

2.4 Zero expansion pressure analysis

To evaluate the possibilities of PDMS - Expancel[®] composite to actuate liquids under the effect of a counter pressure, the pressure provided by the composite when confined was studied. This gives the upper limit on the counter pressure the system might ever provide. Here will be described a methodology as well as some points the reader must be aware of to achieve such a characterisation.

2.4.1 Experimental conditions

A thermalised base and piston were mounted on a force displacement measurement machine (Z010, Zwick GmbH & Co. KG, Ulm, DE with 10 kN force sensor). This allows us to expose the sample to a temperature between 80 and 90 °C, which is the optimal expansion temperature ¹. A cylindrical sample of the material (50 mm in diameter and 4 mm in height) was placed in a sample holder positioned under the piston that was moved until touching the surface with a force of 25N. The experiment was then completed by recording the force as a function of time during material expansion while blocking the movement of the machine's crossbeam. The experiment's duration was set to 500 s, which was enough to insure the nearly complete expansion of the sample. A study of the dependence to volumetric beads' proportion was performed for the same values than the expansion ratio analysis.

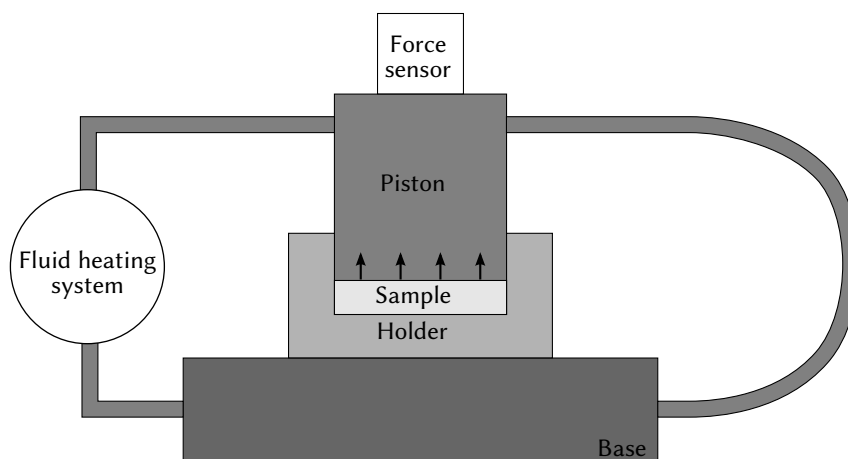


Figure 2.9 Thermalisation and measurement system for force-displacement study

¹see Section 2.2

2.4.2 Results and Discussion

The results of the performed characterisation are presented in Figure 2.10. The first observation that can be made, is that for higher proportions of beads, the pressure provided by the sample goes around 14 bars.

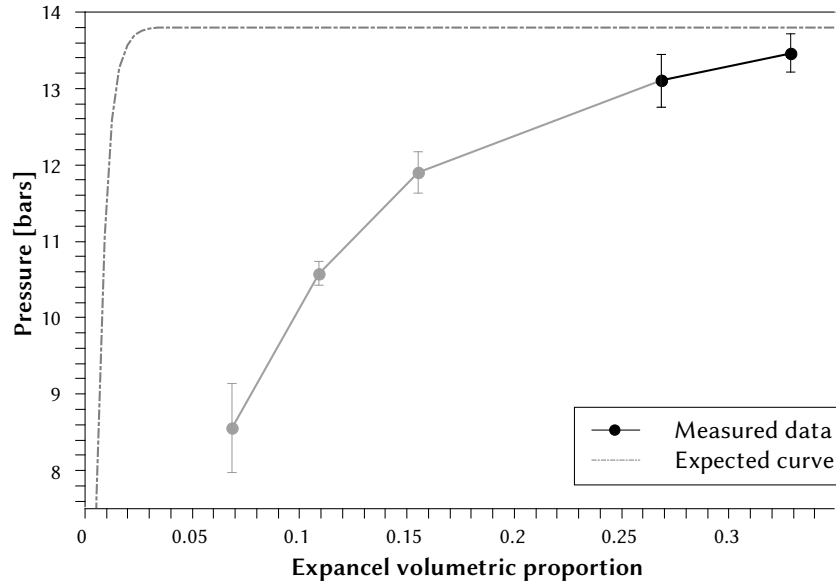


Figure 2.10 Measured pressure after temperature uniformity as function of beads' proportion. Points represent the mean and error bars the standard deviation on three to five measurements. Due to experimental artefacts, the lower proportion points are not accurate. The parasitic expansion lowers the measured value because all the liquid in the beads might be evaporated and the beads' internal pressure drop below the vapour pressure. We expected a curve looking like the dashed one.

Vapour pressure of isobutane is given by equation 2.5, called Antoine's equation [102].

$$\log_{10}(p) = A - \frac{B}{t + C} \quad (2.5)$$

By fitting the handbook data [103] with this equation, one obtains 13.4 bars at 80 °C and 16.2 bars at 90 °C as shown in Figure 2.11. As expected, we can conclude that the ultimate limitation of the composite is defined by the vapour pressure of its blowing agent.

The results for composites with a low proportion of beads (0.06 to 0.15) seem more questionable. As long as enough beads are present in the composite to cover

2.4. Zero expansion pressure analysis

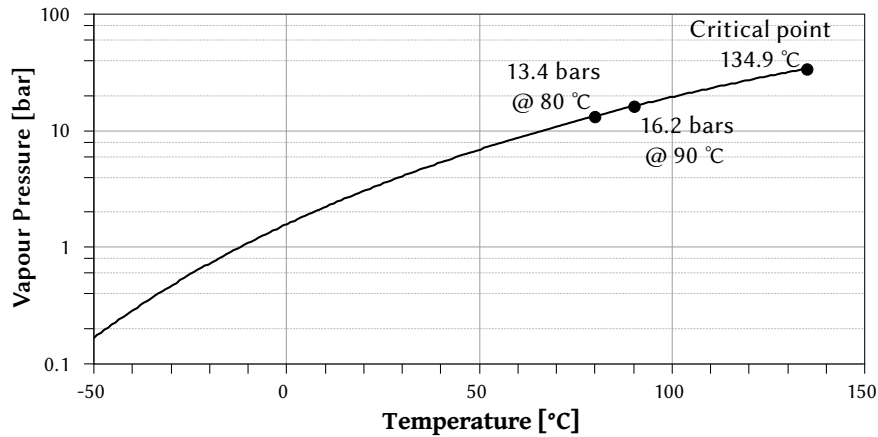


Figure 2.11 Vapour pressure of isobutane in function of temperature obtained by fitting the handbook data [103] with Antoine's equation. In this way, vapour pressure is 13.4 bars at 80 °C and 16.2 bars at 90 °C

the whole sample surface, the pressure given by the system should not drop, unless the beads expand effectively to the point where they are no more filled with liquid.

In the lower proportion, a pressure drop is observed. This might be a measurement artefact. Indeed, if the PDMS is considered incompressible, as long as a single layer of beads covering the whole surface is present in the composite, the provided pressure shall not drop. In the lowest beads' proportion composite tested (6.85%), the amount of beads in a 5 mm thick sample could form a 350 μm thick film. This corresponds to at least 35 layers of 10 μm beads. Thus, this amount of blowing material should not allow the pressure drop observed. With this hypothesis of incompressible PDMS, the pressure should decrease for beads' proportions lower than 0.2%. This behaviour is illustrated by the "Expected curve" of Figure 2.10.

This effect is setup-dependant and is due to the force sensor compliance, which still allows the piston to move even once the machine stops moving. The available amount of gas expanding in the sample is proportional to the volumetric proportion of beads. Thus, if less gas is available, the deformation threshold before the pressure drops will be lower, due to the complete evaporation of the blowing agent.

Such error does not permit to make a complete analysis on the pressure provided by such material. To prevent this artefact, the system must correct the position of the machine's crossbeam to keep the piston's position fixed. This system would enable the knowledge of the precise proportion of beads at which the pressure would drop.

As previously discussed, the pressure in a micro system environment is typically of a few bars². Those measurements prove that despite the error made by the setup, the pressure provided by a composite of lower proportion provides more than 8 bars, making them suitable to actuate liquids in microsystems.

It can also be observed that, once all the blowing agent is evaporated, the pressure provided drops. This follows the perfect gas law giving a constant product of pressure and volume for isothermal gas. This effect is more visible in lower beads' proportion composite where the amount of liquid to evaporate before seeing the pressure drop is lower.

2.4.3 Conclusions

No quantitative data could be derived from this experiment, but a solution to produce more reliable results was proposed. On the other hand, it was observed that the pressure provided by the composite drops as it expands and as all the blowing agent is evaporated. This effect is more present in lower beads' proportion composite where the amount of blowing agent is lower. Moreover, it has been deduced by former experiments, that even a low Expancel[®] proportion composite seems suitable for microfluidic actuation, since they provide pressures higher than the ones generally observed in such systems.

²See Section 2.5

2.5 Volumetric expansion ratio characterisation

This section presents a characterisation of PDMS - Expancel® expansion ratio, or ratio between expanded and unexpanded volume. This information was gathered by expanding the composite and measuring its density before and after the expansion. To be able to plan this expansion under a counter pressure, the expansion was done under a different pressure. Those data will provide a base for the understanding of the expansion phenomenon.

2.5.1 Experimental conditions

Sample preparation and expansion

Samples were prepared as described in Appendix A.1. They were then cut into small pieces of about $1\text{-}2\text{ mm}^3$. Samples were expanded using a pressurised cavity in an oven as shown in Figure 2.12. A thermocouple was sealed inside the cavity and a pressure meter placed on the line between the cavity and the pressure source, to permit the monitoring of the temperature and pressure near the sample during the expansion. The pressure measurement was done using a ISE8H (SMC Corporation, Tokyo, JP) digital pressure meter and temperature was measured with a K junction whose signal was amplified with an Entran PS-30A amplifier. Final signals were recorded with a NI-6008 acquisition card from National Instruments, Austin, USA and a custom LabView program.

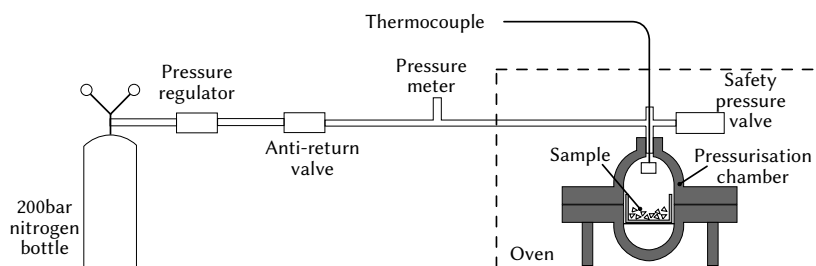


Figure 2.12 Schematic of setup used to expand the composite under controlled pressure.

To prevent leakage due to high pressure, the system was constantly connected to a gas bottle to compensate the pressure loss.

The pressure source was a nitrogen bottle equipped with a pressure reducer. For security purposes, an anti-return valve was mounted at the output of the pressure reducer.

Sample measurement

To determine the expansion ratio, a part of each sample of composite was conserved unexpanded as reference. Both expanded and unexpanded samples had their density measured and the ratio of those values gave the expansion ratio used in further analyses.

All density measurements were performed using a 5 ml pycnometer bottle and ethanol. The detailed experiment protocol is provided in Appendix A.3.

Each sample density used in this study was measured three times. More measurements have been performed on samples with standard deviation of density greater than 2 % to remove erroneous data points.

2.5.2 Results and Discussion

Volumetric expansion ratio: Expancel[®] proportion study

The tested proportions were based on weight ratio between base PDMS and Expancel[®]. Table 2.2 shows correspondence between ratios, mass Expancel[®] proportions and volumetric Expancel[®] proportions. In following results' analyses, volumetric ratio were used except when stated otherwise.

PDMS : Expancel [®] ratio	Expancel [®] mass ratio	Expancel [®] volumetric ratio
10:1	8.33%	6.85%
6:1	13.16%	10.91%
4:1	18.52%	15.52%
2:1	31.25%	26.87%
1.5:1	37.74%	32.88%

Table 2.2 Correspondence between PDMS base : Expancel[®] ratio, weight and volumetric percentage of Expancel[®] in the mix at unexpanded state.

The range of studied proportions of Expancel[®] beads in the composite goes from 6.85 %-vol to 32.88 %-vol. This range is ultimately limited by the random loose pack

2.5. Volumetric expansion ratio characterisation

filling, with the hypothesis of equal diameter sphere, which stands at around 55 % [104]. Such a proportion was not attained due to technological limits like mix high viscosity making homogenisation and moulding nearly impossible.

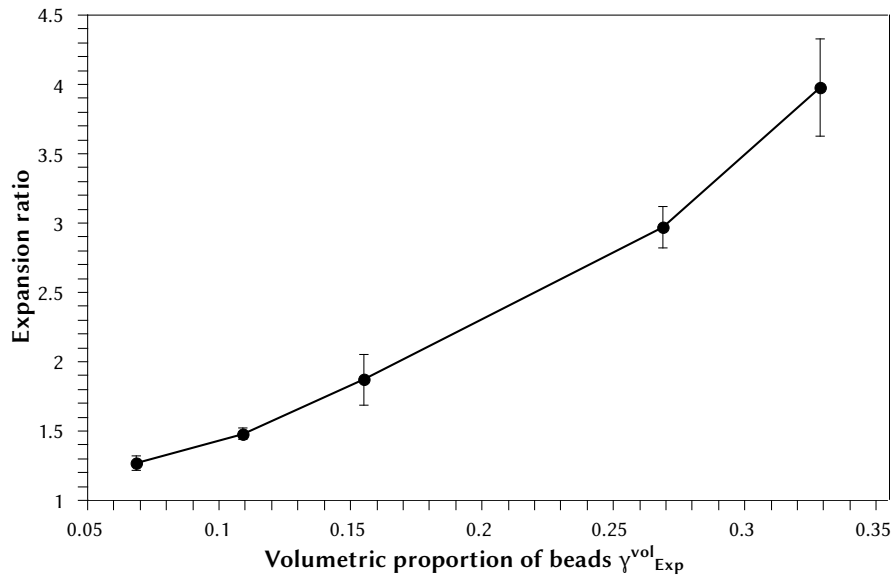


Figure 2.13 Expansion ratio versus volumetric proportion. Each point is the mean of four to five tested samples. The error bars refer to the standard deviation on the multiple experiments performed. The effect is not linear³. Experimental variation grows with the proportion of beads implying varying expansion properties of the latter.

Figure 2.13 shows the relationship between volumetric proportion and expansion ratio. A non linear growing behaviour can be observed. It will be more deeply studied with the development of an analytical model in Section 3.2.

The experimental variation observed on those measurements are more important on higher proportions than on lower ones. The variation may thus reside in the Expancel[®] beads, since they are the expanding part of the composite, PDMS's volume staying constant.

Two main imprecision factors are present: the mixing ratio, the gas content and the Young's modulus. The Young's modulus may vary from one preparation to another as described in Section 2.3. But this variation is present in the whole proportion range. The impact of this parameter will be studied in Chapter 3. The

³See Section 3.2 for more detailed explanations and modelling

mixing ratio imprecision was lowered as much as possible by mixing large quantities of composite to reduce the weighing error. Moreover, the relative error due to weighing is more important on lower proportion of beads. On the other hand, the gas content is highly dependent on the beads' quality which is out of control of the operator. In the datasheet, no precise data is provided and only a range between 10 and 15 % of gas content is given. Furthermore, as discussed in Section 2.1, the smaller particles probably have different expansion properties than the bigger ones. Normally, their weight is taken into account in the given data. But their proportion might change from one mix to another depending on sedimentation of smaller particles during storage and transportation. It is thus expected that this variation might be reduced by controlling Expancel[®] composition more precisely.

Volumetric expansion ratio: pressure-dependant study

In order to know the effect of pressure on expansion ratio, an experiment where a pressure is applied on the polymer during its expansion was performed. The results are shown in Figure 2.14.

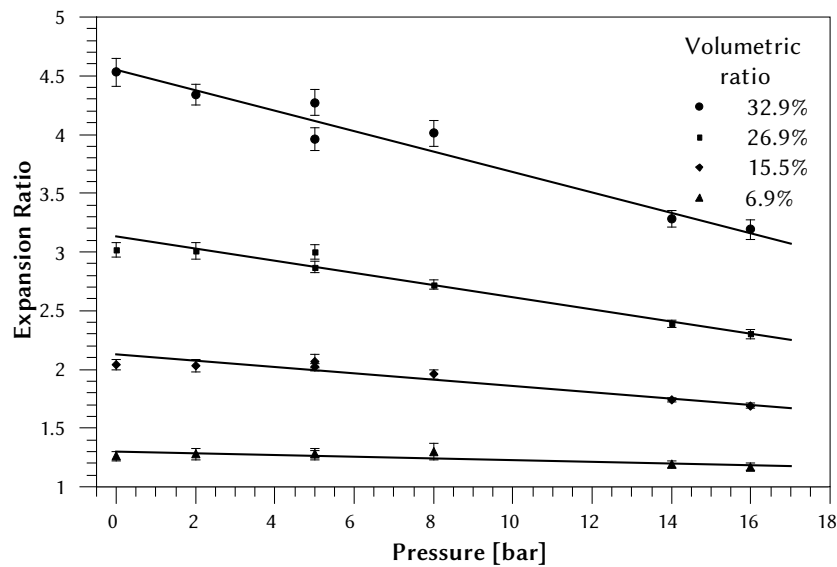


Figure 2.14 Expansion ratio of PDMS - Expancel[®] composite as a function of external pressure. Each point corresponds to an expanded sample. The value is the mean as the error bars correspond to the standard deviation on three density measurements performed on each sample. The expansion ratio decreases in a linear manner as the pressure rises.

2.5. Volumetric expansion ratio characterisation

The dependency of expansion ratio on Expancel[®] proportion is, as expected, still present. The expansion ratio also decreases in a linear manner with counter pressure. The decreasing slope of the expansion ratio as pressure rises is more important for higher beads' proportion.

When designing a system based on PDMS - Expancel[®], two factors can be modified to reach the desired volume displacement: beads' proportion and thickness of the composite layer. Higher beads' proportion composites allow to have thinner layers, but in case of a high counter pressure, the expansion will vary more than for composites with lower beads' proportion. This means that systems needing to actuate liquid in a large range of pressure might require lower beads' proportion and thicker composite layer in order to have less variations on the expansion ratio during their use.

In a microfluidic environment, typical pressures are of a few bars. For example, flowing a liquid through a 30x30 μm channel with a length of 10 mm at a flow rate of 1 $\mu\text{l/s}$ requires around 4 bars [105]. From the presented measurements, the counter pressure in microsystems should only slightly affect the expansion ratio of the material. This shall allow the use of such material to actuate liquid efficiently even through small channels where required pressures are higher than for larger ones.

2.5.3 Conclusions

As expected, the expansion ratio grows with the proportion of beads. The system is sensitive to pressure: expansion diminishes as pressure rises. For lower beads' proportion, the diminution of expansion is less important than for higher ones. At pressures typically present in microsystems, the expansion ratio of the composite still allows a high enough volume displacement to actuate liquids efficiently.

Since composites with lower beads' proportion are less dependant to pressure, for systems facing a large range of pressures, it might become interesting to decrease the proportion of beads in the composite. In this case, the expansion ratio loss needs to be compensated by creating thicker layer of composite in order to get the same volume displacement.

Experimental variations increase in the same way. Thus, the reliability of the system is limited by the homogeneity of beads, and a reliable expansion ratio shall be attained only by refining the beads in size and composition.

2.6 Characterisation roundup

The bulk Expancel® as well as the PDMS-Expancel® composite characterisations have given us an insight on the advantages and weaknesses of this material as well as information on its implementation.

From DMA analysis, an optimal activation temperature of 90°C has been determined. Young's modulus analysis gave us confirmation of the linear dependence on the beads' volumetric proportion and the consequent limitation of this proportion to allow the forming by injection or moulding which are the technology which were used in this study⁴.

Expansion ratio and force analysis methodology were developed. The expansion ratio has been characterised in terms of Expancel® proportion and counter pressure. Typical expansion ratios are between 1.1 and 4 depending on beads' proportion and counter pressure. Modelling of expansion phenomena will be presented in Chapter 3. No direct quantitative data could be extracted from force displacement analysis, but intermediate results show a pressure high enough for microfluidic actuation for all tested composites. Moreover, the highest pressure recorded is close to the vapour pressure of the blowing agent contained inside the beads.

Expancel® is a large-scale manufactured product and has very varying properties such as gas proportion. PDMS suffers from varying Young's modulus depending on the crosslinking process. Those changing properties of each component result in disparity of the composite's functional attributes such as expansion ratio. The impact of these imperfections and thus the potential improvements will also be studied in Chapter 3.

Investigations on pure Expancel® could be carried out in order to define the exact impact of smaller particles on expansion ratio. For example, Focus Ion Beam (FIB) could be used on those small particles to see if they are hollow and contain gas or not. Also, glass phase transition of the polymer shell could be more deeply investigated to explain the two steps expansion of the composite. This could be done by studying heat flux with Differential Scanning Calorimetry (DSC) which allows us to determine phase transitions. All this information could give hints on solutions to refine the product or to modify its fabrication process to get less impurities and have a better reproducibility.

⁴See Appendix A.1

2.6. *Characterisation roundup*

If dynamical and geometrical numerical modelling of expansion is required, thermal parameters (specific heat and thermal conductivity) of the composite material are required. Both specific heat and thermal conductivity can be measured using DSC [106, 107].

Contents

3.1	Expansion of a single Expancel [®] bead	44
3.2	Model of expansion for a PDMS coated bead	46
3.2.1	Hypothesis	46
3.2.2	Equations and their resolution	47
3.3	Beads' internal pressure after expansion	54
3.4	Modelling roundup	58

The goal of this chapter is to understand the phenomenon taking place during the expansion of the PDMS - Expancel[®] composite. Various phenomena could be studied on this material such as local deformations inside the material, or gas permeability of the Expancel[®] membrane. In this work, the focus will be on the realisation of a model for the expansion of the material and its comparison with the results of the previously presented characterisation. The reference variable evaluated was the ratio of final over initial volume of the material. It will be later referred as “expansion ratio”.

3.1. Expansion of a single Expancel[®] bead

3.1 Expansion of a single Expancel[®] bead

From the datasheet, Expancel[®] 820 DU 40 used in this work is composed of 10 to 15% of blowing agent (isobutane). A mass ratio of 12.5% of isobutane corresponds to a volumetric ratio of 25% as shown in Equation 3.2 with numerical values from Table 3.1.

$$\gamma_{iso}^v = \frac{V_{iso}}{V_{tot}^{Exp}} = \frac{\frac{\gamma_{iso}^m}{\rho_{liq}}}{\frac{1}{\rho_{Exp}}} = \gamma_{iso}^m \frac{\rho_{Exp}}{\rho_{liq}} = 0.25 \quad (3.1)$$

$$\Rightarrow \gamma_{shell}^v = 1 - \gamma_{iso}^v = 0.75 \quad (3.2)$$

The mass of Expancel[®] is considered 1 and γ_{iso}^v is the volumetric proportion of isobutane in beads, γ_{shell}^v the volumetric proportion of copolymer shell in beads, γ_{iso}^m the mass proportion of isobutane, V_{iso} the volume of isobutane, V_{tot}^{Exp} the total volume of a bead, ρ_{liq} the density of liquid isobutane, ρ_{Exp} the density of Expancel[®]. Later, ρ_{gas} , the density of gaseous blowing agent will also be used.

As explained in Section 1.1, the blowing agent is in its liquid phase and, when the shell undergoes a glass phase transition under the action of heat, the liquid evaporates. The phase transition of isobutane heated at 70 °C results in a $\frac{\rho_{liq}}{\rho_{gas}}=281$ times volume increase. 70 °C is the temperature at which the beads begin to expand, as discussed in Section 2.2, but also the lowest temperature at which the beads will harden when cooled down. Below this temperature, the volume of the composite will remain constant.

ρ_{Exp} [$\frac{kg}{m^3}$]	γ_{iso}^m [%]	ρ_{liq} [$\frac{kg}{m^3}$]	ρ_{gas} [$\frac{kg}{m^3}$]
1200 [45]	10-15 [45]	593 [108]	2.11 [108]

Table 3.1 Numerical values for the variables used in the determination of the expansion ratio Γ_{Exp} .

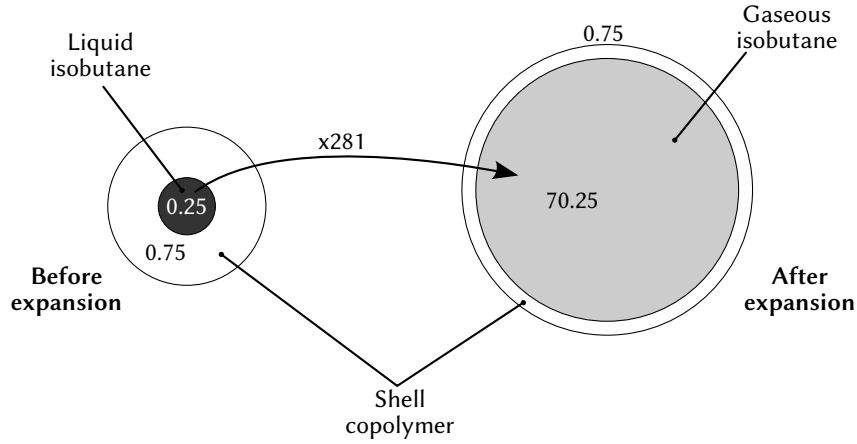


Figure 3.1 Expansion of a single Expancel® bead with a blowing agent mass ratio of 12.5 %. If the volume of a bead is considered 1 before expansion, the volume of liquid isobutane is 0.25,0 and the volume of the shell 0.75. When evaporating at atmospheric pressure, the isobuane expands 281 times to get a volume of 70.25. Thus, the overall expansion ratio, Γ_{Exp} should be 71. Since the data provided by the manufacturer gives an expansion ratio around 40, the effect of the shell is not negligible and results in pressure inside the beads in the order of magnitude of 0.8 bar.

In this way, the global volume expansion of a single Expancel® bead is linearly dependant on the proportion of gas in Expancel® as shown in Figure 3.1 and Equation 3.3. The numerical data in Table 3.1 were used.

$$\Gamma_{Exp} = \frac{V_{fin}^{Exp}}{V_{ini}^{Exp}} = \frac{\gamma_{shell}^v + \gamma_{iso}^v \frac{\rho_{liq}}{\rho_{gas}}}{\gamma_{shell}^v + \gamma_{iso}^v} \quad (3.3)$$

$$= \frac{(1 - \gamma_{iso}^m \frac{\rho_{Exp}}{\rho_{liq}}) + \gamma_{iso}^m \frac{\rho_{Exp}}{\rho_{liq}} \frac{\rho_{liq}}{\rho_{gas}}}{1} = 71$$

Theoretically, Γ_{Exp} is 52 for a mass ratio of 10 % and 86 for a mass ratio of isobutane of 15 %. In the data sheet provided by the manufacturer, the expansion ratio can go up to 40. One possible reason for this value lower than calculated is that the pressure induced by the shell prevents the gas from plainly expanding, maintaining it at a pressure which can be calculated to be between 0.3 and 1.15 bars.

3.2 Model of expansion for a PDMS coated bead

In order to model expansion of PDMS - Expancel[®] composite, two phenomena must be taken into account: (a) the evaporation of the blowing agent after which the gas will follow the perfect gas law and (b) the effect of PDMS preventing gas from expanding to atmospheric pressure because its deformation requires energy.

The presented model will represent the composite as a single bead coated with a layer of PDMS as shown in Figure 3.2. The radius of the beads and their coats correspond to the beads and matrix proportion in the composite. This representation has been used on several occasions in dynamical modelling of bubble formation, for example in foams expansion [109].

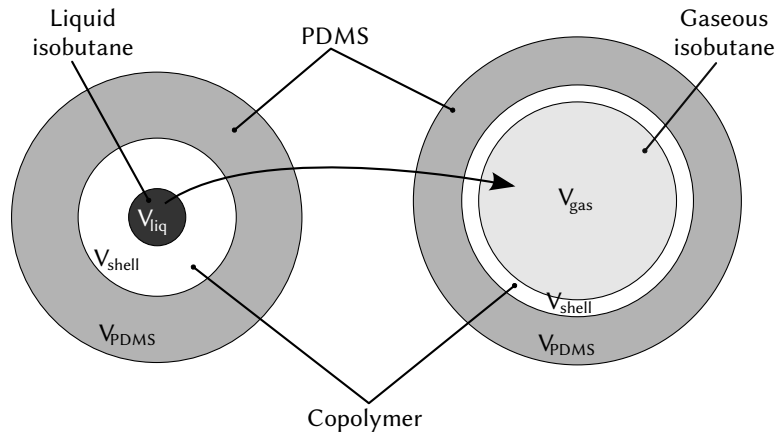


Figure 3.2 Expansion of a single Expancel[®] bead coated with a PDMS volume corresponding to proportion of beads and PDMS in the modelled composite

3.2.1 Hypothesis

The model chosen is a single bead coated with a layer of PDMS corresponding to the beads' proportion in composite. It will be assumed that this bead and its PDMS have the same expansion properties than the bulk material.

We will consider the PDMS and the shell incompressible. Thus, their volume will be constant before and after expansion.

Another effect happening during expansion is the beads' deformation due to their presence near other expanding beads. Figure 3.3 illustrates this effect. In this model, it is neglected as the whole composite is represented by a single bead. But

since PDMS is an elastomer and the blowing agent becomes gaseous and can take any shape, it should be minimal.

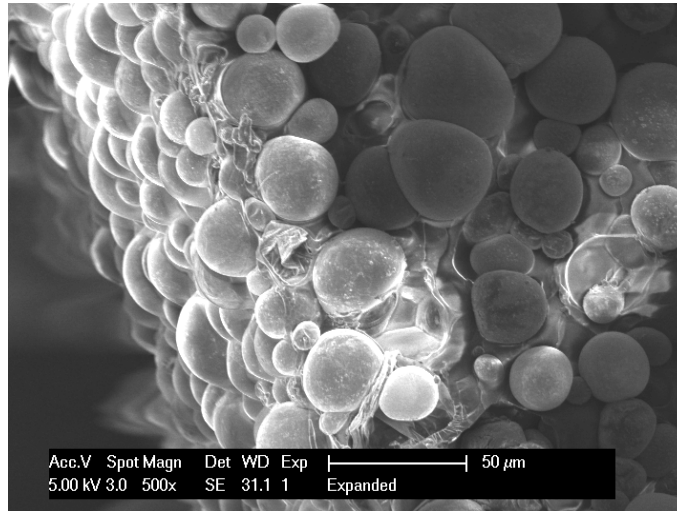


Figure 3.3 PDMS - Expancel[®] composite after expansion imaged with SEM. It can be seen that because of high beads' proportion, beads lose their spherical shape to accommodate each other's space.

As it will also be stated in Section 3.3, the shell volume remains constant as the blowing agent expands several tens of times. Thus, the thickness of the shell in the expanded state is neglected.

To be able to apply the perfect gas law, it must be ensured that all the gas has been evaporated at the end of the expansion. From calculations performed in Section 3.3, it is the case, even if composites with lower beads' proportions are very close to this limit. It was also considered that all the expansion occurs at 70 °C from where the shell hardens again and fixes the final volume. Thermal dilatation of different elements was neglected.

3.2.2 Equations and their resolution

The resolution of the model is done by calculating the deformation of the PDMS hollow sphere due to an internal pressure using Roark's formulas [110] and comparing it to the relation between pressure and volume of gas given by the perfect gas law. Figure 3.4 gives a schematic view of the situation.

3.2. Model of expansion for a PDMS coated bead

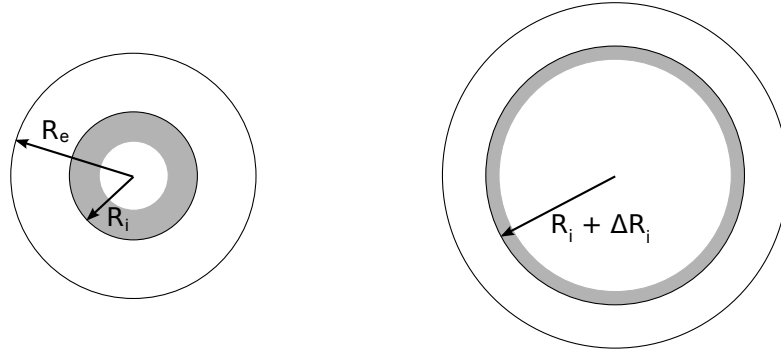


Figure 3.4 Representation of a bead coated with PDMS before and after expansion. The bead's shell is neglected in the internal radius, R_i , which determines the place where the force is applied.

This model tries to determine Γ , the expansion ratio of the PDMS - Expancel[®] composite as a function of the volumetric proportion of beads in the composite, γ_{Exp}^v . This value is the ratio between the final and the initial volume:

$$\Gamma = \frac{V_{fin}}{V_{ini}} \quad (3.4)$$

Figure 3.2 allows visualising the different elements of the initial and final volumes V_{ini} and V_{fin} :

$$\begin{aligned} V_{ini} &= V_{liq} + V_{shell} + V_{PDMS} \\ V_{fin} &= V_{gas} + V_{shell} + V_{PDMS} \end{aligned} \quad (3.5)$$

The sum of the volume of the liquid isobutane and of the shell, V_{liq} and V_{shell} is V_{Exp} the volume of a single bead. This volume is calculated by knowing the external radius of beads which has been measured to be $6.5 \mu\text{m}$ in Section 2.1.

$$\begin{aligned} V_{Exp} &= V_{liq} + V_{shell} \\ &= \frac{4}{3}\pi R_i^3 \end{aligned} \quad (3.6)$$

The proportion of blowing agent in Expancel[®], γ_{iso}^m , the density of Expancel[®], ρ_{Exp} , are also provided by the manufacturer [45]. The density of liquid isobutane, ρ_{liq} , is also known [108]. From those data, V_{liq} and V_{shell} can be calculated.

$$m_{iso} = \gamma_{iso}^m m_{Exp} = \gamma_{iso}^m V_{Exp} \rho_{Exp} = \gamma_{iso}^m \frac{4}{3} \pi R_i^3 \rho_{Exp} \quad (3.7)$$

$$V_{liq} = \frac{m_{iso}}{\rho_{liq}} = \frac{\gamma_{iso}^m \frac{4}{3} \pi R_i^3 \rho_{Exp}}{\rho_{liq}} \quad (3.8)$$

$$V_{shell} = V_{Exp} - V_{liq} = \frac{4}{3} \pi R_i^3 - \frac{\gamma_{iso}^m \frac{4}{3} \pi R_i^3 \rho_{Exp}}{\rho_{liq}} = \frac{4}{3} \pi R_i^3 \left(1 - \gamma_{iso}^m \frac{\rho_{Exp}}{\rho_{liq}}\right) \quad (3.9)$$

To have a good representation of the studied composite, the ratio PDMS : Expancel[®] must correspond to the one in the real composite. In this way, R_e , the external radius of the PDMS coating, is dependant on the volumetric proportion of beads, γ_{Exp}^v , in the composite to be modelled. This radius can be geometrically determined as function of this proportion:

$$\gamma_{Exp}^v = \frac{V_{Exp}}{V_{ini}} = \frac{\frac{4}{3} \pi R_i^3}{\frac{4}{3} \pi R_e^3} \quad (3.10)$$

$$R_e = \frac{R_i}{\sqrt[3]{\gamma_{Exp}^v}} \quad (3.11)$$

In this way, the PDMS volume can be calculated by subtracting from the total volume defined by R_e the volume of the bead V_{Exp} :

$$\begin{aligned} V_{PDMS} &= V_{tot} - V_{Exp} = \frac{4}{3} \pi R_e^3 - \frac{4}{3} \pi R_i^3 \\ &= \frac{4}{3} \pi \frac{R_i^3}{\gamma_{Exp}^v} - \frac{4}{3} \pi R_i^3 \\ &= \frac{4}{3} \pi R_i^3 \left(\frac{1}{\gamma_{Exp}^v} - 1 \right) \end{aligned} \quad (3.12)$$

Now the volume of gas must be determined since it is the only unknown variable to calculate Γ . The perfect gas law gives the relation between the gas pressure and its volume:

$$pV = nRT \Rightarrow V = \frac{nRT}{p} \quad (3.13)$$

with p the pressure of gas, V the volume of gas, n the number of molecules in the gas, $R = 8.31 \frac{J}{mol \cdot K}$ the perfect gas constant and T the temperature in Kelvin.

In other words, the relation between pressure and volume is only affected by the amount of gas, since R is a physical constant and we consider T also constant. The number of moles of gas in a single bead n can be computed from several data provided by the manufacturer.

3.2. Model of expansion for a PDMS coated bead

$$m_{Exp} = \rho_{Exp} V_{Exp} \quad (3.14)$$

$$m_{iso} = \gamma_{iso}^m m_{Exp} \quad (3.15)$$

$$n = \frac{m_{iso}}{M_{iso}} = \frac{\gamma_{iso}^m \rho_{Exp} \frac{4}{3} \pi R_i^3}{M_{iso}} \quad (3.16)$$

where M_{iso} is the molar mass of isobutane.

This finally gives the volume of the gas in the bead as a function of its pressure, T being considered constant:

$$V_{gas}(p) = \frac{\gamma_{iso}^m \rho_{Exp} \frac{4}{3} \pi R_i^3}{M_{iso}} \frac{RT}{p} \quad (3.17)$$

The PDMS behaviour can be seen as the one of a hollow sphere subjected to an internal pressure. This deformation is described by solid mechanics formulas such as developed in Equation 3.18 [110]:

$$\Delta R_i = \frac{(p - p_{atm}) R_i}{E} \left[\frac{(1 - \nu)(R_e^3 + 2R_i^3)}{2(R_e^3 - R_i^3)} + \nu \right] \quad (3.18)$$

This formula depends on Poisson ratio ν and Young's modulus E . It is also dependant on the internal (R_i) and external (R_e) radius of the hollow sphere. R_i is a fixed parameter and R_e was calculated earlier as a function of volumetric proportion of Expancel® in the composite. The pressure is differential and thus $p - p_{atm}$, where p_{atm} is the atmospheric pressure, is used.

Knowing all parameters of Equation 3.18 the internal volume of the hollow sphere after expansion, V_{int}^{fin} , can also be expressed as a function of applied internal pressure:

$$\begin{aligned} V_{int}^{fin}(p) &= \frac{4}{3} \pi (R_i + \Delta R_i)^3 \\ &= \frac{4}{3} \pi \left(R_i + \frac{(p - p_{atm}) R_i}{E} \left[\frac{(1 - \nu) \left(\left(\frac{R_i}{\sqrt[3]{\gamma_{Exp}^{vol}}} \right)^3 + 2R_i^3 \right)}{2 \left(\left(\frac{R_i}{\sqrt[3]{\gamma_{Exp}^{vol}}} \right)^3 - R_i^3 \right)} + \nu \right] \right)^3 \end{aligned} \quad (3.19)$$

By knowing the volume inside the hollow sphere, the volume of the gas as function of pressure, as well as the volume of the shell of a single bead, a volume

assessment can be done to find the equilibrium pressure at which the system is stable.

$$V_{int}^{fin}(p) = V_{gas}(p) + V_{shell} \quad (3.20)$$

Which gives, by replacing the variable previously determined:

$$\begin{aligned} & \frac{4}{3}\pi \left(R_i + \frac{(p - p_{atm})R_i}{E} \left[\frac{(1 - \nu) \left(\left(\frac{R_i}{\sqrt[3]{\gamma_{Exp}^{vol}}} \right)^3 + 2R_i^3 \right)}{2 \left(\left(\frac{R_i}{\sqrt[3]{\gamma_{Exp}^{vol}}} \right)^3 - R_i^3 \right)} + \nu \right] \right)^3 \\ & = \frac{\gamma_{iso}^m \rho_{Exp} \frac{4}{3}\pi R_i^3}{M_{iso}} \frac{RT}{p} + \frac{4}{3}\pi R_i^3 - \frac{\gamma_{iso}^m \rho_{Exp} \frac{4}{3}\pi R_i^3}{\rho_{liq}} \end{aligned} \quad (3.21)$$

The result of the equation is the expression of the pressure inside the cavity as a function of volumetric beads' proportion and mass proportion of blowing agent in Expancel[®], since all other data are numerically known. From this value can be deduced the gas volume from Equation 3.17. Thus, all parameters of Equation 3.4 and Equation 3.5 are known and Γ can be computed as a function of volumetric beads' proportion and displayed in Figure 3.5 using numerical values provided in Table 3.2. Since the mass proportion of blowing agent in Expancel[®] is not precisely provided, a minimum-maximum interval was calculated and shown as a grey area in the graph. The Young's modulus used in those calculation is the one of pure PDMS and not the one measured in Section 2.3 because, at this temperature, the beads are not rigid any more and do not contribute to the augmentation of the material rigidity any more. Further Young's modulus measurements on expanded sample above 70 °C should be performed to get a more precise value.

ρ_{Exp} [$\frac{kg}{m^3}$]	γ_{iso}^m [%]	M_{mol} [$\frac{g}{mole}$]	ρ_{liq} [$\frac{kg}{m^3}$]	R_i [μm]
1200 [45]	10-15 [45]	58.123 [103]	593 [108]	6.5

ν [—]	E [MPa]
0.5	0.75 [101]

Table 3.2 Numerical values used for the calculus of expansion ratio Γ .

3.2. Model of expansion for a PDMS coated bead

Figure 3.5 also shows a confrontation between the model and the measurements performed. One can observe that for lower and higher proportions, the model seems less accurate. For lower proportions, explanations will be given in the next Section. For higher proportions, a divergence from the model might be due to the interactions between beads, which were not taken into account in this model. As the proportion increases, the expanding beads have more and more interactions with their neighbours, and getting a non spherical shape.

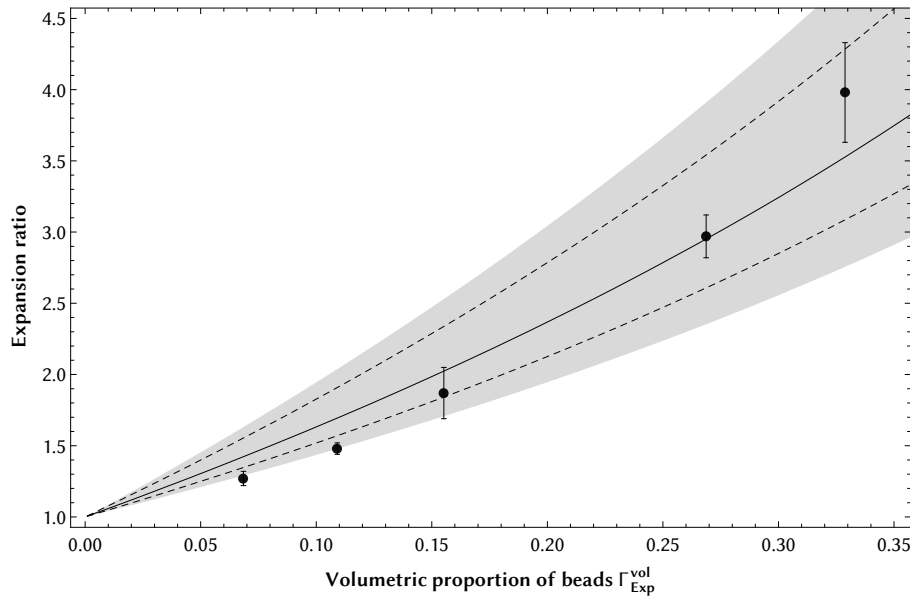


Figure 3.5 Analytical model of bead expansion confronted to bulk material expansion measurement. Each point is the mean of four to five tested samples in the experiment presented in Section 2.5. The error bars refer to the standard deviation on the multiple experiments performed. The three lines were calculated with an isobutane proportion in Expancel[®] γ_{iso}^m of 12.5%. The plain line has a Young's modulus of 0.75 MPa, the dashed lines have Young's moduli of 0.5 (upper) and 1 (lower) MPa. The grey area represents solutions for gas proportions of 10 and 15% for the extreme values of modulus.

This model can be compared to the calculation of a single bead expansion without constraint, which should correspond to a volumetric proportion of beads of 1 (or R_{ext} tends to 0). The expansion ratio tends to 73.5 as R_{ext} tends to 0, thus closely corresponding to the result found in Section 3.1.

Comparisons can also be made with previously published data as represented in Figure 3.6 which confronts the model with results from Samel *et al.* [95]

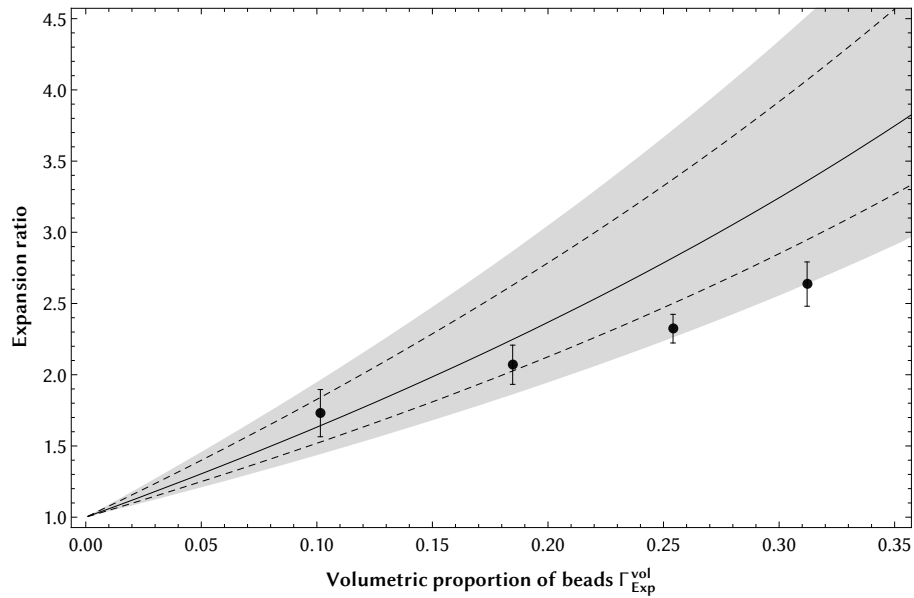


Figure 3.6 Confrontation of the model with results from Samel *et al.* [95]. Each point is the mean of samples tested in the publication. The error bars refer to the standard deviation on the multiple experiments performed. The curves correspond to the same numerical values as in Figure 3.5. The results obtained in this study are lower than the ones in the present work. They seem to correspond to a Young's modulus around 1Mpa rather than 0.75MPa. This might be explained by a difference in the crosslinking procedure.

We can see that even if those data are quite different from the ones obtained here, they still are in the error zone of the model. A plausible explanation is that there might be a different gas proportion in Expancel[®] and/or a different Young's modulus of the PDMS.

Since different batches of Expancel[®] were used, the gas proportion may vary up to 50% (the proportion is between 0.1 and 0.15).

The sample preparation protocols have different curing times. In this paper, 4 h at 65 °C, since our curing procedure was 16 h at room temperature followed by 6 h at 55 °C. In previous publications [99], a dependency on curing temperature and time has been reported but only on temperatures higher than 100 °C. Higher curing temperatures have shown to lower the Young's modulus. Longer curing time also lower this mechanical property. In our case, both parameters are changed in a contradictory manner, making it difficult to know if the Young's modulus has been modified and by which amount. To our knowledge, no experiment were done on curing with two different temperatures as done in our experiment.

3.3. Beads' internal pressure after expansion

3.3 Beads' internal pressure after expansion

One of the explanations for the previous model to overestimate the expansion ratio at lower proportions would be that the pressure in the beads comes close to the vapour pressure of the blowing agent. In order to confirm this, we need to know the pressure inside the beads after expansion. As previously undertaken done in Section 3.1, we will use a very naive model neglecting all pressure applied on the beads by the PDMS to know the volume they should have at atmospheric pressure. Then, comparing this value to the measured expansion ratio will give us the pressure of gas inside the beads. Such an approach is illustrated in Figure 3.7.

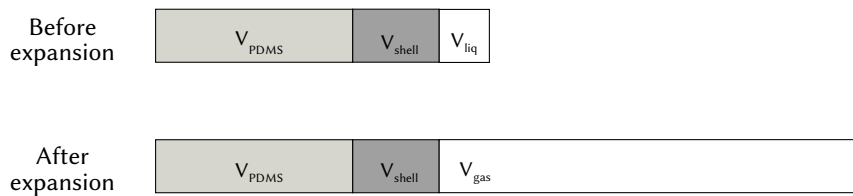


Figure 3.7 Volumetric assessment before and after expansion. The volume of PDMS and of the beads' shell does not change during the expansion of a single bead. On the contrary, the volume of blowing agent is increased due to phase change from liquid to gaseous state. For isobutane the volume increase is of 236-fold.

First, let us define the total volume of a single bead with its PDMS shell before expansion, V_{ini} :

$$V_{ini} = V_{liq} + V_{shell} + V_{PDMS} \quad (3.22)$$

with V_{liq} the liquid isobutane volume, V_{shell} the volume of copolymer forming the shell and V_{PDMS} the PDMS volume.

To develop further those relations, the determination of volumetric proportion of isobutane in unexpanded beads must be found. First, the copolymer shell density is required. This is obtained by making a volume count of the different elements

forming Expancel[®] for a normalized mass of Expancel[®] containing liquid isobutane as shown in equation 3.23.

$$\begin{aligned}
 V_{Exp} &= V_{liq} + V_{shell} \\
 \frac{1}{\rho_{Exp}} &= \frac{\gamma_{iso}^m}{\rho_{liq}} + \frac{1 - \gamma_{iso}^m}{\rho_{shell}} \\
 \Rightarrow \rho_{shell} &= \frac{1 - \gamma_{iso}^m}{\frac{1}{\rho_{Exp}} - \frac{\gamma_{iso}^m}{\rho_{liq}}}
 \end{aligned} \tag{3.23}$$

where V_{Exp} is the volume of Expancel[®], ρ_{shell} the beads' shell density, ρ_{Exp} the complete beads' density, γ_{iso}^m is the mass proportion of blowing agent in the beads, ρ_{liq} the density of liquid isobutane, ρ_{Exp} the overall density of Expancel[®].

The volumetric proportion of liquid isobutane in Expancel, γ_{iso}^v , can now be calculated from this result:

$$\begin{aligned}
 \gamma_{iso}^v &= \frac{V_{iso}}{V_{Exp}} = \frac{V_{iso}}{V_{iso} + V_{shell}} \\
 &= \frac{\frac{\gamma_{iso}^m}{\rho_{liq}}}{\frac{\gamma_{iso}^m}{\rho_{liq}} + \frac{1 - \gamma_{iso}^m}{\rho_{shell}}} \\
 &= \frac{\rho_{shell} \gamma_{iso}^m}{\rho_{shell} \gamma_{iso}^m + \rho_{liq} (1 - \gamma_{iso}^m)}
 \end{aligned} \tag{3.24}$$

The three volumes expressed in Equation 3.22 can be calculated from values provided in datasheets for PDMS and Expancel[®]:

$$\begin{aligned}
 V_{liq} &= \gamma_{Exp}^v \gamma_{iso}^v V_{ini} \\
 V_{shell} &= \gamma_{Exp}^v (1 - \gamma_{iso}^v) V_{ini} \\
 V_{PDMS} &= (1 - \gamma_{Exp}^v) V_{ini}
 \end{aligned} \tag{3.25}$$

with γ_{Exp}^v the volumetric Expancel[®] proportion in the studied composite. As expected, the sum of these three volumes is 1 because normalised volumetric proportions were used.

To determine the expansion ratio, the final volume of our bead, V_{fin} must be determined. All volumes stay the same except the volume of liquid blowing agent, V_{liq} becoming the volume of gaseous blowing agent, V_{gas} .

$$V_{fin} = V_{gas} + V_{shell} + V_{PDMS} \tag{3.26}$$

3.3. Beads' internal pressure after expansion

The relation between the volume of liquid and the volume of gas is given by the density ratio for the two given states:

$$V_{gas} = \frac{\rho_{liq}}{\rho_{gas}} V_{liq} \quad (3.27)$$

giving:

$$V_{fin} = \frac{\rho_{liq}}{\rho_{gas}} V_{liq} + V_{shell} + V_{PDMS} \quad (3.28)$$

Then, the expansion ratio with the hypothesis of atmospheric pressure inside the beads can be expressed by:

$$\begin{aligned} \Gamma_{atm} &= \frac{V_{fin}}{V_{ini}} = \frac{\frac{\rho_{liq}}{\rho_{gas}} V_{liq} + V_{shell} + V_{PDMS}}{V_{liq} + V_{shell} + V_{PDMS}} \\ &= \frac{\frac{\rho_{liq}}{\rho_{gas}} \gamma_{Exp}^v \gamma_{iso}^v + \gamma_{Exp}^v (1 - \gamma_{iso}^v) + (1 - \gamma_{Exp}^v)}{\gamma_{Exp}^v \gamma_{iso}^v + \gamma_{Exp}^v (1 - \gamma_{iso}^v) + (1 - \gamma_{Exp}^v)} \\ &= \left(\frac{\rho_{liq}}{\rho_{gas}} - 1 \right) \gamma_{iso}^v \gamma_{Exp}^v + 1 \end{aligned} \quad (3.29)$$

Table 3.3 gives the numerical values for the previously cited variables.

ρ_{Exp} [$\frac{kg}{m^3}$]	γ_{iso}^m [%]	ρ_{liq} [$\frac{kg}{m^3}$]	ρ_{gas} [$\frac{kg}{m^3}$]	ρ_{PDMS} [$\frac{kg}{m^3}$]	γ_{Exp}^v [%]
1200	10-15	593	2.11	970	5 to 35

Table 3.3 Numerical values for the variables used in the determination of the expansion ratio Γ_{atm} .

Finally, the pressure can be calculated:

$$\frac{p_{int}}{p_{atm}} = \frac{V_{gas}^{theo}}{V_{gas}^{meas}} = \frac{V_{gas}}{\Gamma_{meas} V_{ini} - V_{shell} - V_{PDMS}} \quad (3.30)$$

where p_{int} is the pressure inside the beads, V_{gas}^{theo} the theoretical volume of gas in the composite, V_{gas}^{meas} the volume of gas in our measurement, which is deduced from Γ_{meas} the mean value of expansion ratio measured for different proportion of Expancel® in the composite. Figure 3.8 shows the evaluated pressure inside the beads deduced from our measurement. The error bars correspond to the incertitude due to the imprecise value of the blowing agent proportion in Expancel®.

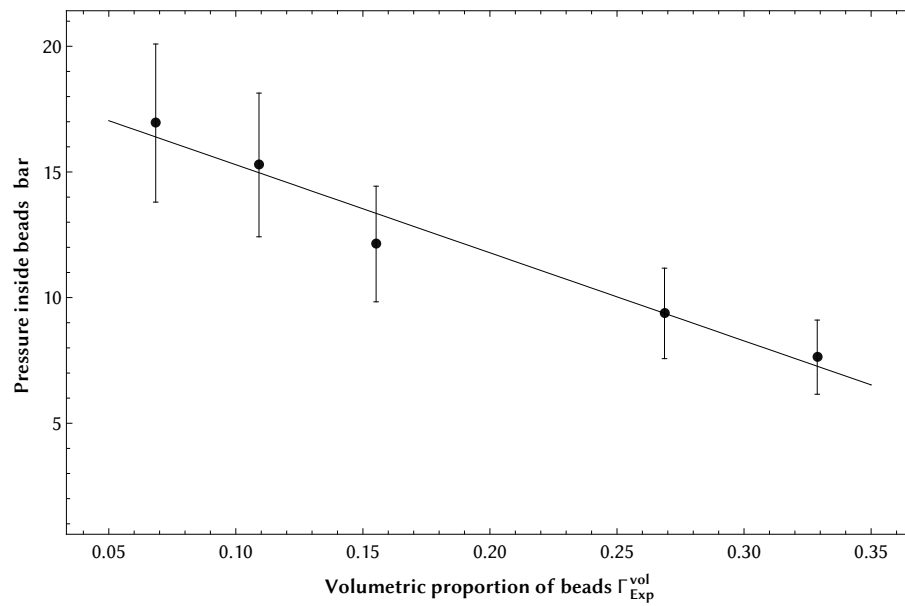


Figure 3.8 Pressure inside the beads for performed experiments. The error bars correspond to the incertitude due to the imprecise value of the blowing agent proportion in Expancel®.

One can observe that the value for lower proportion is near 14 bars¹ which is close to the vapour pressure of isobutane at 70 °C², making it possible to have some liquid remaining in the beads. Thus, models based on the assumption that the only state of isobutane present is gaseous are less accurate, which is the case on lower beads' proportion in the previously presented model.

¹See Section 2.4.2 for details

²See Section 3.1 for explanations on the choice of temperature

3.4 Modelling roundup

Calculations have been made to predict the expansion ratio of PDMS - Expancel® for different proportions of beads. The model fits the experimental results. Limitations of the model, such as non-spherical beads and high internal gas pressure after expansion, have been described and enable to explain the differences between the model and the experimental results.

This model also proves the limitations of the material in term of reproducibility. Indeed, it highlights the dependency on Young's modulus and blowing agent proportion in Expancel®. This model provides a way to calculate the intrinsic reproducibility limit of the material depending on the change of blowing agent proportion and on the Young's modulus variation due to the fabrication process.

Heating system for PDMS - Expancel[®] composite activation

Contents

4.1	Screen-printed heaters with temperature control	60
4.1.1	Working principle	60
4.1.2	Experimentals	61
4.1.3	Results	66
4.1.4	Conclusion	68
4.2	Other activation methods	70
4.3	Heating system roundup	72

In the first demonstration of use of PDMS - Expancel[®] composite, the heating was done using PCB copper tracks. In this chapter, other alternatives will be discussed. Some aimed at getting cheaper mountings of the expandable composite, others are proofs of concepts and prototyping methods.

4.1 Screen-printed heaters with temperature control

In previous studies [95–98], the PDMS - Expancel[®] composite was activated by copper tracks on PCB. The heating was controlled by the power applied on the tracks.

This implementation of the composite will use screen-printed heaters thermally controlled in order to perform the activation. Previously used copper tracks have a relatively low resistivity due to the intrinsic electrical properties of copper. Moreover, the tracks width is limited by the PCB manufacturing process to around 100 μm . Resistive pastes are much more resistive than copper, allowing to get much higher resistance on the same surface, and thus enabling the use of much smaller currents to get the same power generation.

This section will present the implementation of such a system. We will also study the geometry of a free-expanding composite layer and its dependency on temperature.

4.1.1 Working principle

Screen-printing, also known as thick film technology [111], allows us to deposit and structure layers of paste. It is commonly used to fabricate resistors on a substrate. It was considered an alternative to PCB copper tracks for heating the PDMS - Expancel[®] composite.

Two main kinds of paste are usually used to create thick film resistors: ceramic and polymer (mainly epoxy). The principle is to structure photosensitive resin on a mesh and to scrape the paste through the mesh on the substrate. The structured photoresist acts as a mask and allows for the deposition on the substrate only on the selected areas.

Ceramic thick film technology was put aside because the thermal conductivity of the substrate¹ is much higher than the conductivity of PDMS² and lower than the resolution due to thermal diffusion.

The evaluation was done by characterising the expansion of a layer of composite moulded on top of PCB holding resistive parts. Heating was performed by a screen-printed resistor (see Figure 4.1) and the power supplied was controlled by a temperature driven Proportional Integral Derivative (PID) controller. Since the

¹Alumina: $30 \text{ Wm}^{-1}\text{K}^{-1}$ [103]

²PDMS: $0.15 \text{ Wm}^{-1}\text{K}^{-1}$ [16]

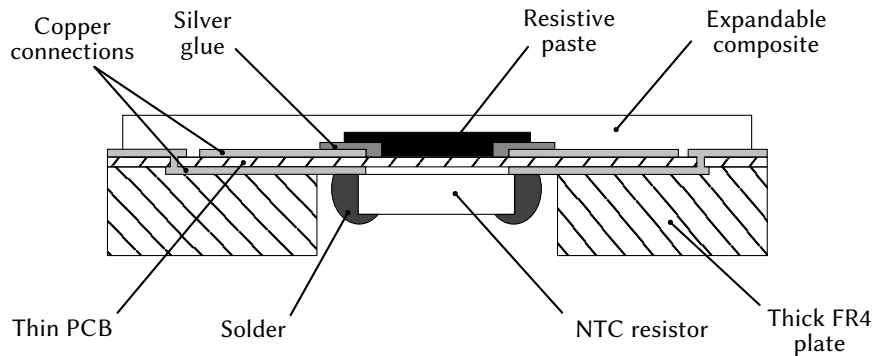


Figure 4.1 Working principle of thick film technology used as heater for PDMS - Expancel® composite activation. A thin PCB is supporting copper tracks for connection. First a Silver glue layer is screen-printed on this PCB to insulate the heater from the heat sink. Then the resistive paste is screen-printed to form the heater. This thin screen-printed PCB is cold pressed on a thick FR4 plate with holes where NTC resistors are soldered to measure temperature. Finally the composite is moulded directly on top of the obtained chip.

screen-printing was performed on a 0.1 mm thick FR4 PCB, the temperature was recorded by soldering a Negative Temperature Coefficient (NTC) resistor on the back of the heating resistor.

4.1.2 Experimentals

This section will present the different stages of fabrication of the presented system, as shown on the process flow in Figure 4.2.

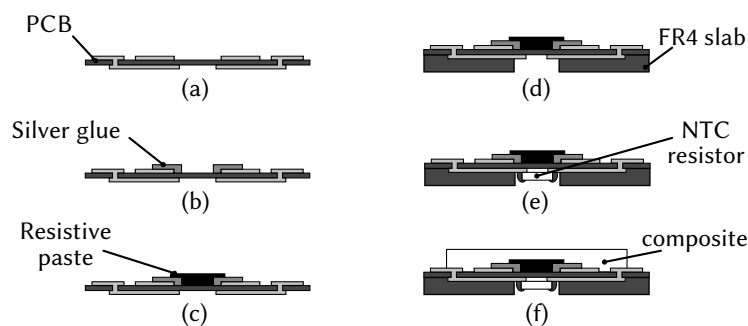


Figure 4.2 Process flow of the fabrication: Double-sided PCB fabrication. (b) Silver glue screen-printing. (c) Resistive paste screen-printing. (d) Reinforcement slab pressing. (e) NTC resistor soldering. (f) Composite moulding.

4.1. Screen-printed heaters with temperature control

Heater design

The heaters were designed in a circular shape, to prevent detachment of the composite from the PCB due to corners singularities. Connection to the resistive paste was done with electrically but not thermally conductive glue to prevent copper tracks from acting as heat sink and thus avoid energy losses. Instead of straight, the connections were rounded to correspond to the shape of the resistor to allow a uniform repartition of current through the resistor. This design is shown in Figure 4.3.

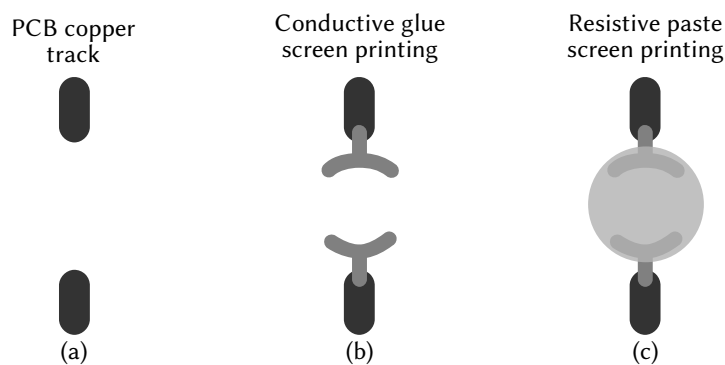


Figure 4.3 Design and fabrication process of the screen-printed heaters. First (a) the PCB is fabricated with standard manufacturing process. The contact tracks are Ni/Au coated to prevent corrosion. Then (b) conductive glue is screen-printed on the PCB to make the connection to the resistor. Finally (c), resistive paste is screen-printed to form the heaters.

PCB fabrication

A thin (0.1 mm) double layer FR4 PCB with all tracks is fabricated by usual PCB fabrication process; that is, photolithography and chemical copper etching. Tracks were Ni/Au plated to prevent corrosion. The top side contains tracks connecting the heaters, and the bottom side the temperature sensor. All external connections were made on the top side through vias.

Screen-printing

A first step of screen-printing was undertaken using silver glue (E212 Silver Glue, Épotecny, Levallois Perret, FR) to create connections between the resistive paste and the tracks. This prevents heat dissipation through highly conductive copper

connections. The frame used was 325 mesh with 20 µm emulsion. The glue was cured at 150 °C during 15 min.

The paste (ED7100-200Ohm ELECTRA^ΩD'OR®, Electra Polymers LTD, Tonbridge, UK) was then screen-printed using a 400 mesh frame with 20 µm emulsion. Some systems were screen-printed on both sides, so the protocol was to screen-print one side, dry the paste 1h, then screen-print the second side and dry 1h, and finally cure the paste for 5h. All the drying and curing phases were done at 155 °C.

Chip assembly

As shown on Figure 4.1, screen-printing was performed on a 0.1 mm PCB layer. A mechanical reinforcement was needed to insure the stability of the system and prevent fissuring of the paste. Thus a thick (1.6 mm) FR4 part was stuck on the back of the thin PCB layer by cold pressing with solid glue. The thick PCB layer was drilled to allow access to the NTC resistor pad for soldering. The 20 kΩ NTC resistor was tin soldered after pressing. Finally, thermal paste was applied on the NTC to ensure a good thermal contact with the PCB.

Composite moulding

The composite is moulded directly on top of the screen-printed PCB. This is required since using thick film technology results in non-flat chips. Thus a normal membrane cannot be superimposed without being significantly deformed.

A dedicated mould was fabricated to allow the chip to be inserted in the mould. This operation is shown in Figure 4.4. On one part of the mould the form of the membrane is carved. On the other part, a cavity (suited for the chip) is present. In this cavity one can put an o-ring, then the chip; the hole thing covered with the first part of the mould, allowing the membrane to be directly moulded on the chip.

Electrical control system

Thermal control was done with a LabView program featuring a PID. A NI-6008-USB card from National Instruments, Austin, USA was used to measure NTC tension and generate control potential on the heating resistor. The signal given by the NI card was amplified with an operational amplifier circuit to ensure there was enough current to power the resistor. The PID was adjusted using Ziegler-Nicols [112] methods. A temperature set point was chosen and the proportional coefficient of

4.1. Screen-printed heaters with temperature control

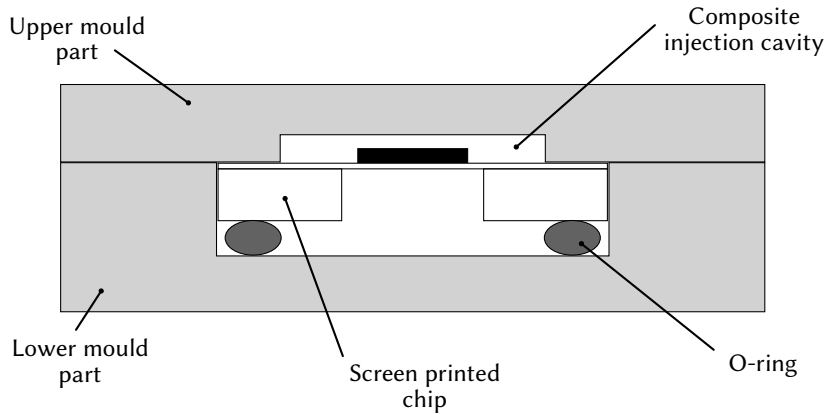


Figure 4.4 Moulding system. The chip lays in a cavity of its size on top of an o-ring. The upper part of the mould holds the shape of the membrane and closes the mould on top of the chip. This allows the liquid composite to adhere to the chip and prevents the membrane from buckling.

the PID was raised until obtaining an oscillation. This value is named K_p and the oscillation period T_c . Then the different parameters were given by the Ziegler-Nichols formulas, where K is the proportional factor, K_i the integral factor and K_d the derivative factor:

$$\begin{aligned} K &= 0.6K_p \\ K_i &= 0.5T_c \\ K_d &= 0.125T_c \end{aligned} \quad (4.1)$$

The measurement performed for a set point of 75 °C gave 5.4, 0.002, 0.001 for K , K_i , K_d respectively.

System calibration

In order to limit the error due to NTC resistor mounting, a temperature calibration of the sensor was performed using the system shown in Figure 4.5.

The calibration was done by maintaining the heater at a certain known temperature and measuring the temperature with the sensor. By performing this with several temperatures, a correspondence curve could be established and was used to determine the actual temperature of the operating heater from the measured one.

A large, thermally conductive (aluminium) mass was heated by a wire powered by a current source (E3631A, Hewlett-Packard, Palo Alto, USA) to a temperature measured by a thermocouple inserted in its core.

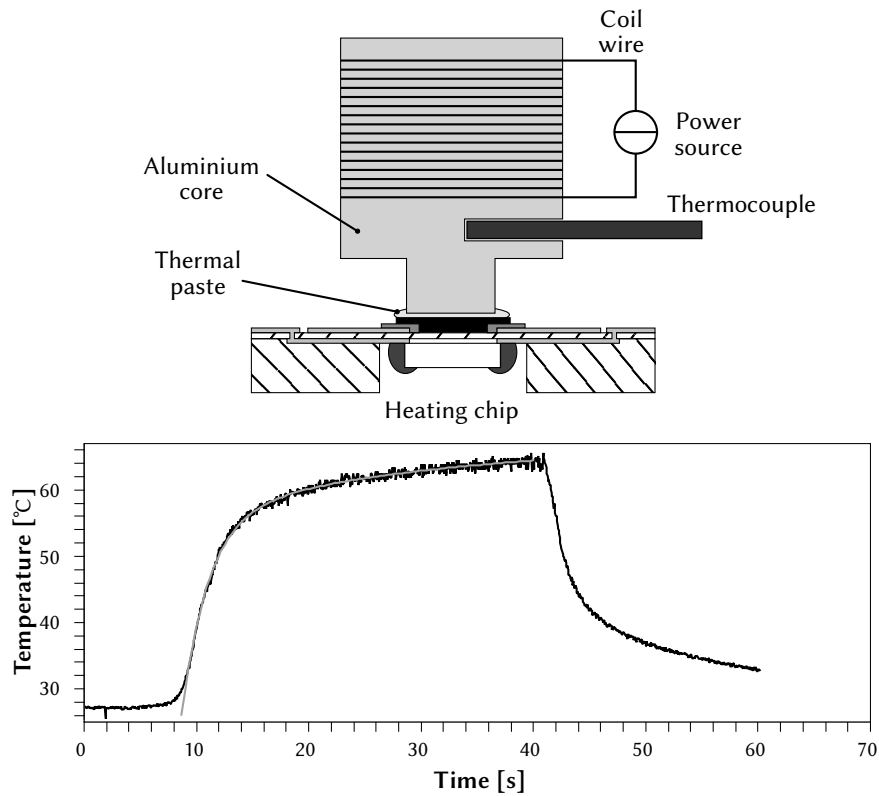


Figure 4.5 Calibration system (top) and result (bottom). A large, thermally conductive (aluminium) mass is heated to a temperature measured by a thermocouple inserted in its core. This mass is then applied on the heater with thermal paste to get a good thermal contact. The temperature progression measured by the sensor due to this thermal step is recorded and an offset is deduced from the result of a fitting on the curve.

The three reference temperatures were 80, 90 and 100°C in order to have a good reliability around the temperatures relevant for the performed experiment. Each measurement was performed six times to make up for experimental errors such as bad contact between the aluminium core and the heater. On each measurement a fitting was done using the function:

$$T(t) = y_0 + A_1 e^{\frac{-(t-t_0)}{\tau_1}} + A_2 e^{\frac{-(t-t_0)}{\tau_2}} \quad (4.2)$$

The y_0 parameter is considered the offset we were looking for. A correspondence map was done for each chip between measured and real temperatures and measurements were corrected according to it.

4.1. Screen-printed heaters with temperature control

Expansion protocol

Temperature profile applied to the sample is shown in Figure 4.6. The principle of the measurement is to fix a temperature set point (T_2) during a given time and measure the geometrical properties of the expanded zone. To avoid measurement artefacts due to external temperature, a conditioning step was added to the temperature profile applied (T_1). First, a temperature ramp to reach $40\text{ }^\circ\text{C}$ (T_1) in 10 s (t_1) was performed, then an isotherm was kept during 10 s (t_2). After the isotherm, a rapid step of 0.2 s (t_3) to the temperature set point was made. Finally, the set point temperature was kept during 20 s (t_4) to perform the expansion. The set point temperature was set way below the theoretical expansion temperature because of the offset due to the 0.1 mm thick FR4 membrane between the heater and the measurement resistor. The studied temperatures were set between 65 and $75\text{ }^\circ\text{C}$.

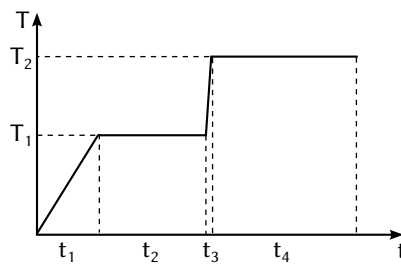


Figure 4.6 Temperature profile applied on composite layers through the temperature control system.

Geometrical measurement

After expansions were performed, the expanded parts of the membrane were studied with an optical profiler (Wyko NT1100, Veeco, Plainview, USA) to determine their height and geometry. A qualitative analysis on the expansion shape was also made.

4.1.3 Results

From the qualitative shape analysis, it can be said that a lower activation temperature results in highly non-circular shapes as shown in Figure 4.7. As expected, the highest temperature has resulted in a larger expanded zone, in height and diameter. This is representative of the inhomogeneity of heat generation on a circular heater.

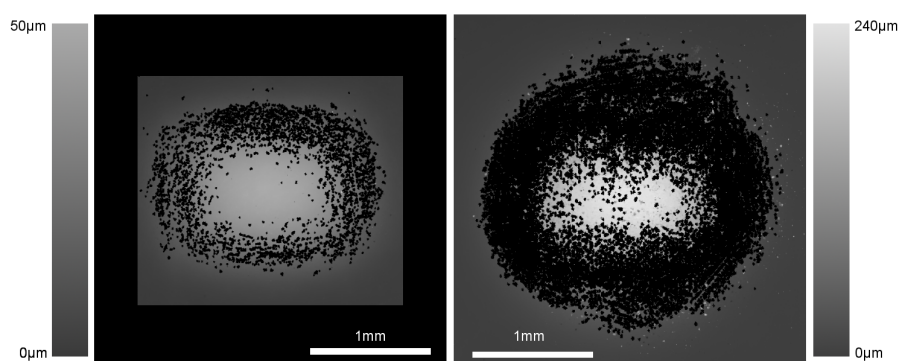


Figure 4.7 Geometrical comparison of the expanded zone for two different activation temperatures. The temperature was maintained around 90 °C (left) and 105 °C (right).

Obviously, the heat loss is higher at the circle perimeter. Moreover, since connections to the paste are much more conductive and at the same time create a heat sink, those areas are less hot. This results in a rectangular shape. For a higher activation temperature, this phenomenon is hidden by a higher heat diffusion through the composite, making the expansion wider. In this way, the periphery is less hot and thus expands less due to thermal repartition of expansion as discussed in Section 2.2.

From a more quantitative point of view, the height achieved can be represented as a function of the activation temperature as shown in Figure 4.8. Temperatures were corrected according to calibration. A linear behaviour is seen. This is due to the effect presented in Section 2.2; which is that the material does not expand at a precise temperature, but over a range. All experiments were done with the same batch of composite mix and with the same curing protocol, reducing the variations of the material itself.

It can be observed that the activation temperature needed here is much higher than the one presented in Section 2.2. This is due to the fact that, unlike in the characterisation experiment, the temperature of the composite is not homogeneous. Indeed, the composite thermal conductivity lowers as it expands, making it more difficult to have an homogeneous temperature in the composite layer. In this way, the temperature of the heater needs to be higher in order to achieve expansion on the whole composite membrane thickness.

4.1. Screen-printed heaters with temperature control

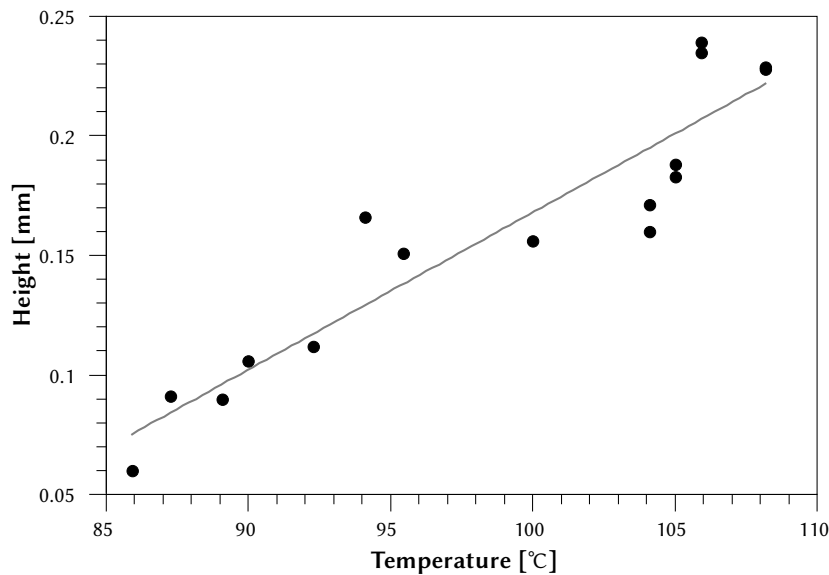


Figure 4.8 Relation between temperature and height. A linear behaviour is observed. This would enable the control of the expanded volume through the applied temperature. The applied temperature is higher than expected with the previous expansion vs. temperature measurements³. This is due to the fact that the temperature is not homogeneous in the composite layer and a high temperature is needed at the heater level in order to have expansion over the whole membrane thickness.

4.1.4 Conclusion

The integration of a thermally controlled screen-printed heating system was successfully achieved. A general relation between temperature and expanded height is observed, but some variations still persist with our experimental setup. Calibration shows large variations between the different heaters, hinting at different thermal couplings between heater and measurement resistor. The calibration step might not be precise enough to insure a perfect correction of this coupling variation.

A better thermal coupling between the temperature sensor and heater might be achieved by using a screen-printed resistor as sensor, as proposed by Nicolics *et al.* [113]. Such an implementation was tested, but NTC characteristic of the ED7100 has resulted in poor sensitivity, preventing a precise enough control of the

³See Section 2.2.

temperature. Engineering a more sensitive NTC polymeric paste would solve this issue and give a more reliable temperature/geometry relation.

Control of the expansion geometry through activation would permit a control over the dispensed volume. In contrary to previously developed systems [95], the dispensed volume could be defined by the activation temperature instead of the geometry. It would result in a flexible system where the amount of liquid dispensed would not be set at the manufacturing. It would require improvement of Expancel® reproducibility to reduce theoretical variations of expansion ratio described in Section 3.2.

4.2 Other activation methods

Several other approaches of PDMS - Expancel[®] heating have been examined. A qualitative approach of the results will be presented for two of them: Titanium - Platinum electrodes on glass and conducting PDMS.

Titanium - Platinum electrodes

Some tests have been performed using Ti/Pt electrodes structured on glass. Those were fabricated by plasma etching of sputtered Ti/Pt layer. The titanium layer was very thin and helped the platinum adhere to the glass. Membranes of PDMS - Expancel[®] composite have been plasma bonded on top of this electrode, to be thermally activated.

The advantages of such a system are its ease of assembly, requiring no alignment, and the use of very well-known and controlled fabrication processes such as sputtering and Pt plasma etching. The heaters' high resolution of such systems allows for the implementation of more features using the same technology, such as temperature sensors enabling close-loop temperature controls. On the other hand, the main drawback is the use of clean-room technologies to manufacture every single heater, greatly increasing the price of a technology mainly aimed at disposable devices.

The main technical failure observed was the impact of the relatively high thermal conductivity of glass. Indeed, the expanded zone was always much larger than the heater, making it difficult to control the amount of expanded composite. If the application requires the actuation of a precise volume, a geometrically constrained system can be used. In such a system, the composite does not expand freely but in a cavity, which restrains its final volume.

Conducting PDMS

In the optic of low cost devices, the possibility of an all-polymer device was studied. To this aim, the use of conductive fillers in PDMS was investigated. Polymers have been made conductive by particles on several occasions [114–116]. Based on previous works, which aim was to make PDMS conductive [114, 115, 117], a PDMS - Expancel[®] composite expansion was performed. As previously proposed [114], 4 μm silver-coated copper flakes have been used as fillers to make PDMS conductive. 80 weight-% of copper flakes and PDMS mix has been used. PDMS structures

holding channels corresponding to the wanted resistor shape were moulded and filled with the conductive mix. To allow for a better filling of the channel, some heptane was used to make uncured PDMS less viscous. Finally, an expandable composite membrane was plasma bonded on the heater. The resulting setup is shown in Figure 4.9.

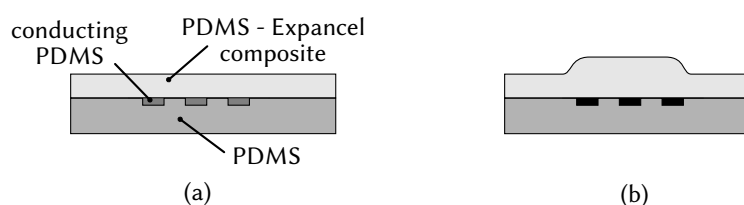


Figure 4.9 Design and operation of a conducting PDMS heating system. (a) The system is composed of a PDMS layer where channels corresponding to resistors are moulded. Those channels are then filled with conducting PDMS containing a copper flakes filler. A PDMS - Expancel® composite is then plasma bonded on top of the PDMS layer. (b) When a current is applied on the resistors, heat is generated and the composite expands

This solution provides a simple and cheap way of manufacturing the heater layer of a PDMS - Expancel® composite-based system. It is suitable for systems requiring large area heaters, since small resistors are hard to implement using this technology. This is due to the viscosity of conducting PDMS but also to the low conductivity of the paste.

4.3 Heating system roundup

In this chapter was studied a solution for activation of PDMS - Expancel[®] composite in microsystems using screen-printed resistors. Two other alternatives were briefly described.

Screen-printing is a good choice for activation of PDMS - Expancel[®] composite because its resolution is good, the technology is already well developed and rather cheap. As described here, it allows for on-chip temperature sensors to control the heating, which is quite important, bearing in mind the narrow temperature range at which the composite is fully activated, but not damaged.

Improvements have to be made on the sensor to make it more reliable and easier to put together. This might be done by finding a reliable conductive paste with stable and sensitive NTC or PTC properties to achieve precise temperature measurements to replace the SMD (Surface Mounted Device) NTC resistor.

Conductive PDMS heaters might be interesting in some applications, but because of the poor resolution of the manufacturing process, it will not be possible to integrate temperature sensors. However, for patch-like systems with low precision on injected volumes, or external volume control like predefined doses, the low cost of such technology might overcome its drawback.

Finally Ti/Pt electrodes have a very good resolution, far better than the one of the composite itself, in which the smallest active components are 10 μm in diameter. The high cost of fabrication however, makes this system difficult to apply in a disposable industrial product.

Applications of PDMS - Expancel[®] composite

Contents

5.1	Micro-injector	74
5.1.1	Principle and operation	74
5.1.2	Experimental conditions	75
5.1.3	Results	77
5.1.4	Conclusion	80
5.2	Miniaturized blood coagulation testing tool	81
5.2.1	Principle and operation	82
5.2.2	Experimental conditions	83
5.2.3	Results	84
5.2.4	Conclusion	87
5.3	Applications roundup	88

This chapter will focus on possible applications of PDMS - Expancel[®] in medical and / or diagnostic devices. Two applications will be presented and their applicability will be studied. The first is a micro injector, or pipetting device. It sucks liquid to store it in an internal cavity and ejects it later, without energy consumption between the two phases. The second application is a fluidic actuator used as coagulation testing system.

5.1 Micro-injector

Samel *et al.* have proposed a system to suck up and eject liquids [97]. This is used, for example, to take liquid from a reservoir and inject it in a microfluidic system. In this section, a system allowing the study of the possibilities offered by such a device in terms of reliability in automated systems will be presented. Contrary to previously proposed systems where activation time was manually applied, this setup will provide an automated power supply to the heaters. In this way, the properties of such technology included in a “Lab-on-chip” system will be highlighted.

A study of the liquid movement in the system will be done by adding a planar measuring channel on top of it, which will be filled with coloured liquid. Thus, when the system is operated, the amount of liquid inside the cavity can be monitored through the filling of the measuring channel. Stroke volumes will be observed to determine if automatisisation affects reproducibility.

5.1.1 Principle and operation

The operation principle of such a system is shown in Figure 5.1. The presented device shows a demonstration prototype, which just sucks and ejects liquid. The system layers are the following: the heating layer, which is a PCB holding copper tracks, an expansible layer of PDMS - Expancel[®] composite, a flexible PDMS closing layer, a rigidifying glass layer and finally a measuring channel in PDMS allowing the evaluation of dispensed volumes.

The heating layer features two heating tracks: a round heater in the centre and a ring heater in the periphery. The heaters are two nested spirals. The connections are made on the back side of the wafer and through vias. In the central heater, the spacing of the loops of the spiral are not constant. Since tighter loops get hot faster, it enables the progressive closing of the cavity from the outer side to the centre, preventing the clogging of the fluidic connection before a complete ejection. The expansible layer is spin-coated on top of the PCB. The closing layer is bonded by oxygen plasma on the expansible layer except in the centre upon the round heater. The unbonded zone can be opened to create a cavity for the liquid. In this implementation of the system, the cavity is connected to a channel whose dimensions are well-known, making it possible to know how much liquid goes inside the cavity and out.

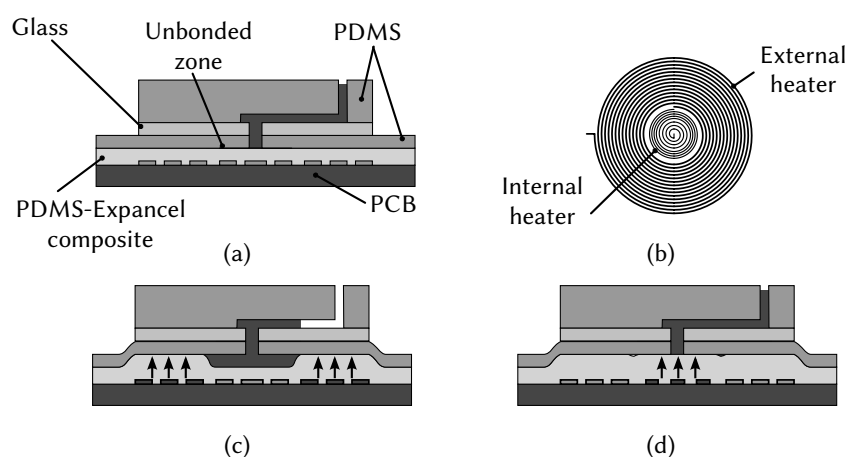


Figure 5.1 Schema of operation of the micro injector. (a) The system is composed of several stacked layers. The PCB holding the heater is covered by a membrane of PDMS - Expancel® composite. A layer of PDMS is selectively bonded of top of it to have an unbounded area to create a cavity. Finally, a planar measurement channel is connected on the output to enable the monitoring of the volume of liquid in the cavity. (b) The heaters are two nested spirals. The connections are made on the back side of the PCB and through vias. (c) To suck the liquid in, the external ring is powered and the cavity is created. (d) To eject the liquid the internal heater is activated and the cavity is closed.

5.1.2 Experimental conditions

Fabrication of the device

The fabrication occurs in several steps presented in Figure 5.2. The heating layer is a PCB holding several ring/centre pairs, fabricated only once and reused. This layer is spin coated with PDMS - Expancel® composite. The polymer is crosslinked at 60 °C for 4 h. The ratio of Expancel® in the composite was 1:4 Expancel® to base PDMS ratio, corresponding to a volumetric proportion of beads of 15.52%.

The closing layer is poured on a wafer (glass or silicon). The thickness is determined by the amount of PDMS poured on the wafer. It is then crosslinked at 80 °C during 20 min. The closing layer is removed from the wafer and punched to create the connection hole at the proper location to correspond to the heating layer.

Both the heating layer and the closing layer are then exposed to an oxygen plasma (300 mTorr, 50 W, 30 s). On the heating layer, a PDMS mask hides the zones of the cavities to prevent them from being activated by the plasma. The two layers are then put together. To facilitate the opening of the cavity during the operation

5.1. Micro-injector

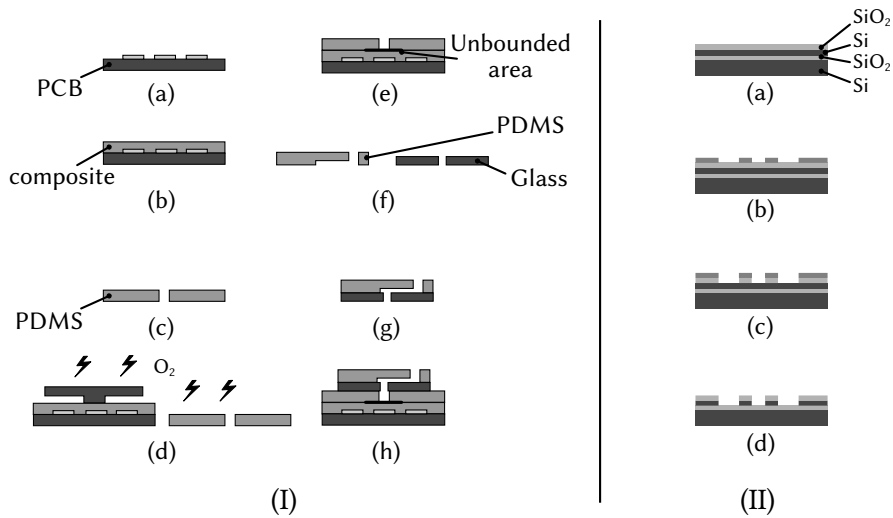


Figure 5.2 Fabrication process of a complete micro-injector (I) and of the measurement capillary masters (II). For the complete system, a PCB is fabricated (I-a) and composite is spin-coated and cured on it (I-b). A slab of PDMS is cured and punched to create fluidic connections (I-c). The coated PCB and the PDMS slab are exposed to oxygen plasma and bonded (I-d,I-e). During this process, the composite is masked with a PDMS stamp to prevent locally the activation and bonding. Capillaries are cast-moulded on a master and a corresponding slab of glass is drilled for fluidic connections (I-f). Both pieces are bonded together (I-g). The formed capillary is finally bonded on the PCB stack to obtain the full system (I-h). The masters used for the casting of the capillaries are SOI wafer (2 μm SiO₂, 100 μm Si) oxydized (2 μm) (II-a). A photolithography was performed on top of the oxide (II-b). Oxide was plasma etched (II-c) to structure the mask. With this mask, Si was dry etched by Bosch process (II-d) to finalise the master.

of the system, it is filled with vegetable oil and emptied before the next fabrication step.

The measuring capillaries are separated elements featuring a square of glass with a hole in its centre and a moulded PDMS part containing a channel of known dimensions. One of the channel's outlets corresponds to the hole in the glass square and the other one will be the interface with the outside.

Finally, those measuring channels are bonded on top of the system with both holes aligned to connect the channel and the cavity.

Experimental procedure

The plate holding the systems is dipped in water (coloured with alimentary dye) and exposed to vacuum. In this way the measuring channel is filled with liquid which can be aspirated in the cavity, making it possible to measure how much liquid is sucked and then ejected. The vacuum removes the air from the channel, but also desaturates the liquid and the PDMS from gas, which makes it possible for remaining bubbles to be absorbed in the PDMS when taking the system out of the vacuum.

The experiment is controlled by an electronic system and a MatLab 7.2, MathWorks program enabling to power the two heaters sequentially. The power supply is made by a current source (E3631A, Hewlett-Packard, Palo Alto, USA), followed by a reed relay selecting the inner or outer heater.

Different sizes of inner heaters and cavity diameters were tested and the thickness of the composite layer varied, using different spinning rates. The progression of the liquid in the measuring channel was recorded and the stroke was deduced from this information.

5.1.3 Results

Pictures in Figure 5.3 show a sequence of aspiration and ejection of the micro-system as well as a graph of the evolution of the cavity's volume. First (1-3), the blue liquid lies only in the measurement channel and, as the ring heater is activated, the composite expands and the liquid fills the cavity. Then (4-6), as the inner heater is powered, the liquid is ejected outside the cavity and refills the measurement channel. As seen on the graph, at the beginning, no expansion takes place, because activation temperature must be reached and the surface to heat is large. As expected, the volume of liquid ejected corresponds to the aspired volume.

Figure 5.4 shows the average stroke for three different sizes of heaters. The inner heaters were of 3.5 mm, 5 mm and 6 mm in diameter.

The variation of the stroke is much higher for larger diameter systems. Most probably because they have a higher chance of getting stuck and not opening normally. This hypothesis is reinforced by the fact that a linear behaviour is observed on the measurement mean, but a quadratic one is expected because of the relation between the diameter and the volume.

5.1. Micro-injector

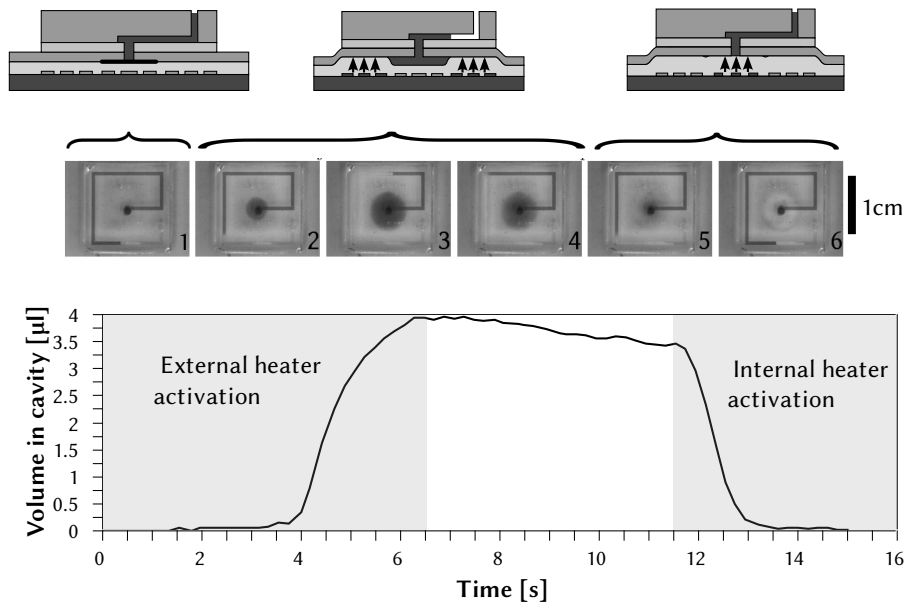


Figure 5.3 Operation of the micro-injector (top) and evolution of the volume inside its cavity with time (bottom). Image 1 shows the system before activation. Images 2-4 are taken during the cavity filling, and the last two (5-6) show the ejection of the liquid. The graph shows the evolution of the volume of liquid present in the cavity during the operation of the system. At the beginning, no expansion takes place, because activation temperature must be reached. As expected, the volume of liquid ejected corresponds to the aspired volume.

Spin coating is a process highly dependant on the viscosity of the material deposited. According to measurements done on unexpanded parts of the system, the thickness of the composite may vary more than 20 % from one fabrication to another. Considering only systems from the same fabrication batch greatly reduces the observed experimental variations. This impacts on the final height of the cavity, because a thicker composite layer will expand more than a thinner one, but also because the heating time for such material will thus vary. On previous systems presented in the literature, the activation time was controlled by the experimenter, avoiding the risk of an incomplete expansion of the material. With an automated system, this correction is not possible any more. The thickness error is also emphasised by the fact that, as explained before¹, the composite itself does not have a reliable expansion ratio.

In order to know the best theoretical reproducibility of this system, which is limited by the fluctuation of gas proportion in Expancel[®], the variation of the vol-

¹See Section 2.5

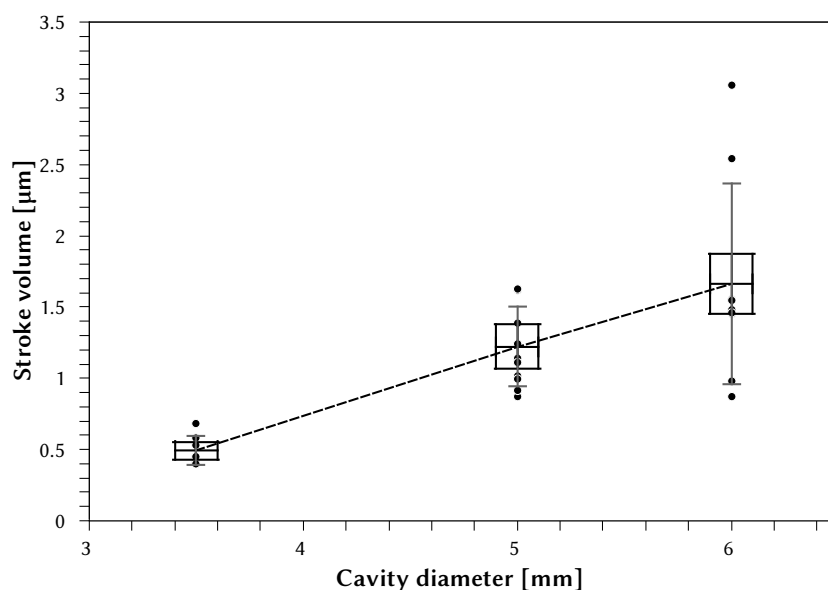


Figure 5.4 Stroke for different sizes of heaters. Each point corresponds to a measurement, error bars are standard deviations and boxes correspond to the theoretical variation of 12.64%. Even if the results are significantly different for the three different sizes, the reproducibility is rather low. Different explanations are possible, such as intrinsic material variation, cavity sticking, misalignment or micro-leakage.

ume of the central cavity was calculated. For a proportion of beads of 15.5%, the expansion ratio theoretically varies between 1.86 and 2.17 if the Young's modulus of PDMS is set at 0.75MPa and the gas proportion is comprised between 0.1 and 0.15. This results in a variation of the chamber's height of 12.64%².

Another variation source in automated systems is the variation of heater resistance. For each imperfection or variation of the resistor, a controlled current results in a change of power and thus of the applied energy. This might induce changes in final expanded volume due to a variable thermal diffusion in the material. This could be corrected by using the heater implementation proposed in the previous chapter, enabling to control the temperature instead of the electrical current.

²See Appendix B.1 for detailed calculations

5.1. *Micro-injector*

5.1.4 **Conclusion**

In the current state of the art, the Expancel[®]-based microinjector system has a theoretical dosing reproducibility around 12 %. Applications using such systems should not be sensitive to reproducibility or should have other systems limiting its variation like pre-dosing the volume of liquid before actuation.

For applications of higher precision, this point can be improved by reducing the expansion ratio variation of Expancel[®] by having a better control on its gas content. Using temperature controlled heating as described in Section 4.1 might also improve the reproducibility, since the expansion rate of the material is also dependant on temperature³.

³See Section 2.2

5.2 Miniaturized blood coagulation testing tool

This section was published as an article in *Micro and Nano Systems* [118], thus some redundancies could be found in the rest of the work.

Nowadays, people undergoing cardiac surgery, suffering from pulmonary embolism, thrombosis or excessive blood clotting are treated with oral anticoagulants such as Warfarin [119]. This treatment requires long term monitoring of blood coagulation parameters to ensure the stability of the patient's coagulation time and to prevent an accident due to change in the living habits of the patient. Home prothrombin time monitoring was reported as a good alternative to control treatment of patients undergoing anticoagulant therapy [119].

Blood coagulation is a complex cascading catalytic reaction, involving several coagulation factors [120]. The use of Warfarin reduces the liver's ability to use vitamin K to produce active forms of proteins needed in the coagulation cascade. This results in slowing down the clotting process. The measurement of this modification of coagulation process is done by the prothrombin time (PT) also called Quick time. PT is often reported as International Normalized Ratio (INR) which compares the PT of the patient to a healthy PT [121]. INR is used to monitor the dosing of oral anti-vitamin K anticoagulant such as Warfarin [122].

PT is measured in a laboratory in presence of an excess of thromboplastin, one of the proteins involved in coagulation [120]. To measure this time, many different detection methods have been described, such as optical measurement [123], impedometric measurement [124, 125], changes in the blood's mechanical properties [126, 127] and channel obstruction [128]. Some are used in laboratory equipment to get high precision results as others have been implemented in point-of-care devices. One of the current point-of-care system using the channel obstruction method is implemented in the ProTime® system (ITC, Edison, US). This patented technology includes syringe pumps linked to a sample channel by fluidic connections [128].

The methodology proposed in this Section will be applicable to handheld devices and is based on the same detection principle: observing the obstruction of a microfluidic channel by the blood due to its clotting. The improvement proposed in the present study is to include the actuation mechanism directly on the disposable test strip and not in the permanent device.

5.2. Miniaturized blood coagulation testing tool

5.2.1 Principle and operation

The microfluidic system was obtained by superimposing several functional layers as described in Figure 5.5. The bottom layer is a printed circuit board on which copper tracks are patterned to define heating elements. A layer of PDMS - Expancel[®] composite is placed on top of the PCB. Finally, a microfabricated glass or PDMS chip containing the cavities and channels is sealed on the thermoexpandable composite to form the channels [96].

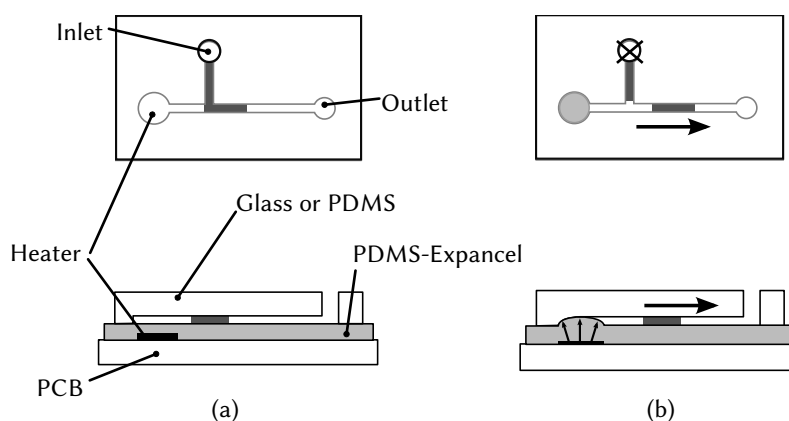


Figure 5.5 Design and operation of the system: (a) the device is composed of several layers. The bottom layer is a PCB on which tracks are acting as heaters. A thermoexpandable composite membrane is placed on top of the PCB. Finally, a PDMS or glass chip containing channels is sealed on the latter. To operate the system, liquid is inserted in the inlet and fills the channel through the outlet by capillarity. The inlet is closed (b) and the thermoexpandable composite is heated and swells. This pushes the air and the liquid in the channel towards the outlet.

The proposed microfluidic system forms a simple T-junction, where one branch leads to actuation cavities through a channel network, while the other two lead to the inlet and outlet. The liquid is inserted in the inlet and flows by capillarity towards the outlet. The inlet is subsequently closed. Several heating elements are placed under the cavities and are powered sequentially, inducing a rise in temperature which leads to the swelling of the thermoexpandable composite, pushing air and therefore the sample toward the outlet.

5.2.2 Experimental conditions

Device fabrication

Spiral heating resistors (600 μm in external diameter and 25 μm wide track) were patterned on a flexible, double sided PCB. Heating tracks lay on one side and interconnections on the other side. Connections between front and back side are performed through 80 μm diameter vias. PCB were fabricated by Cicorel SA, Boudry, Switzerland. To make them rigid, they have been glued on glass chips. A dedicated mold made in polymethyl metacrylate (PMMA) was used to produce 300 μm thick membranes in PDMS - Expancel[®] composite by cast moulding and curing at 55°C overnight.

Glass chips containing channels and cavities have been fabricated by wet 10 %-HF etching of Pyrex. Masking was done by superimposing a Cr / Au / Cr / Au [129–131] mask and a 14 μm thick AZ9268 photoresist, with an intermediate Cr adhesion layer for the resist. After a first 50 μm etch using the photoresist to form the cavities, this mask was removed and a second 50 μm wet etch was performed with the Cr / Au / Cr / Au mask to structure the channels and deepen the cavities. Finally, the Cr / Au mask was stripped in standard Au etch and Cr etch baths. All fabrication steps were realized at the EPFL clean room facility (CMI). The typical volume of the resulting cavities is 20 nl.

The PCB, PDMS - Expancel[®] membranes and glass chip were finally aligned and maintained in a holder.

Chemicals and blood

In all the experiments, the polymer composite has been prepared in 10:2.5:1 PDMS : Expancel[®]: curing agent proportion. The PDMS base was first mixed with the beads and then the curing agent was added. All mixing steps were done by hand and the obtained material was degassed in a vacuum chamber for 20 minutes before molding or spin coating. The PDMS is Sylgard 184 from Dow Corning and the beads are Expancel[®] 820 DU from Azko Nobel provided by Alberto Luosoni SA, Bassecourt, Switzerland. The dye was Patent Blue V obtained from Sigma-Aldrich. Rat blood was obtained from the EPFL animal facility. It was collected in S-Monovette 3ml 9NC citrated syringe and stored at 4°C until the experiment was performed. Calcium solutions were made from calcium chloride dihydrate obtained from Fluka. Prior to performing coagulation experiments on-chip, blood

5.2. Miniaturized blood coagulation testing tool

was mixed with a 100 mM CaCl₂ solution in a 3:1 ratio. As the blood samples were stored for some days before experimentation, the time required for the blood to coagulate was longer than for fresh samples. It has been measured to be between 4 and 5 minutes by preliminary in vitro experiments.

Measurement protocol

A custom experimental setup was developed to perform experiments. A current source (E3136A Triple output, Hewlett-Packard) was used to power the heating elements. MOS transistors (SPP 47N10L, Distrelec, Switzerland) were used to switch sequentially between each heating element. The current source was interfaced via a GPIB-USB connector (GPIB-USB-B, National Instruments) and the transistors via a NiDAQ card (NiDAQ PCI-6251, National Instruments), both connected to a computer and controlled through a MatLab user interface (MatLab 7.2, MathWorks). The progression of the liquid in the channels was recorded by a USB camera (uEye UI-2230-C, IDE). The frame rate was controlled in the MatLab interface and was 2.5 image/s. The liquid progression was analyzed by the same MatLab program.

Once the liquid sample has filled the main channel and the inlet closed by adhesive tape, the heating elements were sequentially activated with a power of 200mW for a duration of 8s with an interval of 1s.

5.2.3 Results

Characterization of the system

Figure 5.6 shows the implemented system (a) and its operation when using blue dye as liquid sample (b). The heaters have been sequentially powered, closing the cavities one at a time and pushing the liquid sample plug in the channel as shown in Figure 5.6-(b). Table 5.1 reports typical initial actuation flow depending on power provided to a heater for a single actuation on the presented system.

By appropriately choosing the actuation sequence, the liquid plug can either be moved continuously in the channel or actuated in steps separated by moments when the sample is immobile, which can be of interest because biological or chemical reactions can take place.

in Figure 5.6-(b) the per-step actuated volume is between 7 to 10 nl, which provides a typical flow of 60 nl/min. Compared to other actuation systems, the flow

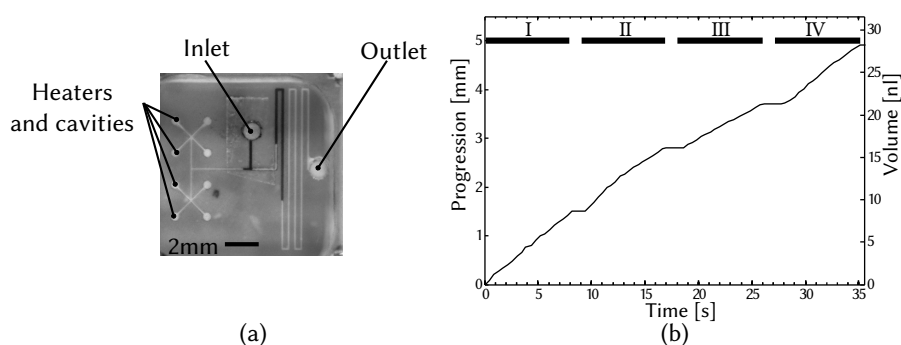


Figure 5.6 Design and operation of the system.(a) The cavities and the associated heaters on the left of the picture are connected to the main channel by a tree connection network. The test liquid is inserted in the inlet and flows through the outlet. The inlet is closed and the heaters are sequentially powered, as indicated by horizontal thick lines, providing the actuation profile showed in (b).

Power [mW]	100	150	175	200
Flow [nl/min]	20	40	47	50

Table 5.1 Averages of reported initial flows for different actuation power in single actuation tests. The experiments were performed by applying the given power to a single heater and measure the resulting flow during the first 5s to 15s depending on the duration of the actuation. We estimated the overall experimental variation on our measurements at 35%.

provided by the system we developed is much smaller than the ones that can be obtained with mechanical actuators; it is also smaller than the flows resulting from some non-mechanical systems such as phase transfer, electrowetting or electrochemical pumps. It is on the same order of magnitude as electrokinetic and electrodynamic flows [57].

As suggested by the results of Table 5.1 and studies of similar systems [98], the expansion dynamic, and thus the liquid flow, can be fine tuned by changing the power provided to the heaters. This allows for more flexibility during the system design and the channel size to fit the application needs better.

Control experiment

A test using recalcified citrated blood was performed on a similar system to demonstrate the capability of the system to perform a coagulation test. For ease of ma-

5.2. Miniaturized blood coagulation testing tool

nipulation during the mixing of the blood with calcium and the insertion in the channels, a coarser setup featuring the same actuation principle was used (Figure 5.7).

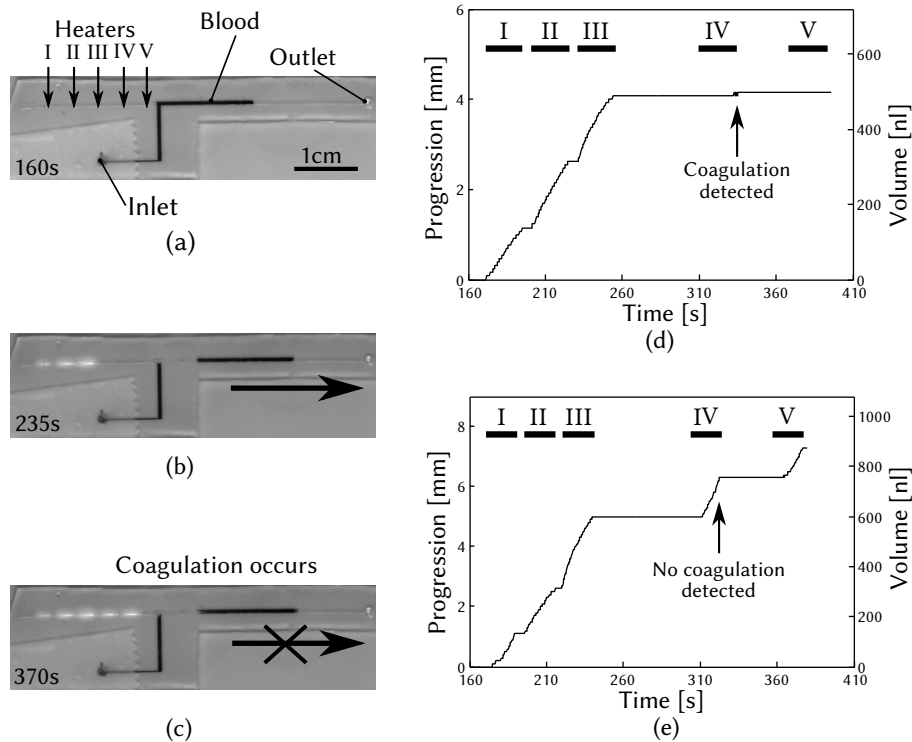


Figure 5.7 Demonstration of the capability of PDMS - Expancel® based systems to test coagulation. Pictures (a)-(c) show the actuation and when the blood stops due to coagulation. (d) shows the actuation profile of recalcified blood. Heaters I, II, III, IV and V, are activated sequentially as indicated by horizontal thick lines. When heaters I, II and II are powered, the blood moves freely in the channel. For heaters IV and V the blood has coagulated and remains stationary. (e) shows a negative control performed by doing the same experiment without adding calcium to the blood, preventing it from coagulating. Again, the activation of heaters I, II, III, IV and V are indicated by horizontal thick lines. Here, even during the activation of heaters IV and V the blood could move freely.

Blood and calcium were inserted in the channel and heaters I-V were sequentially activated. In comparison, a negative control was performed with no calcium addition to the blood, preventing it from coagulating. The blood was inserted on the chip 160s after the addition of calcium, allowing the mixing of the blood and CaCl_2 solution off-chip during the positive test. Figure 5.7 shows the progression of the blood samples in the channels due to the actuation. The result of the coag-

ulation test is shown in Figure 5.7-(d): the blood is flowing during the actuation of heaters I to III, but after the actuation of heaters IV and V no more movement is observed, indicating that coagulation occurred between 4min20s and 5min10sec after the addition of calcium. On the other hand, as shown in Figure 5.7-(e), on the negative control, the displacement of the blood continues during all the actuation phases. The experiments performed with this test device demonstrate the principle of the blood coagulation test on PDMS - Expancel® actuated systems.

5.2.4 Conclusion

A system allowing the actuation of liquid in a flow range of 60nl/min using a thermoexpandable PDMS - Expancel® actuator on a chip was realised. We also demonstrated the capability of this system to perform blood coagulation testing on-chip using a thermoexpandable composite as fluid flow actuator for moving the sample in a microchannel until coagulation occurs and stops the liquid movement.

The coagulation of blood was demonstrated not to be prevented by the temperature rise induced by the activation heaters. Deeper investigations could be made to know the impact of temperature on the final result, for example by in situ temperature measurement or coagulation time comparison with a “cold” actuation system.

This system has a good flexibility in pressure and flow applied on the fluid. The pressure applied on the liquid can be tuned by adapting the fluidic resistance between the actuation site and the liquid. The speed of the sample can be chosen by changing the power supplied to the heaters and the number of steps during the actuation can be adapted by the number of heaters. This type of sequential actuation can be promising for the implementation of the different reaction steps required in prothrombin time measurements, such as citration, addition of thromboplastin and recalcification of blood.

5.3 Applications roundup

Two applications of PDMS - Expancel[®] composite as microfluidic actuator were proposed. They coherently illustrate how the imperfections of the PDMS - Expancel[®] composite can influence the application.

The first application, the micro-injector, has a reproducibility highly dependant on the expansion ratio of the composite. This will lead to a quite low reproducibility. This application would profit a lot from an improvement of the reproducibility of the material, either by refining it or by improving the fabrication process.

On the other hand, the coagulation testing system is an application where the actuation precision is much less critical. Thus, it is less influenced by the variation of the expansion ratio. In this way, it is a perfect example of how to by-pass the imperfection of the material.

Contents

6.1	Summary of results	90
6.1.1	Characterisation and modelling	90
6.1.2	Heating systems	91
6.1.3	Applications	91
6.2	Perspectives	92

6.1 Summary of results

6.1.1 Characterisation and modelling

One of the goals of this work was to develop tools to assess the use of PDMS - Expancel[®] as microfluidic actuator and help the design of systems using it. Since this composite relies on materials sourced from different manufacturers, it is subject to reformulation modifying the properties of its components. Providing a set of experiments in order to determine the properties of the material allows to perform a full characterisation on new formulations of the components and on the composite itself. Thus, the characterisation part of this work provides a methodology to evaluate the properties of similar materials.

The proposed methodology allows to define the expansion ratio of the composite under different environments. The pressure provided by the system can also be measured if the proposed correction to the setup of Section 2.4 are applied in order to get reliable measurements. The activation temperature range can be determined using DMA.

Modelling allows to assess the mechanical and physical parameters that will influence the expansion ratio.

Results of material characterisation have highlighted some points of interest for the use of the PDMS - Expancel[®] composite as microfluidic actuator:

- The material expands between 1.1 and 4 folds depending on the amount of Expancel[®] in the composite.
- The best actuation temperature is around 90 °C, because at that temperature most beads have expanded and no degradation seems to occur.
- The composite expansion suffers from a large dependence on the properties of both its components.
- The size of the beads, their gas proportion and the Young's modulus of the matrix can vary to a large extent, making the expansion ratio hardly reproducible on large series.
- Expansion ratio is also altered by the environment of the composite.

Those properties make it difficult to have reliable free expansion ratios: this material is, at the moment, more suitable to use confined in cavities in order to gain in reproducibility.

6.1.2 Heating systems

Several systems have been evaluated and a temperature controlled device has been fabricated. The latter highlights the possibility to control the geometry of the expansion through temperature. However, inaccuracies in temperature control were due to the mounting of the temperature sensor. In order to get better results, a more reliable thermal connection needs to be implemented between the temperature sensor and the heater. This can be done by using a screen printed resistor as sensor. This was already achieved in previous work, but would require better NTC characteristic of the paste or more sensitive electronics to have a sufficient thermal resolution.

In other systems without temperature control, the use of Ti/Pt electrodes is too expensive to ever be combined with a disposable device. Thus, it is not a possible alternative to be used with PDMS - Expancel[®] composites. On the other hand, conducting PDMS is, in terms of cost, compatible with PDMS - Expancel[®] composites. Compared to screen-printed systems, the size of the heaters fabricated in conductive PDMS is much bigger. It is thus not applicable for actuation of small amount of liquid (hundreds of nl), but might be a good alternative to inject higher volumes (hundreds of μ l).

6.1.3 Applications

The two applications proposed were a micro-injection system and a coagulation testing system. In the former, it has been demonstrated that a reliable system will be hard to fabricate because it expands freely and suffers from the fluctuation of the material. On the other hand, the coagulation testing tool proves it is suitable as actuation if reliability is not a requirement for the good function of the system.

The PDMS - Expancel[®] composite is thus a good solution for liquid displacement in microsystems, but not for dosing until the lack of reproducibility is corrected. It is of course only suitable for disposable devices due to its irreversibility and its implementation being compatible with relatively compact systems such as handheld devices.

6.2 Perspectives

As shown by the results stated above, the PDMS - Expancel[®] composite is currently very limited by the lack of reproducibility of its two components. Expancel[®] suffers from its primary application where expansion ratio reliability is not an issue. Its fabrication process does not permit a constant size and composition of the particles. In order to achieve better material reproducibility, work needs to be done either on particles synthesis or in refining them. If particles of the same size have the same expansion temperature and blowing agent proportion, selection based on this criteria might improve the reproducibility. Since size segregation attempts discussed in this work were performed, Azko Nobel created a new formulation of Expancel[®] with a lower tendency to aggregate (031 DUX 40). This enable further work to succeed in selection of size.

Young's modulus of PDMS is also a varying factor, but it seems that this variation can be correlated with processing factors. Thus, by controlling precisely the crosslinking time and temperature, one could achieve reliable enough mechanical properties of the matrix to allow for a reproducible expansion ratio.

Looking at applications, the actuation temperature of 90 °C might be an important drawback in the case of biological applications. Indeed, this high temperature may interfere with biological processes or change properties of sensitive elements such as proteins. Consequently, it would be of interest to synthesise beads with a different expansion temperature to get more flexibility in design and avoid the need to create thermal insulation when using Expancel[®] in biological applications. By being able to choose the temperature, it can be set to a value triggering thermally sensitive biological reaction like PCR.

PDMS - Expancel[®] composites currently provide a low cost and disposable actuation system for applications where reproducibility of actuation itself is not an issue. On the other hand, as shown by the model proposed in this work, it is highly dependant on properties of its components and suffers from their imperfections. Nevertheless, with some developments to improve reproducibility, it will provide a smart and easily manufactured actuation method for disposable devices as needed in medicine and biology.

Bibliography

- [1] T. A. Franke and A. Wixforth. “Microfluidics for miniaturized laboratories on a chip” *ChemPhysChem*, Vol. 9, No. 15, pp. 2140–2156, 2008, doi: 10.1002/cphc.200800349.
- [2] P. Yager, T. Edwards, E. Fu, K. Helton, K. Nelson, M. Tam, and B. Weigl. “Microfluidic diagnostic technologies for global public health” *Nature*, Vol. 442, No. 7101, pp. 412–418, 2006, doi: 10.1038/nature05064.
- [3] A. de Mello and R. Wootton. “But what is it good for? Applications of microreactor technology for the fine chemical industry” *Lab on a Chip - Miniaturisation for Chemistry and Biology*, Vol. 2, No. 1, 2002, doi: 10.1039/b200736n.
- [4] H. Becker and L. Locascio. “Polymer microfluidic devices” *Talanta*, Vol. 56, No. 2, pp. 267–287, 2002, doi: 10.1016/S0039-9140(01)00594-X.
- [5] M. Behl and A. Lendlein. “Actively moving polymers” *Soft Matter*, Vol. 3, No. 1, pp. 58–67, 2007, doi: 10.1039/b610611k.
- [6] F. Liou and Y. Wang. “Preparation and characterization of crosslinked and heat-treated pva-ma films” *Journal of Applied Polymer Science*, Vol. 59, No. 9, pp. 1395–1403, 1996, doi: 10.1002/(SICI)1097-4628(19960228)59:9<1395::AID-APP7>3.0.CO;2-6.
- [7] A. Baldi, Y. Gu, P. Loftness, R. Siegel, and B. Ziaie, “A hydrogel-actuated smart microvalve with a porous diffusion barrier back-plate for active flow control,” in *Proceedings of the IEEE Micro Electro Mechanical Systems (MEMS)*, 2002, pp. 105–108.

- [8] J. McDonald, D. Duffy, J. Anderson, D. Chiu, H. Wu, O. Schueller, and G. Whitesides. "Fabrication of microfluidic systems in poly(dimethylsiloxane)" *Electrophoresis*, Vol. 21, No. 1, pp. 27–40, 2000, doi: 10.1002/(SICI)1522-2683(20000101)21:1<27::AID-ELPS27>3.0.CO;2-C.
- [9] J. Ng, I. Gitlin, A. Stroock, and G. Whitesides. "Components for integrated poly(dimethylsiloxane) microfluidic systems" *Electrophoresis*, Vol. 23, No. 20, pp. 3461–3473, 2002, doi: 10.1002/1522-2683(200210)23:20<3461::AID-ELPS3461>3.0.CO;2-8.
- [10] C. Friedel and J. M. Crafts. "Sur quelques nouvelles combinaisons organiques du silicium et sur le poids atomique de cet element" *Comptes Rendus des Séances de l'Académie des Sciences*, Vol. 56, pp. 590–594, 1863.
- [11] F. S. Kipping and L. L. Lloyd. "XLVII.-organic derivatives of silicon. triphenylsilicol and alkyloxysilicon chlorides" *Journal of the Chemical Society, Transactions*, Vol. 79, pp. 449–459, 1901, doi: 10.1039/CT9017900449.
- [12] Dow Corning Corporation. *Dow corning website*, Online: <http://www.dowcorning.com>, last visited on August 10th, 2010.
- [13] N. Ravo. "J. Franklin Hyde, 96, the 'Father of Silicones'" *New York Times*, October 16th, 1999.
- [14] L. B. Loeb, *Electrical coronas : their basic physical mechanisms* Berkeley : University of California Press, 1965.
- [15] Dow Corning Silicones. *Highlights from the history of Dow Corning Corporation, the silicone pioneer*, Online: <http://www.dowcorning.com/content/publishedlit/01-4027-01.pdf>, last visited on August 10th, 2010.
- [16] J. E. Mark, *The polymer data handbook* Oxford University Press, 2009.
- [17] A. Colas. "Silicone: Preparation, properties and performances" *Chimie Nouvelle*, Vol. 8, No. 30, p. 847, 1990.
- [18] S. Sia and G. Whitesides. "Microfluidic devices fabricated in poly(dimethylsiloxane) for biological studies" *Electrophoresis*, Vol. 24, No. 21, pp. 3563–3576, 2003, doi: 10.1002/elps.200305584.

- [19] M. A. Unger, H. P. Chou, T. Thorsen, A. Scherer, and S. R. Quake. “Monolithic microfabricated valves and pumps by multilayer soft lithography” *Science*, Vol. 288, No. 5463, pp. 113–116, 2000, doi: 10.1126/science.288.5463.113.
- [20] C. S. Effenhauser, G. J. M. Bruin, A. Paulus, and M. Ehrat. “Integrated capillary electrophoresis on flexible silicone microdevices: analysis of dna restriction fragments and detection of single dna molecules on microchips” *Analytical Chemistry*, Vol. 69, No. 17, pp. 3451–3457, 1997, doi: 10.1021/ac9703919.
- [21] M. A. Eddings, M. A. Johnson, and B. K. Gale. “Determining the optimal PDMS–PDMS bonding technique for microfluidic devices” *Journal of Micromechanics and Microengineering*, Vol. 18, No. 6, p. 067001, 2008, doi: 10.1088/0960-1317/18/6/067001.
- [22] B. Samel, M. Chowdhury, and G. Stemme. “The fabrication of microfluidic structures by means of full-wafer adhesive bonding using a poly(dimethylsiloxane) catalyst” *Journal of Micromechanics and Microengineering*, Vol. 17, No. 8, pp. 1710–1714, 2007, doi: 10.1088/0960-1317/17/8/038.
- [23] S. Satyanarayana, R. Karnik, and A. Majumdar. “Stamp-and-stick room-temperature bonding technique for microdevices” *Microelectromechanical Systems, Journal of*, Vol. 14, No. 2, pp. 392 – 399, april 2005, doi: 10.1109/JMEMS.2004.839334.
- [24] M. A. Eddings and B. K. Gale. “A PDMS-based gas permeation pump for on-chip fluid handling in microfluidic devices” *Journal of Micromechanics and Microengineering*, Vol. 16, No. 11, p. 2396, 2006, doi: 10.1088/0960-1317/16/11/021.
- [25] J. El-Ali, I. Perch-Nielsen, C. Poulsen, D. Bang, P. Telleman, and A. Wolff. “Simulation and experimental validation of a su-8 based pcr thermocycler chip with integrated heaters and temperature sensor” *Sensors and Actuators, A: Physical*, Vol. 110, No. 1-3, pp. 3–10, 2004, doi: 10.1016/j.sna.2003.09.022.
- [26] M. Ni, W. H. Tong, D. Choudhury, N. A. A. Rahim, C. Iliescu, and H. Yu. “Cell culture on mems platforms: A review” *International Journal of Molecular Sciences*, Vol. 10, No. 12, pp. 5411–5441, 2009, doi: 10.3390/ijms10125411.

- [27] J. Lee, C. Park, and G. Whitesides. "Solvent compatibility of poly(dimethylsiloxane)-based microfluidic devices" *Analytical Chemistry*, Vol. 75, No. 23, pp. 6544–6554, 2003, doi: 10.1021/ac0346712.
- [28] R. Mukhopadhyay. "When PDMS isn't the best" *Analytical Chemistry*, Vol. 79, No. 9, pp. 3248–3253, May 2007, doi: 10.1021/ac071903e.
- [29] H. Makamba, J. Kim, K. Lim, N. Park, and J. Hahn. "Surface modification of poly(dimethylsiloxane) microchannels" *Electrophoresis*, Vol. 24, No. 21, pp. 3607–3619, 2003, doi: 10.1002/elps.200305627.
- [30] S. Hu, X. Ren, M. Bachman, C. E. Sims, G. P. Li, and N. Allbritton. "Surface modification of poly(dimethylsiloxane) microfluidic devices by ultraviolet polymer grafting" *Analytical Chemistry*, Vol. 74, No. 16, pp. 4117–4123, 2002, doi: 10.1021/ac025700w.
- [31] H. Hillborg and U. Gedde. "Hydrophobicity recovery of polydimethylsiloxane after exposure to corona discharges" *Polymer*, Vol. 39, No. 10, pp. 1991 – 1998, 1998, doi: DOI: 10.1016/S0032-3861(97)00484-9.
- [32] K. Efimenko, W. E. Wallace, and J. Genzer. "Surface modification of sylgard-184 poly(dimethyl siloxane) networks by ultraviolet and ultraviolet/ozone treatment" *Journal of Colloid and Interface Science*, Vol. 254, No. 2, pp. 306 – 315, 2002, doi: 10.1006/jcis.2002.8594.
- [33] M. Chaudhury and G. Whitesides. "Direct measurement of interfacial interactions between semispherical lenses and flat sheets of poly(dimethylsiloxane) and their chemical derivatives" *Langmuir*, Vol. 7, No. 5, pp. 1013–1025, 1991, doi: 10.1021/la00053a033.
- [34] M. Morra, E. Occhiello, R. Marola, F. Garbassi, P. Humphrey, and D. Johnson. "On the aging of oxygen plasma-treated polydimethylsiloxane surfaces" *Journal of Colloid and Interface Science*, Vol. 137, No. 1, pp. 11 – 24, 1990, doi: 10.1016/0021-9797(90)90038-P.
- [35] B. Kim, E. Peterson, and I. Papautsky, "Long-term stability of plasma oxidized PDMS surfaces," in *26th Annual International Conference of the IEEE Engineering in Medicine and Biology Society, EMBC*, vol. 26 VII, 2004, pp. 5013–5016.

- [36] S. M. Hong, S. H. Kim, J. H. Kim, and H. I. Hwang. “Hydrophilic surface modification of PDMS using atmospheric RF plasma” *Journal of Physics: Conference Series*, Vol. 34, No. 1, p. 656, 2006, doi: 10.1088/1742-6596/34/1/108.
- [37] D. Bodas and C. Khan-Malek. “Formation of more stable hydrophilic surfaces of pdms by plasma and chemical treatments” *Microelectronic Engineering*, Vol. 83, No. 4-9, pp. 1277 – 1279, 2006, doi: 10.1016/j.mee.2006.01.195.
- [38] D. Eddington, J. Puccinelli, and D. Beebe. “Thermal aging and reduced hydrophobic recovery of polydimethylsiloxane” *Sensors and Actuators, B: Chemical*, Vol. 114, No. 1, pp. 170–172, 2006, doi: 10.1016/j.snb.2005.04.037.
- [39] D. Duffy, J. McDonald, O. Schueller, and G. Whitesides. “Rapid prototyping of microfluidic systems in poly(dimethylsiloxane)” *Analytical Chemistry*, Vol. 70, No. 23, pp. 4974–4984, 1998, doi: 10.1021/ac980656z.
- [40] J. Anderson, D. Chiu, R. Jackman, O. Chmiavskaya, J. McDonald, H. Wu, S. Whitesides, and G. Whitesides. “Fabrication of topologically complex three-dimensional microfluidic systems in pdms by rapid prototyping” *Analytical Chemistry*, Vol. 72, No. 14, pp. 3158–3164, 2000, doi: 10.1021/ac9912294.
- [41] H. Becker and C. Gärtner. “Polymer microfabrication methods for microfluidic analytical applications” *Electrophoresis*, Vol. 21, No. 1, pp. 12–26, 2000, doi: 10.1002/(SICI)1522-2683(20000101)21:1<12::AID-ELPS12>3.0.CO;2-7.
- [42] A. Bernard, E. Delamarche, H. Schmid, B. Michel, H. R. Bosshard, and H. Biebuyck. “Printing patterns of proteins” *Langmuir*, Vol. 14, No. 9, pp. 2225–2229, 1998, doi: 10.1021/la980037l.
- [43] Azko Nobel. *Expancel*, Online: <http://www.akzonobel.com/expancel/>, last visited on August 13th, 2010.
- [44] US Patent 3 615 972 “Expansible thermoplastic polymer particles containing volatile fluid foaming agent and method of foaming the same” October, 1971.
- [45] Alberto Luisoni, “Expancel 820DU40 safety datasheet,” 2009.
- [46] P. Griss, H. Andersson, and G. Stemme. “Expandable microspheres for the handling of liquids” *Lab on a Chip*, Vol. 2, No. 2, pp. 117–120, 2002, doi: 10.1039/b111040n.

- [47] H. Aglan, S. Shebl, M. Morsy, M. Calhoun, H. Harding, and M. Ahmad. “Strength and toughness improvement of cement binders using expandable thermoplastic microspheres” *Construction and Building Materials*, Vol. 23, No. 8, pp. 2856 – 2861, 2009, doi: 10.1016/j.conbuildmat.2009.02.031.
- [48] M. Ahmad. “Flexible vinyl resiliency property enhancement with hollow thermoplastic microspheres” *Journal of Vinyl and Additive Technology*, Vol. 7, No. 3, pp. 156–161, 2001.
- [49] K. F. Jensen. “Microreaction engineering – is small better?” *Chemical Engineering Science*, Vol. 56, No. 2, pp. 293 – 303, 2001, doi: 10.1016/S0009-2509(00)00230-X.
- [50] H. Stone, A. Stroock, and A. Ajdari. “Engineering flows in small devices: Microfluidics toward a lab-on-a-chip” *Annual Review of Fluid Mechanics*, Vol. 36, No. 1, pp. 381–411, 2004, doi: 10.1146/annurev.fluid.36.050802.122124.
- [51] G. M. Whitesides. “The origins and the future of microfluidics” *Nature*, Vol. 442, No. 7101, pp. 368–373, Jul. 2006, doi: 10.1038/nature05058.
- [52] S. Terry, J. Jerman, and J. Angell. “A gas chromatographic air analyzer fabricated on a silicon wafer” *Electron Devices, IEEE Transactions on*, Vol. 26, No. 12, pp. 1880 – 1886, dec 1979, doi: 10.1016/0160-4120(81)90126-4.
- [53] A. Manz, N. Graber, and H. Widmer. “Miniaturized total chemical analysis systems: A novel concept for chemical sensing” *Sensors and Actuators B: Chemical*, Vol. 1, No. 1-6, pp. 244 – 248, 1990, doi: 10.1016/0925-4005(90)80209-I.
- [54] S. Haeberle and R. Zengerle. “Microfluidic platforms for lab-on-a-chip applications” *Lab on a Chip*, Vol. 7, No. 9, pp. 1094–1110, 2007, doi: 10.1039/b706364b.
- [55] K. Oh and C. Ahn. “A review of microvalves” *Journal of Micromechanics and Microengineering*, Vol. 16, No. 5, 2006, doi: 10.1088/0960-1317/16/5/R01.
- [56] N.-T. Nguyen and Z. Wu. “Micromixers - a review” *Journal of Micromechanics and Microengineering*, Vol. 15, No. 2, pp. R1–R16, 2005, doi: 10.1088/0960-1317/15/2/R01.

- [57] N. T. Nguyen, X. Huang, and T. K. Chuan. “MEMS-micropumps: A review” *Journal of Fluids Engineering*, Vol. 124, No. 2, pp. 384–392, 2002, doi: 10.1115/1.1459075.
- [58] B. Iverson and S. Garimella. “Recent advances in microscale pumping technologies: A review and evaluation” *Microfluidics and Nanofluidics*, Vol. 5, No. 2, pp. 145–174, 2008, doi: 10.1007/s10404-008-0266-8.
- [59] R. C. Wong and H. Y. Tse, Eds., *Lateral Flow Immunoassay* Humana Press, 2009.
- [60] Abaxis. *Abaxis medical diagnostics: PiccoloXpress*, Online: <http://www.piccoloxpress.com/>, last visited on August 17th, 2010.
- [61] N. G. Anderson. “Computer interfaced fast analyzers” *Science*, Vol. 166, No. 3903, pp. 317–324, 1969.
- [62] C. A. Burtis, J. C. Mailen, W. F. Johnson, C. D. Scott, T. O. Tiffany, and N. G. Anderson. “Development of a miniature fast analyzer” *Clin Chem*, Vol. 18, No. 8, pp. 753–761, 1972.
- [63] M. Madou, J. Zoval, G. Jia, H. Kido, J. Kim, and N. Kim. “Lab on a cd” *Annual Review of Biomedical Engineering*, Vol. 8, No. 1, pp. 601–628, 2006, doi: 10.1146/annurev.bioeng.8.061505.095758.
- [64] S. F. Bart, L. S. Tavrow, M. Mehregany, and J. H. Lang. “Microfabricated electrohydrodynamic pumps” *Sensors and Actuators A*, Vol. 21, No. 1-3, pp. 193–197, 1990.
- [65] D. J. Harrison, A. Manz, and P. G. Glavina, “Electroosmotic pumping within a chemical sensor system integrated on silicon,” in *Proceeding Transducers '91*, 1991, pp. 792–795.
- [66] H. Matsumoto and J. E. Colgate, “Preliminary investigation of micropumping based on electrical control of interfacial tension,” in *Proc. IEEE Micro Electro Mechanical Systems*, 1990, pp. 105–110.
- [67] M. Lewandowski, D. A. Ateya, A. A. Shah, and S. Z. Hua, “Sequential electrolytic bubble-based micro-pump dosing system,” in *Proceeding. ASME 2003 International Mechanical Engineering Congress and Exposition*, vol. 5, 2003, pp. 379–383.

- [68] S. Böhm, B. Timmer, W. Olthuis, and P. Bergveld. “Closed-loop controlled electrochemically actuated micro-dosing system” *Journal of Micromechanics and Microengineering*, Vol. 10, No. 4, pp. 498–504, 2000, doi: 10.1088/0960-1317/10/4/303.
- [69] L. Metref, F. Herrera, D. Berdat, and M. Gijs. “Contactless electrochemical actuator for microfluidic dosing” *Journal of Microelectromechanical Systems*, Vol. 16, No. 4, pp. 885–892, 2007, doi: 10.1109/JMEMS.2007.892893.
- [70] K. Pitchaimani, B. C. Sapp, A. Winter, A. Gispanski, T. Nishida, and Z. H. Fan. “Manufacturable plastic microfluidic valves using thermal actuation” *Lab on a Chip*, Vol. 9, No. 21, pp. 3082–3087, 2009, doi: 10.1039/b909742b.
- [71] H. Takagi, R. Maeda, K. Ozaki, M. Parameswaran, and M. Mehta, “Phase transformation type micro pump,” in *Proc. of the International Symposium on Micro Machine and Human Science*, 1994, pp. 199–202.
- [72] T. Braschler, L. Metref, R. Zvitov-Marabi, H. Van Lintel, N. Demierre, J. Theytaz, and P. Renaud. “A simple pneumatic setup for driving microfluidics” *Lab on a Chip*, Vol. 7, No. 4, pp. 420–422, 2007, doi: 10.1039/b617673a.
- [73] H.-P. Chou, M. Unger, and S. Quake. “A microfabricated rotary pump” *Biomedical Microdevices*, Vol. 3, No. 4, pp. 323–330, 2001, doi: 10.1023/A:1012412916446.
- [74] A. Groisman, M. Enzelberger, and S. Quake. “Microfluidic memory and control devices” *Science*, Vol. 300, No. 5621, pp. 955–958, 2003, doi: 10.1126/science.1083694.
- [75] C.-C. Lee, G. Sui, A. Elizarov, C. Shu, Y.-S. Shin, A. Dooley, J. Huang, A. Daridon, P. Wyatt, D. Stout, H. Kolb, O. Witte, N. Satyamurthy, J. Heath, M. Phelps, S. Quake, and H.-R. Tseng. “Multistep synthesis of a radiolabeled imaging probe using integrated microfluidics” *Science*, Vol. 310, No. 5755, pp. 1793–1796, 2005, doi: 10.1126/science.1118919.
- [76] J. Liu, M. Enzelberger, and S. Quake. “A nanoliter rotary device for polymerase chain reaction” *Electrophoresis*, Vol. 23, No. 10, pp. 1531–1536, 2002, doi: 10.1002/1522-2683(200205)23:10<1531::AID-ELPS1531>3.0.CO;2-D.
- [77] T. Thorsen, S. Maerkl, and S. Quake. “Microfluidic large-scale integration” *Science*, Vol. 298, No. 5593, pp. 580–584, 2002, doi: 10.1126/science.1076996.

- [78] H. T. G. van Lintel, F. C. M. van De Pol, and S. Bouwstra. “A piezoelectric micropump based on micromachining of silicon” *Sensors and Actuators*, Vol. 15, No. 2, pp. 153–167, 1988.
- [79] B. Büstgens, W. Bacher, W. Bier, R. Ehnes, D. Maas, R. Ruprecht, W. K. Schomburg, and L. Keydel, “Micromembrane pump manufactured by molding,” in *Proceedings. Actuator '94*, 1994, pp. 86–90.
- [80] J. Ni, F. Huang, B. Wang, B. Li, and Q. Lin. “A planar pdms micropump using in-contact minimized-leakage check valves” *Journal of Micromechanics and Microengineering*, Vol. 20, No. 9, p. 095033, 2010, doi: 10.1088/0960-1317/20/9/095033.
- [81] J. G. Smits. “Piezoelectric micropump with three valves working peristaltically” *Sensors and Actuators A*, Vol. 21, No. 1-3, pp. 203–206, 1990, doi: 10.1016/0924-4247(90)85039-7.
- [82] E. Stemme and G. Stemme. “A valveless diffuser/nozzle-based fluid pump” *Sensors and Actuators A*, Vol. 39, No. 2, pp. 159–167, 1993, doi: 10.1016/0924-4247(93)80213-Z.
- [83] C. H. Ahn and M. G. Allen, “Fluid micropumps based on rotary magnetic actuators,” in *Proc. of the IEEE Micro Electro Mechanical Systems*, 1995, pp. 408–412.
- [84] K. Gall, P. Kreiner, D. Turner, and M. Hulse. “Shape-memory polymers for microelectromechanical systems” *Microelectromechanical Systems, Journal of*, Vol. 13, No. 3, pp. 472 – 483, june 2004, doi: 10.1109/JMEMS.2004.828727.
- [85] A. Lendlein and S. Kelch. “Shape-memory polymers” *Angewandte Chemie International Edition*, Vol. 41, No. 12, pp. 2034–2057, 2002, doi: 10.1002/1521-3773(20020617)41:12<2034::AID-ANIE2034>3.0.CO;2-M.
- [86] E. S. Gil and S. M. Hudson. “Stimuli-responsive polymers and their bioconjugates” *Progress in Polymer Science*, Vol. 29, No. 12, pp. 1173 – 1222, 2004, doi: 10.1016/j.progpolymsci.2004.08.003.
- [87] D. Eddington and D. Beebe. “A valved responsive hydrogel microdispensing device with integrated pressure source” *Journal of Microelectromechanical Systems*, Vol. 13, No. 4, pp. 586–593, 2004, doi: 10.1109/JMEMS.2004.832190.

- [88] M. Harmon, M. Tang, and C. Frank. “A microfluidic actuator based on thermoresponsive hydrogels” *Polymer*, Vol. 44, No. 16, pp. 4547–4556, 2003, doi: 10.1016/S0032-3861(03)00463-4.
- [89] J. Hoffmann, M. Plötner, D. Kuckling, and W. J. Fischer. “Photopatterning of thermally sensitive hydrogels useful for microactuators” *Sensors and Actuators A*, Vol. 77, No. 2, pp. 139–144, 1999, doi: 10.1016/S0924-4247(99)00080-1.
- [90] D. Eddington and D. Beebe. “Flow control with hydrogels” *Advanced Drug Delivery Reviews*, Vol. 56, No. 2, pp. 199–210, 2004, doi: 10.1016/j.addr.2003.08.013.
- [91] D. J. Beebe, J. S. Moore, J. M. Bauer, Q. Yu, R. H. Liu, C. Devadoss, and B. H. Jo. “Functional hydrogel structures for autonomous flow control inside microfluidic channels” *Nature*, Vol. 404, No. 6778, pp. 588–590, 2000, doi: 10.1038/35007047.
- [92] E. J. Geiger, A. P. Pisano, and F. Svec. “A polymer-based microfluidic platform featuring on-chip actuated hydrogel valves for disposable applications” *Microelectromechanical Systems, Journal of*, Vol. 19, No. 4, pp. 944–950, aug. 2010, doi: 10.1109/JMEMS.2010.2048702.
- [93] P. Selvaganapathy, E. T. Carlen, and C. H. Mastrangelo. “Electrothermally actuated inline microfluidic valve” *Sensors and Actuators A: Physical*, Vol. 104, No. 3, pp. 275–282, 2003, doi: 10.1016/S0924-4247(03)00030-X.
- [94] G. Kaigala, V. Hoang, and C. Backhouse. “Electrically controlled microvalves to integrate microchip polymerase chain reaction and capillary electrophoresis” *Lab on a Chip*, Vol. 8, No. 7, pp. 1071–1078, 2008, doi: 10.1039/b802853b.
- [95] B. Samel, P. Griss, and G. Stemme. “A thermally responsive pdms composite and its microfluidic applications” *Journal of Microelectromechanical Systems*, Vol. 16, pp. 50–57, Feb. 2007, doi: 10.1109/JMEMS.2006.886025.
- [96] B. Samel, V. Nock, A. Russom, P. Griss, and G. Stemme. “A disposable lab-on-a-chip platform with embedded fluid actuators for active nanoliter liquid handling” *Biomedical Microdevices*, Vol. 9, No. 1, pp. 61–67, 2007, doi: 10.1007/s10544-006-9015-5.

- [97] B. Samel, P. Griss, and G. Stemme, “Active liquid aspiration and dispensing based on an expanding PDMS composite,” in *Proceedings IEEE International Conference on Micro Electro Mechanical Systems (MEMS)*, Jan. 2007, pp. 565–568.
- [98] B. Samel, J. Chretien, R. Yue, P. Griss, and G. Stemme. “Wafer-level process for single-use buckling film microliter-range pumps” *Journal of Microelectromechanical Systems*, Vol. 16, No. 4, pp. 795–801, 2007, doi: 10.1109/JMEMS.2007.901642.
- [99] M. Liu, J. Sun, and Q. Chen. “Influences of heating temperature on mechanical properties of polydimethylsiloxane” *Sensors and Actuators A*, Vol. 151, No. 1, pp. 42 – 45, 2009, doi: 10.1016/j.sna.2009.02.016.
- [100] D. Fuard, T. Tzvetkova-Chevolleau, S. Decossas, P. Tracqui, and P. Schiavone. “Optimization of poly-di-methyl-siloxane (PDMS) substrates for studying cellular adhesion and motility” *Microelectronic Engineering*, Vol. 85, No. 5-6, pp. 1289 – 1293, 2008, doi: 10.1016/j.mee.2008.02.004.
- [101] D. Armani, C. Liu, and N. Aluru, “Re-configurable fluid circuits by pdms elastomer micromachining,” in *Proceedings of the IEEE Micro Electro Mechanical Systems (MEMS)*, Anon, Ed. IEEE, 1999, pp. 222–227.
- [102] C. Antoine. “Tensions des vapeurs; nouvelle relation entre les tensions et les températures” *Comptes Rendus des Séances de l’Académie des Sciences*, Vol. 107, pp. 681–684, 1888.
- [103] D. R. Lide, Ed., *CRC Handbook of Chemistry and Physics*, 74th ed. CRC Press, 1993.
- [104] C. Song, P. Wang, and H. A. Makse. “A phase diagram for jammed matter” *Nature*, Vol. 453, No. 7195, pp. 629–632, May 2008, doi: 10.1038/nature06981.
- [105] P. Tabeling, *Introduction à la microfluidique* Belin, 2003.
- [106] DIN 51 007, Deutsches Institut für Normung Std., *Thermal analysis; differential thermal analysis; principles*, June 1994.
- [107] S. Marcus and R. Blaine. “Thermal conductivity of polymers, glasses and ceramics by modulated dsc” *Thermochimica Acta*, Vol. 243, No. 2, pp. 231–239, Sep. 1994, doi: 10.1016/0040-6031(94)85058-5.

- [108] Air Liquide. *Isobutane*, Online: <http://encyclopedia.airliquide.com/encyclopedia.asp?GasID=38>, last visited on August 6th, 2010.
- [109] M. Amon and C. D. Denson. “A study of the dynamics of foam growth: Analysis of the growth of closely spaced spherical bubbles” *Polymer Engineering & Science*, Vol. 24, No. 13, pp. 1026–1034, 1984, doi: 10.1002/pen.760241306.
- [110] W. C. Young, R. G. Budynas, and R. J. Roark, *Roark’s formulas for stress and strain*, 7th ed. McGraw-Hill, 2002.
- [111] K. Pitt, *Handbook of thick film technology* Electrochemical Publications, 2005.
- [112] R. Longchamp, *Commande numérique de systèmes dynamiques* Presses Polytechniques et Universitaires Romandes, 1995.
- [113] J. Nicolics, M. Mundlein, G. Hanreich, A. Zluc, H. Stahr, and M. Franz, “Thermal analysis of multilayer printed circuit boards with embedded carbon black-polymer resistors,” in *Proc. th International Spring Seminar on Electronics Technology*, May 9-13, 2007, pp. 46–52.
- [114] H.-S. Chuang and S. Wereley. “Design, fabrication and characterization of a conducting pdms for microheaters and temperature sensors” *Journal of Micromechanics and Microengineering*, Vol. 19, No. 4, p. 045010 (7pp), 2009, doi: 10.1088/0960-1317/19/4/045010.
- [115] X. Niu, S. Peng, L. Liu, W. Wen, and P. Sheng. “Characterizing and patterning of pdms-based conducting composites” *Advanced Materials*, Vol. 19, No. 18, pp. 2682–2686, 2007, doi: 10.1002/adma.200602515.
- [116] S. Jiguet, A. Bertsch, H. Hofmann, and P. Renaud. “Conductive su8 photoresist for microfabrication” *Advanced Functional Materials*, Vol. 15, No. 9, pp. 1511–1516, 2005, doi: 10.1002/adfm.200400575.
- [117] X. Gong and W. Wen. “Polydimethylsiloxane-based conducting composites and their applications in microfluidic chip fabrication” *Biomicrofluidics*, Vol. 3, No. 1, pp. 012 007.1–012 007.14, 2009, doi: 10.1063/1.3098963.
- [118] L. Metref, F. Bianchi, V. Vallet, N. Blanc, R. Goetschmann, and P. Renaud. “Microfluidic system based on thermoexpandable polymer for on chip blood coagulation testing” *Micro and Nanosystems*, Vol. 1, pp. 41–45, 2009.

- [119] D. T. Yang, R. S. Robetorye, and G. M. Rodgers. "Home prothrombin time monitoring: A literature analysis" *American Journal of Hematology*, Vol. 77, No. 2, pp. 177–186, 2004, doi: 10.1002/ajh.20161.
- [120] M. M. Wintrobe, *Clinical Hematology*, 6th ed. Lea & Febiger: Philadelphia, 1967.
- [121] S. Caldwell and N. Shah. "The prothrombin time-derived international normalized ratio: Great for warfarin, fair for prognosis and bad for liver-bleeding risk" *Liver International*, Vol. 28, No. 10, pp. 1325–1327, 2008, doi: 10.1111/j.1478-3231.2008.01881.x.
- [122] C. Heneghan, P. Alonso-Coello, J. M. Garcia-Alamino, R. Perera, E. Meats, and P. Glasziou. "Self-monitoring of oral anticoagulation: A systematic review and meta-analysis" *Lancet*, Vol. 367, No. 9508, pp. 404–411, 2006, doi: 10.1016/S0140-6736(06)68139-7.
- [123] G. P. Carpenter, T. G. Neel, and J. R. Parker, "Overview of a novel point of care instrument system for measuring whole blood prothrombin time," in *Proceeding of SPIE*, vol. 2136, 1994, pp. 205–213.
- [124] A. Ur. "Changes in the electrical impedance of blood during coagulation" *Nature*, Vol. 226, No. 5242, pp. 269–270, 1970, doi: 10.1038/226269a0.
- [125] R. L. Rosenthal and C. W. Tobias. "Measurement of the electric resistance of human blood use in coagulation studies and cell volume determinations" *The Journal of Laboratory and Clinical Medicine*, Vol. 33, No. 9, pp. 1110–1122, 1948.
- [126] L. G. Puckett, G. Barrett, D. Kouzoudis, C. Grimes, and L. G. Bachas. "Monitoring blood coagulation with magnetoelastic sensors" *Biosensors & Bioelectronics*, Vol. 18, No. 5-6, pp. 675–681, 2003, doi: 10.1016/S0956-5663(03)00033-2.
- [127] M. Andersson, J. Andersson, A. Sellborn, M. Berglin, B. Nilsson, and H. Elwing. "Quartz crystal microbalance-with dissipation monitoring (qcm-d) for real time measurements of blood coagulation density and immune complement activation on artificial surfaces" *Biosensors and Bioelectronics*, Vol. 21, No. 1, pp. 79–86, 2005, doi: 10.1016/j.bios.2004.09.026.
- [128] US Patent 5 591 403 "Portable prothrombin time test apparatus and associated method of performing a prothrombine time test" 1997.

- [129] C. Iliescu, B. Chen, and J. Miao. “On the wet etching of pyrex glass” *Sensors and Actuators A*, Vol. 143, No. 1, pp. 154–161, 2008, doi: 10.1016/j.sna.2007.11.022.
- [130] F. E. H. Tay, C. Iliescu, J. Jing, and J. Miao. “Defect-free wet etching through pyrex glass using Cr/Au mask” *Microsystem Technologies*, Vol. 12, No. 10-11, pp. 935–939, 2006, doi: 10.1007/s00542-006-0116-0.
- [131] A. Berthold, P. Sarro, and M. Vellekoop, “Two-step glass wet-etching for micro-fluidic devices,” in *Proceedings of the SeSens workshop*, 2000, pp. 613–616 Online: <http://engineering.dartmouth.edu/microeng/processing/etching/PyrexEtch2.pdf>

List of Symbols

Abbreviations

CIME	Centre Interdisciplinaire de Microscopie Electronique
DMA	Dynamical Mechanical Analysis
FIB	Focus Ion Beam
INR	International Normalised Ratio
MEMS	Microelectromechanical Systems
NTC	Negative Temperature Coefficient
PCB	Printed Circuit Board
PDMS	Polydimethylsiloxane
PID	Proportional Integral Derivative
PMMA	Polymethyl metacrylate
PT	Prothrombine Time
SEM	Secondary Electron Microscopy
SMD	Surface Mounted Device
SMP	Shape Memory Polymers
μ TAS	Micro Total Analysis

Variables and constants

α	Thermal expansion coefficient	$[\text{m}^{-1}]$
ΔR_i	Variation of radius of an Expancel [®] bead before and after expansion	$[\text{m}]$
γ_{iso}^m	Mass proportion of isobutane in an Expancel [®] bead	$[-]$
γ_{eff}^{vol}	Effective proportion of beads in composite	$[-]$
γ_{iso}^v	Volumetric proportion of isobutane in an Expancel [®] bead	$[-]$
γ_{shell}^v	Volumetric proportion of copolymeric shell in an Expancel [®] bead	$[-]$
Γ_{atm}	Theoretical expansion ratio if internal pressure is atmospheric	$[-]$
ν	Poisson's ratio	$[-]$
ρ_{eth}	Density of ethanol	$[\text{kg}\cdot\text{m}^{-3}]$
ρ_{Exp}	Density of Expancel [®]	$[\text{kg}\cdot\text{m}^{-3}]$
ρ_{gas}	Density of gaseous isobutane at room temperature	$[\text{kg}\cdot\text{m}^{-3}]$
ρ_{liq}	Density of liquid isobutane	$[\text{kg}\cdot\text{m}^{-3}]$
ρ_{PDMS}	Density of PDMS	$[\text{kg}\cdot\text{m}^{-3}]$
ρ_{sample}	Density of composite sample	$[\text{kg}\cdot\text{m}^{-3}]$
A, B, C	Parameters of Antoine's equation	$[-]$
E	Young's modulus	$[\text{Pa}]$
K	PID proportional factor	$[-]$
K_i	PID integral factor	$[-]$
K_p	PID derivative factor	$[-]$
K_p	PID proportional factor at system oscillation	$[-]$

List of Symbols

$m_{bot+eth+sample}$	Mass of pycnometric bottle containing a sample and filled with ethanol	[kg]
$m_{bot+eth}$	Mass of pycnomteric bottle filled with ethanol	[kg]
m_{bot}	Mass of an empty pycnometric bottle	[kg]
m_{Exp}	Mass of Expancel® inside composite	[kg]
M_{iso}	Molecular mass of isobutane	[kg·mol ⁻¹]
m_{iso}	Mass of isobutane in composite	[kg]
m_{PDMS}	Mass of PDMS inside composite	[kg]
m_{sample}	Mass of composite sample	[kg]
n	Number of molecules of gas	[-]
p	Beads' internal pressure	[Pa]
p_{atm}	Atmospheric pressure	[Pa]
R	Perfect gas constant	[J·mol ⁻¹ ·K ⁻¹]
R_e	External radius of equivalent PDMS coated Expancel® bead	[m]
R_i	Radius of an Expancel® bead	[m]
T	Temperature	[K]
$V_{eth,full}$	Volume of ethanol in a pycnometric bottle	[m ³]
$V_{eth,meas}$	Volume of ethanol during a pycnometric measurement	[m ³]
V_{Exp}	Volume of Expancel® beads inside composite	[m ³]
V_{fin}	Volume of composite after expansion	[m ³]
V_{fin}^{Exp}	Volume of Expancel® after expansion	[m ³]
V_{gas}	Volume of Expancel® gaseous isobutane in composite after expansion	[m ³]
V_{ini}	Volume of composite before expansion	[m ³]

V_{ini}^{Exp}	Volume of Expancel [®] before expansion	[m ³]
V_{int}^{fin}	Volume of a bead coated with PDMS after expansion	[m ³]
V_{iso}	Volume of isobutane in an Expancel [®] bead	[m ³]
V_{liq}	Volume of liquid isobutane in composite before expansion	[m ³]
V_{PDMS}	Volume of PDMS inside composite	[m ³]
V_{sample}	Volume of composite sample	[m ³]
V_{shell}	Volume of Expancel [®] shell polymer in composite	[m ³]
V_{tot}	Volume of composite	[m ³]
V_{tot}^{Exp}	Volume of an Expancel [®] bead	[m ³]



Detailed experimental protocol

Contents

A.1	PDMS-Expancel [®] composite preparation	112
A.2	Crosslinked PDMS removal procedure	114
A.3	Density measurement protocol	115
A.4	Conducting PDMS preparation protocol	116
A.5	Ti/Pt electrode fabrication and implementation with composite	118

A.1. PDMS-Expancel[®] composite preparation

A.1 PDMS-Expancel[®] composite preparation

The PDMS used for all experiments in this work is Sylgard 184 from Dow Corning. Expancel[®] beads are 820 DU 40 from Azko Nobel provided by Luosoni SA (Bassecourt, CH)

Preparation

1. PDMS and Expancel[®] beads are mixed with the desired ratio. If large amounts are required, the mix is homogenised with an extruder provided by the LTPC (Laboratoire de technologies polymères et composites). The extrusion was done at room temperature and the water cooling system was used when the product's temperature raised above 28°C. Each run contained 4ml of mix and was extruded for 3min. The resulting product was then stocked until used, but not more that 40 days to prevent degradation.
2. Crosslinker is added to the mix with a 10:1 pure PDMS: crosslinker ratio and manually mixed.
3. The polymer is formed either by injection, or by casting

Forming

Injection

1. The composite is sucked in a syringe and is degassed under vacuum (water pump) for 30 min
2. The mix is injected in the mould

Cast moulding

1. The mix is degassed under vacuum (water pump) for 30min
2. The composite is cast on the mould or spin coated.

Crosslinking

Two crosslinking protocols are proposed depending on the time available for fabrication. The standardised protocol was used for all characterisation steps as the quick protocol was used for quick testing and debugging.

Standardised First polymerisation step occurs at room temperature during 16h and then at 55°C for 6h. The first polymerisation step at room temperature allows to have the composite crosslinked on a very flat surface to have flat films.

Quick At 60°C for at least 10h.

A.2. Crosslinked PDMS removal procedure

A.2 Crosslinked PDMS removal procedure

Removing of crosslinked PDMS bounded on a surface was done with the following procedure:

1. Remove mechanically a maximum of PDMS.
2. Let the system in the cleaning solution for one night, or a shorter time if the part can not handle such a treatment.
3. Rinse the substrate with water.

The cleaning solution has the following composition:

- 1ml deionized water
- 2.3ml ethanol
- 0.67g potassium hydroxide (KOH)

A.3 Density measurement protocol

This section describes the protocol used to measure density.

- Weighting of the sample (m_{sample})
- Precise filling of the bottle with the sample and pure ethanol
- Weighting of the bottle filled with the sample and ethanol ($m_{bot+eth+sample}$)

By knowing the mass of the bottle filled exclusively with ethanol ($m_{bot+eth}$) and of the empty bottle (m_{bot}), the sample mass and ethanol density (ρ_{eth}), the volume of sample can be deduced and thus its density.

$$\begin{aligned}
 V_{sample} &= V_{eth,full} - V_{eth,meas} \\
 &= \frac{m_{bot+eth} - m_{bot}}{\rho_{eth}} - \frac{m_{bot+eth+sample} - m_{bot} - m_{sample}}{\rho_{eth}} \\
 &= \frac{m_{bot+eth} - m_{bot+eth+sample} + m_{sample}}{\rho_{eth}} \\
 \Rightarrow \rho_{sample} &= \frac{m_{sample}\rho_{eth}}{m_{bot+eth} - m_{bot+eth+sample} + m_{sample}}
 \end{aligned} \tag{A.1}$$

A.4 Conducting PDMS preparation protocol

PDMS - Expancel[®] expansion were performed using conducting PDMS tracks fabricated as described here.

PDMS substrate

PDMS Master

Masters representing the channels which will hold the conducting composite were fabricated using SU8. The following fabrication process was used on silicon test wafer.

- **Oxygen plasma** The wafer was exposed to an oxygen plasma generated by a Plasmaline oven at 100 W and 1 Torr during 3 min.
- **Dehydration** 10 min at 200 °C on a hotplate.
- **Spin coating** GM1070 was spun 40 s at 900 rpm (10 s acceleration) for a 100 µm layer.
- **Softbake** On a hotplate the following temperature sequence was applied: (i) 30 min at 65°C, (ii) 1h à 95°C, (iii) free cooling to room temperature on the plate.
- **Exposure** 1 min (under vacuum film) with an isel-Vakuum-UV-Belichtungsgerat 4
- **Postexposure Bake** On a hotplate the following temperature sequence was applied: (i) 15 min at 65°C, (ii) 40 min à 95°C, (iii) reducing the hotplate temperature of 20 °C every 5 minutes
- **Development** 5 to 10 min in PGMEA¹ until no more white zones are visible when rinsed with isopropanol.
- **Hardbake** if the resin is not completely polymerized further curing can be performed for up to 2h at 135°C

¹Propylene Glycol Monomethyl Ether Acetate

Moulding and curing

PDMS was mixed using the standard 10:1 base:croslinker ratio. The mix was poured on the master and cured on a hotplate at 100 °C. Curing was stopped once the PDMS was hard.

Conductive mix

Conducting PDMS was obtained by mixing PDMS with silver coated copper flakes to obtain a metal weight ratio of 80 %. This mix was then applied on the previously prepared PDMS channels and cured in a oven at 80 °C for at least 30 min.

Activation

Activation of PDMS - Expancel® composite was done by placing the fabricated resistor a membrane of cured composite and applying a power around 200 mW to it. This power may vary due to the resistance variation of the heater due to the temperature rise.

A.5 Ti/Pt electrode fabrication and implementation with composite

In order to fabricate titan - platinum heater the following process was performed on Pyrex wafer in CMI clean room facilities.

- **Ti/Pt sputtering** 20nm Ti, 100nm Pt on Spider sputterer
- **Photoresist spin coating** AZ9260 5µm on EVG
- **Exposure** twice 9.5sec with 20 sec break on MA6
- **Development** AZ9260 development program on EVG
- **Pt etch** 3-5 min on STS
- **Photoresist removal** PR removal bath at 75 °C
- **Cleaning** Burnt resin removal with acetone



Detailed calculus

Contents

B.1	Variation of volume in a micro injector cavity	120
-----	--	-----

B.1 Variation of volume in a micro injector cavity

In the case of the microinjector, the volume of the cavity depends on the height augmentation of the Expancel. In Figure B.1 is drawn the situation of an expanding layer in a micro injector.

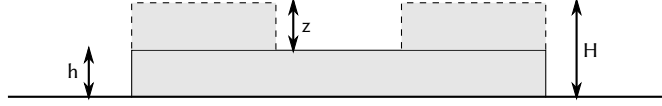


Figure B.1 Schema of the expanded system forming the cavity to be filled with liquid

If we neglect the lateral error in order to have an approximate minimal number, z is given by

$$z = H - h \quad (\text{B.1})$$

with h , the initial thickness of the layer and H the thicknessa after expansion. The thickness after expansion can be deducted from inital thickness and expansion ratio Γ . Since the expansion ratio is volumetric, the linear factor to use for the height is the cubic square of such value.

$$H = \sqrt[3]{\Gamma}h \quad (\text{B.2})$$

Thus z is completely defined.

$$z = \sqrt[3]{\Gamma}h - h = (\sqrt[3]{\Gamma} - 1)h \quad (\text{B.3})$$

In this way, the variation on z , ϵ_z is the difference between the mean value and the minimum, divided by the mean value. It is mainly dependant on the error on Γ , ϵ_Γ :

$$\begin{aligned} \epsilon_z &= \frac{z - z_{min}}{z} \\ &= \frac{(\sqrt[3]{\Gamma} - 1)h - (\sqrt[3]{(1 - \epsilon_\Gamma)\Gamma} - 1)h}{(\sqrt[3]{\Gamma} - 1)h} \\ &= 1 - \frac{\sqrt[3]{(1 - \epsilon_\Gamma)\Gamma} - 1}{\sqrt[3]{\Gamma} - 1} \end{aligned} \quad (\text{B.4})$$

Appendix B. Detailed calculus

In our case, the expansion ratio is comprised between 1.86 and 2.17. Thus, Γ is 2.015 and ϵ_{Γ} is 0.0769. In this way, the volume variation equal to the height variation is 0.1264.

B.1. Variation of volume in a micro injector cavity

Curriculum Vitae



Born November 20th, 1981
Swiss and Algerian
lynda.metref@a3.epfl.ch

Lynda Metref

Education

PhD. in Microsystem Technology

2006 – 2010 Laboratoire de Microsystèmes 4, EPFL, Lausanne, Switzerland
“Fluid manipulation using thermoexpandable polymer based on polydimethylsiloxane and Expancel”

MSc. in Microtechnology

2000 – 2005 Section de Microtechnique, EPFL, Lausanne, Switzerland
Master thesis: “Dosing and sampling system for Lab-on-Chip”
Semester project: “Microfluidic system for cells immobilisation in gel”
Semester projet: “PC104 card prototype for motor control and translator on the SmartEase robot”

Professional experience

R & D Engineer

2006 – 2010 Debiotech SA, Lausanne, Switzerland
Prospective research on medical devices with thermoexpandable materials

Research Assistant

2005 – 2006 Dept. of Chemical Engineering, HKUST, Hong Kong, China
World-to-chip interface for a mRNA detection microsystem

Research Assistant

2005 Laboratoire de Microsystèmes 2, EPFL, Lausanne, Switzerland
Contactless electrochemical actuator for precise sampling on microchip

Teaching assistant

2004 – 2005 Computer Vision Laboratory, EPFL, Lausanne, Switzerland
C programming language course

Trainee

2004 Laboratoire de Microsystèmes 4, EPFL, Lausanne, Switzerland
Cells immobilisation on a porous membrane

Publications

Journal Papers

- 2009 L. Metref, F. Bianchi, V. Vallet, N. Blanc, R. Goetschmann, and P. Renaud. *Microfluidic system based on thermoexpandable polymer for on chip blood coagulation testing*. *Micro and Nanosystems*, 1(1):41-45, 2009.
- 2007 L. Metref, F. Herrera, D. Berdat, and M. Gijs. *Contactless electrochemical actuator for microfluidic dosing*. *Journal of Microelectromechanical Systems*, 16(4):885-892, 2007.
- 2007 T. Braschler, L. Metref, R. Zvitov-Marabi, H. van Lintel, N. Demierre, J. Theytaz, and P. Renaud. *A simple pneumatic setup for driving microfluidics*. *Lab on a Chip*, 7(4):420-422, 2007.
- 2005 T. Braschler, R. Johann, M. Heule, L. Metref, and P. Renaud. *Gentle cell trapping and release on a microfluidic chip by in situ alginate hydrogel formation*. *Lab on a Chip*, 5(5):553-559, 2005.

Conferences & Proceedings

- 2009 P. Lemaire, L. Metref, F. Bianchi, and P. Renaud. *On-chip thermopneumatic actuation system for coagulation time measurement*. In *Procedia Chemistry*, 521-524. Elsevier, 2009.
- 2005 L. Metref, F. Herrera, D. Berdat, and M. A. M. Gijs. *Contactless electrochemical actuator for precise sampling on microchip*. In *Proceedings of μ TAS 2005 Conference*, 69-171, 2005.

Patents

- 2009 EP 08172813.1 *Digital microfluidic* F. Bianchi and L. Metref. Debiotech SA. (pending)
- 2007 PCT/IB2006/054432 *System to measure blood coagulation related parameters* L.-D. Piveteau, V. Vallet, F. Neftel, L. Metref and N. Blanc. Debiotech SA. (published)

Skills & Interests

Languages

French: Native
English: Fluent
German: Basic
Chinese: Travelling knowledge

Interests

Museums, visit of historical sites, cultural events, photography, calligraphy, role-playing games, open-source software, video games.